MATRIX-FRACTURE TRANSFER IN NON-ISOTHERMAL CONDITIONS

A THESIS SUBMITTED TO
THE GRADUATE SCHOOL OF NATURAL AND APPLIED SCIENCES
OF
MIDDLE EAST TECHNICAL UNIVERSITY

BY

YASHAR   TAVAKKOLI OSGOUEI

IN PARTIAL FULFILLMENT OF THE REQUIREMENTS
FOR
THE DEGREE OF DOCTOR OF PHILOSOPHY
IN
PETROLEUM AND NATURAL GAS ENGINEERING

JANUARY 2020

Approval of the thesis:

MATRIX-FRACTURE TRANSFER IN NON-ISOTHERMAL CONDITIONS

submitted by **YASHAR TAVAKKOLI OSGOUEI** in partial fulfillment of the requirements for the degree of **Doctor of Philosophy in Petroleum and Natural Gas Engineering Department, Middle East Technical University** by,

Prof. Dr. Halil Kalıpçılar
Dean, Graduate School of **Natural and Applied Sciences**   _____

Assoc. Prof. Dr. Çağlar Sınayuç
Head of Department, **Petroleum and Natural Gas Eng.**   _____

Prof. Dr. Serhat Akın
Supervisor, **Petroleum and Natural Gas Eng., METU**   _____

Assoc. Prof. Dr. Emre Artun
Co-Supervisor, **Petroleum and Natural Gas Eng., METU-NCC**   _____

Examining Committee Members:

Prof. Dr. Mahmut Parlaktuna
Petroleum and Natural Gas Engineering, METU   _____

Prof. Dr. Serhat Akın
Petroleum and Natural Gas Eng., METU   _____

Prof. Dr. Nurkan Karahanoğlu
Geological Engineering, METU   _____

Prof. Dr. Ö. İnanç Türeyen
Petroleum and Natural Gas Engineering, ITU   _____

Assist. Prof. Dr. Doruk Alp
Petroleum and Natural Gas Engineering, METU-NCC   _____

Date: 20.01.2020

I hereby declare that all information in this document has been obtained and presented in accordance with academic rules and ethical conduct. I also declare that, as required by these rules and conduct, I have fully cited and referenced all material and results that are not original to this work.

Name, Surname: Yashar Tavakkoli Osgouei

Signature:

ABSTRACT

MATRIX-FRACTURE TRANSFER IN NON-ISOTHERMAL CONDITIONS

Tavakkoli Osgouei , Yashar
Doctor of Philosophy, Petroleum and Natural Gas Engineering
Supervisor: Prof. Dr. Serhat Akın
Co-Supervisor: Assoc. Prof. Dr. Emre Artun

January 2020, 168 pages

A numerical and experimental study was carried out to investigate matrix-fracture transfer in fractured porous media. Film type heat flux sensors were installed in four different synthetically fractured core plugs to measure the temperature and heat flux in fracture during cold water injection. Experimental values of heat flux were used to calculate convective heat transfer coefficient. Fracture temperatures were used to calibrate numerical model developed using CMG-STARS simulator to evaluate contributing matrix thermal properties. The results show that the temperature decrease in fracture is lower when rock matrix has higher thermal properties. The variations in heat flux and temperature difference along matrix-fracture interface with respect to time necessitates the use of variable convective heat transfer coefficients for accurate analysis of matrix-fracture heat transfer.

Moreover, results of tracer experiments where Rhodamine B solution was injected at a flow rate of 1 cc/min and outer temperature of 70 °C was used to determine dispersion coefficients using aforementioned numerical model. Sensitivity analysis of the numerical model indicated that thermal properties of matrix are effective in matrix-fracture mass transfer similar to injection rate. To illustrate, the solute penetration is higher in core plugs with larger matrix thermal properties that provide larger temperature gradient over matrix-fracture interface. This can be explained by

the Soret effect that is kind of coupled heat and mass transfer at non-isothermal conditions.

ÖZ

İZOTERMAL OLMAYAN KOŞULLARDA MATRİKS – ÇATLAK TRANSFERİ

Tavakkoli Osgouei , Yashar
Doktora, Petrol ve Doğal Gaz Mühendisliği
Tez Danışmanı: Prof. Dr. Serhat Akın
Ortak Tez Danışmanı: Doç. Dr. Emre Artun

Ocak 2020, 168 sayfa

Çatlaklı gözenekli ortamda çatlak - matriks transferini araştırmak için sayısal ve deneysel bir çalışma yapılmıştır. Film tipi ısı akısı sensörleri, soğuk su enjeksiyonu sırasında çatlaktaki sıcaklığı ve ısı akısını ölçmek için dört farklı sentetik olarak çatlatılmış tapaya yerleştirilmiştir. Konvektif ısı transfer katsayısını hesaplamak için deneysel ısı akısı değerleri kullanılmıştır. Matriks termal özelliklerini değerlendirmek için CMG-STARS simülatörü kullanılarak geliştirilen sayısal modeli kalibre etmek için çatlak sıcaklıkları kullanılmıştır. Sonuçlar, kaya matriksinin daha yüksek termal özelliklere sahip olması halinde çatlaktaki sıcaklık düşüşünün daha az olduğunu göstermektedir. Matriks-çatlak arayüzü boyunca zamana göre ısı akısı ve sıcaklık farkındaki değişimler, matriks-çatlak ısı transferinin doğru analizi için değişken konvektif ısı transfer katsayılarının kullanılması gerektiğini göstermiştir.

Ayrıca, yukarıda belirtilen sayısal model kullanılarak Rhodamine B çözeltisinin 1 cc / dakika akış hızında 70°C dış sıcaklıkta enjekte edildiği izleyici deneylerinin sonuçları dağılım katsayılarını belirlemek için kullanılmıştır. Sayısal modelin duyarlılık analizi, matriksin termal özelliklerinin, enjeksiyon hızına benzer matriks - çatlak kütle transferinde etkili olduğunu göstermiştir. Örnek vermek gerekirse, matriks – çatlak arayüzü üzerinde daha büyük sıcaklık gradyanı sağlayan daha büyük

matris termal özelliklerine sahip tapalarda çözünen penetrasyon daha yüksektir. Bu, izotermal olmayan koşullarda bir tür birleştirilmiş ısı ve kütle transferi olan Soret etkisi ile açıklanabilir.

Anahtar Kelimeler: Çatlaklı poroz ortam, Matriks-çatlak transferi, Konvektif ısı transfer katsayısı, İzleyici testi sayısal modellemesi, ısı ve kütle transferinin birlikte değerlendirilmesi

To my parents and my wife

ACKNOWLEDGEMENTS

TABLE OF CONTENTS

LIST OF TABLES

TABLES

LIST OF FIGURES

FIGURES

LIST OF ABBREVIATIONS

ABBREVIATIONS

BTU: British Thermal Unit

CMG-STARS: Computer Modelling Group Ltd.-STARS

cc: Cubic Centimeter

erfc: Complementary Error Function

ft: Foot

hr: Hour

in.: Inch

LTE: Local Thermal Equilibrium

LTNE: Local Thermal Non-Equilibrium

min: Minute

MW: Molecular weight

μv: MicroVolts

Pe: Peclet Number

ppb: Parts Per Billion

SS: Sandstone

LIST OF SYMBOLS

GREEK SYMBOLS

α: Thermal diffusivity (cm^2/min)

α_m: Thermal diffusivity of matrix (cm^2/min)

α_w: Thermal diffusivity of water (cm^2/min)

ρ_w: Density of water (kg/cm^3)

τ: Tortuosity of matrix

$\varnothing$: Porosity (%)

LATIN SYMBOLS

A: Area (cm^2)

a: Dispersivity (cm)

b: Half aperture of fracture (cm)

C: Concentration of solute (ppb)

C_f: Concentration of solute in fracture (ppb)

C_m: Concentration of solute in matrix (ppb)

c_p: Specific heat capacity (J/kg °C)

$c_{p,w}$: Specific heat capacity of water (J/kg °C)

$(\rho c_p)_m$: Volumetric heat capacity of matrix (J/cm^3 °C)

D: Dispersion coefficient of the solute(cm^2/min)

D_e: Effective diffusion coefficient of matrix (cm^2/min)

D_L: longitudinal dispersion coefficient (cm^2/min)

D_m: Molecular diffusion coefficient of the solute (cm^2/min)

D_T: Transverse dispersion coefficient (cm^2/min)

h: Convective heat transfer coefficient (J/min cm^2 °C)

j: Flux of solute

k: Thermal conductivity (J/min cm °C)

k_m: Thermal conductivity of matrix (J/min cm °C)

k_w: Thermal conductivity of water (J/min cm °C)

$\overset{\bullet}{m}$: Mass flow rate (kg/s)

Q: Volumetric flow rate (cm^3/min)

q: Heat flux (J/min cm^2)

R: Chemical reaction

r: Radius (cm)

t: Time (min)

t_D: Dimensionless time

T_o: Outer surface temperature of the matrix (°C)

T_f: Temperature of flowing fluid in fracture (°C)

T_i: Average temperature of fracture surface of core plug (°C)

T_{in}: Inlet temperature of fluid (°C)

T_m: Temperature of matrix (°C)

T_{out}: Outlet temperature of fluid (°C)

T_s: Temperature of solid surface (°C)

u: Fluid velocity (cm/min)

V: Volume (cm^3)

Y (L): Length (cm)

y_D: Dimensionless space

SUBSCRIPTS

D: Dimensionless

f: Fracture

m: Matrix

s: Fracture surface

w: Water

CHAPTER 1

INTRODUCTION

Over the recent decades, the need for the understanding, characterizing, and modeling of flow and transfers as well as interactions within porous media has mainly been increased (Berre et al., 2019). As porous medium can be defined as a solid structure with interconnected voids, it can cover many areas, ranging from agricultural, chemical, hydrological, environmental, petroleum and geothermal engineering to soil and geo sciences (Olasolo et al., 2016).

Similar to geothermal reservoirs existing commonly as the matrix-fracture systems, approximately 60 % of world's hydrocarbon reservoirs are placed in the fractured porous media. While different kinds of porous media are characterized by fracture network, the scale of fractures can range from millimeters to hundreds of kilometers (Berre et al., 2019; Olasolo et al., 2016).

Fractured porous media are somewhat different from homogeneous porous media in the sense that they are highly heterogeneous systems. This heterogeneity can be referred to the very large contrast in properties such as permeability and storage capacity. Fractured porous media include high storage capacity and low permeability matrix which acts as a storage and low storage capacity and high permeability fracture providing flow path for fluid flow (Berre et al., 2019; Kumar, 2012).

The flow and transport through fractured porous media can be contrasted with those in unfractured porous media. Therefore, there may be early breakthroughs in the former structures compared to the latter ones. In fact, the heterogeneities of flow and transport properties in both fracture networks and surrounding porous matrix result in increasing uncertainties, making characterization of matrix-fracture systems more complicated (Kumar, 2012).

The reason why fracture networks affect the flow and transport in matrix-fracture systems can be clarified that the heterogeneous structure of fractured porous media provides complex fluid velocity profiles. Because the flow velocity in fracture is considerably faster than that in porous matrix, the large velocity gradient between matrix and fracture can produce the potential for matrix-fracture transfers of mass and heat over fluid flow in matrix-fracture systems (Kumar, 2012). In addition, other physical and chemical processes such as chemical reaction and adsorption etc. can affect transport process (Khuzhayorov and Mustofokulov, 2019; Khuzhayorov and Mustofoqulov, 2018). The spatial heterogeneities in fractured porous media and the variability in flow and transport properties make them intricate for analysis of matrix-fracture transfers. That's why, the single fracture-matrix systems are usually used to have a precise analysis of matrix-fracture transfers (Bagalkot et al., 2018).

Although matrix-fracture thermal transport involves heat conduction within matrix and forced heat convection along matrix-fracture interface due to fluid flow in fracture, the analysis of matrix-fracture heat transfer can be simplified by theory of local thermal non-equilibrium describing the convective heat transfer mechanism (Shaik et al., 2011; Yamaguchi and Akibayashi, 1992). Thus, convective heat transfer coefficient can be considered as a representative to determine the amount of heat exchange in matrix-fracture system (Abdallah et al., 1995).

In the way that the large velocity gradient between matrix and fracture causes matrix-fracture heat transfer due to temperature difference, it can also produce concentration difference between matrix and fracture which is responsible for matrix-fracture mass transfer (Kumar, 2012). Tracer testing is the most commonly used approach for the characterization of porous media and the estimate of transport parameters. These properties are usually determined through fitting tracer transport models to real data over tracer testing. In fact, they are determinant quantities to analyze matrix-fracture transfers in fractured porous media (Schmelling and Ross, 1989).

2

Although fractures can contribute heat and mass differences between matrix and fracture for matrix-fracture transfers due to the large velocity gradient, the porous matrix can be controlling factor in transport process along matrix-fracture interface, namely, the properties of matrix can greatly affect matrix-fracture transfers (Wu et al., 2010).

In present study, the single fractured core plugs were synthetically prepared to analyze matrix-fracture transfers. The matrix-fracture transfers can be divided into the main three categories: thermal transport, solute transport, and particles transport. Cold water injection, tracer solution injection, and micro-tracer particles injection through the single fracture-matrix systems were experimentally carried out for analysis of thermal transport, solute transport, and particles transport, respectively. Also, each category can be further divided into four steps: experimental measurements, development of numerical model, history matching, and sensitivity analysis. The values of temperature in fracture and heat flux along matrix-fracture interface over cold water injection and outlet concentration of tracer over tracer injection constitute experimental measurements. The numerical simulation models were developed for all core plugs using CMG-STARS then matching the results of numerical models with the values of experimental measurements were carried out to determine some properties of matrix and fracture involved in matrix-fracture transfers. The calibrated numerical model was used to investigate the effect of flow rate in fracture as well as thermal and physical properties of matrix on matrix-fracture transfers in different core plugs.

Because porous matrix acts as the source to supply heat over cold water injection and the storage to retard tracer breakthrough due to dispersion within matrix over tracer injection, the thermal properties of matrix along with physical properties can determine the amount of matrix-fracture transfers in non-isothermal conditions. In fact, coupled heat and mass transfers is effectively used to analyze simultaneous occurrence of heat and mass transfers between matrix and fracture in non-isothermal

conditions. Figure 1.1. shows the flowchart of stages performed to study matrix-fracture transfers in the single fracture-matrix systems.
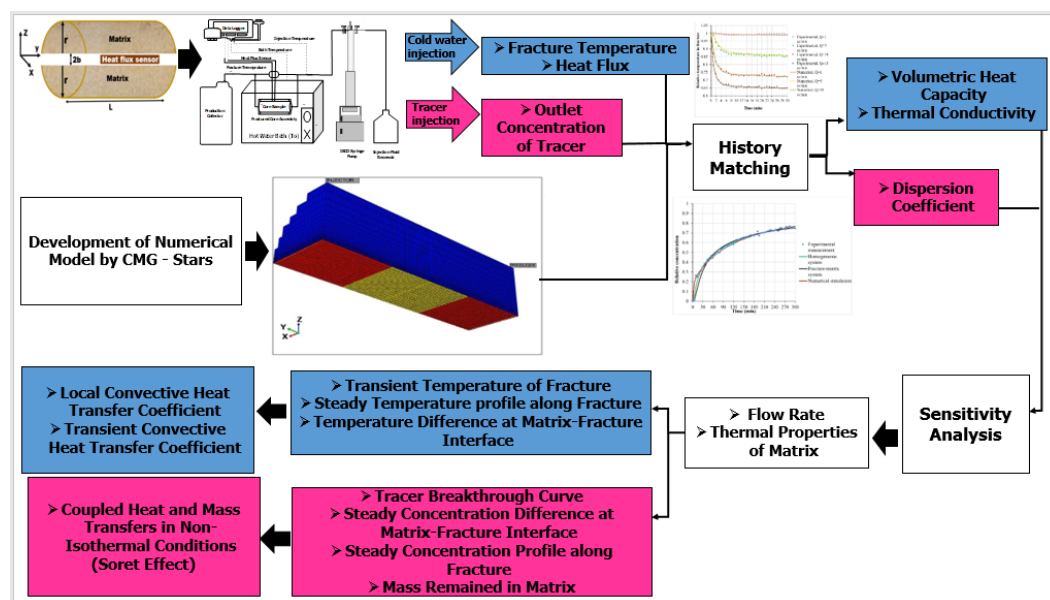
Figure 1.1. The flowchart of study on matrix-fracture transfers in non-isothermal conditions

In this chapter the overall concept of matrix-fracture transfers and the stages of current study were briefly explained.

In **chapter 2**, the statement of the problems about matrix-fracture transfers then the main stages handled in the current study are explained as well.

In **chapter 3**, the preparation of core plugs and fractured core assembly and design of experimental setup used for flow-through experiments to measure heat flux and temperature in fracture over cold water injection and outlet concentration of tracer over tracer injection are described.

In **chapter 4**, the construction of numerical simulation models developed to study heat and mass transfers through the single fractured core plugs are explained. The fundamental of history matching is briefly described to achieve a calibrated numerical

model used for matrix-fracture transfers analysis and determining some uncertain parameters as well.

In **chapters 5**, the investigations of thermal transport in the single fractured core plugs are presented. Firstly, several previous studies and different aspect of heat transfer in matrix-fracture systems reported in the literatures were reviewed. In the next step, the procedures of experimental measurements and calibration of numerical models are described. Then, experimental and numerical as well as analytical results are given and compared for analysis of matrix-fracture heat transfers.

In **chapters 6**, the investigations of solute transport in the single fractured core plugs are presented. Firstly, several previous studies and different aspect of solute transport in matrix-fracture systems reported in the literatures were reviewed. In the next step, the procedures of experimental measurements and calibration of numerical models are described. Then, experimental and numerical as well as analytical results are given and compared for analysis of matrix-fracture mass transfers.

In **chapter 7**, the investigations of particles transport in the single fractured core plugs are presented. Firstly, several previous studies and different aspect of particles transport in matrix-fracture systems reported in the literatures were reviewed. Then, the experimental results of particles transport in the single fracture-matrix systems are given.

In **chapter 8**, the summary of the most outstanding points of the current study in the analysis of matrix-fracture transfers involving methodology, observations, and results is given.

CHAPTER 2

STATEMENT OF PROBLEM

The analysis of matrix-fracture heat transfer can be convenient by calculating convective heat transfer coefficient. In other words, it can be considered as a representative of the amount of heat exchange between matrix and fracture in matrix-fracture systems. The convective heat transfer coefficient depends on flowing fluid properties, geometry of matrix-fracture interface, and temperature difference at matrix-fracture interface. In addition to flow conditions in fracture and fracture properties, thermal properties of matrix by establishing the temperature of fracture surface can affect temperature difference at matrix-fracture interface. Although energy balance method and analytical solution of heat transfer equations in matrix-fracture systems are used to calculate the constant value of convective heat transfer coefficient, it cannot exactly explain matrix-fracture thermal transport. It can be attributable to variations in the values of temperature difference, in turn, heat flux along matrix-fracture interface with respect to space and time in matrix-fracture systems.

To cope with this problem, heat flux sensor was used to measure experimental values of heat flux and fracture temperature. The experimental values of fracture temperature were used to calibrate numerical model by which thermal properties of matrix and temperature difference along matrix-fracture interface in various times were determined. The values of heat flux were used to calculate directly convective heat transfer coefficient as well. Eventually, new form of heat transfer coefficient, namely, local and transient convective heat transfer coefficients are introduced for analysis of matrix-fracture thermal transport.

The level of tracer penetration into matrix can be used for analysis of matrix-fracture mass transfer. It can be considered as a representative of the amount of mass transfer between matrix and fracture in matrix-fracture systems. The rate of penetration depends on flow conditions in fracture and fracture properties as well as matrix properties. A constant and isotropic value of dispersion coefficient cannot adapt the solute penetration in matrix-fracture systems due to their heterogeneous structure.

To analyze solute transport between matrix and fracture the anisotropic values of dispersion coefficient were determined by numerical simulation model calibrated with experimental values of outlet concentration of tracer. These values are compatible with matrix permeability. Moreover, the calibrated numerical model was used to investigate the effect of thermal properties of matrix on matrix-fracture solute transport at different temperatures in non-isothermal conditions transport processes. The Sorret effect as a representative of coupled heat and mass transfers was used to explain the effect of thermal properties of matrix on solute transport through matrix-fracture systems in non-isothermal conditions.

However, the development of numerical simulation model of micro particles transport was impossible due to adsorbing or sticking of particles on fracture wall and surface of the heat flux sensor as well as gravity settling of particles in the fracture.

CHAPTER 3

PREPARATION OF CORE PLUGS AND EXPERIMENTAL SETUP

3.1. Core Plugs Preparation and Properties

The core samples were prepared to the desirable dimensions through cutting and trimming processes by using core drilling and sample cutting machines. The core samples used in this study are limestone with low permeability.

After core plug preparation processes, the samples were then dried in an oven at 110 ºC for 24 hours and cooled in a vacuum chamber until gas porosimeter and permeability measurements were conducted by using core property measurement apparatus available in petroleum and natural gas engineering department (Figure 3.1). Four limestone core samples were selected for fracturing in order to use in flooding experiments.

Figure 3.1. Core plugs preparation and properties measurements

The physical properties of the core plugs used in experiments are listed in the below Table 3.1:

Table 3.1. *The physical properties of core plugs*

Core Plug	Length (cm)	Diameter (cm)	Porosity (%)	Permeability (md)	Pore Volume (cm^3)
# 1	7.21	3.72	17.92	8.39	14.04
# 3	7.13	3.72	19.00	3.79	14.73
# 8	6.77	3.72	16.85	8.83	12.40
# 10	7.09	3.72	17.91	4.31	13.80

3.2. Fractured Core Assembly

For creating the single fracture and installing heat flux sensor within it, the core samples were bisected along their length to install the heat flux sensor.

The thin film type heat flux sensor (Omega HFS-3) was used to measure the heat flux and fracture temperature (Figure 3.2). The heat flux sensor sensor is a flexible and self-generating thermopile transducer that the data was recorded by using a digital data logger. It outputs microvolts with 4-wire sensor with thermocouple and the nominal sensitivity 3.0 (μv/BTU/ft2hr).

Whereas the fracture including heat flux sensor was situated in the middle of the two matrix blocks, the outside surface of the core plugs was sealed with epoxy resin. The coating of core plugs was performed by placing fractured cores in the middle of the cast acrylic tube and filling their surrounding space with epoxy resin of Neodecanoic acid glycidyl ester type ER2188 with MW<=700. The sealing outer surface of core plugs ensures fluid flow through single fracture and not along the outer surface, creating a no flow boundary condition at the radial boundary. Consequently, it provides a gap between top and bottom of core plugs' halves to give only fluid flow through a horizontal fracture with the aperture 0.01778 cm that is equal to thickness of the film heat flux sensor.

Then the fractured core is positioned in a Teflon core holder with two end caps at the top and bottom of the core for fluid flow in and out of the core holder. In order to

distribute fluid in all direction of fractured core, the end cap faces that meet the rock sample have spider-web-shaped channels (Figure 3.3).
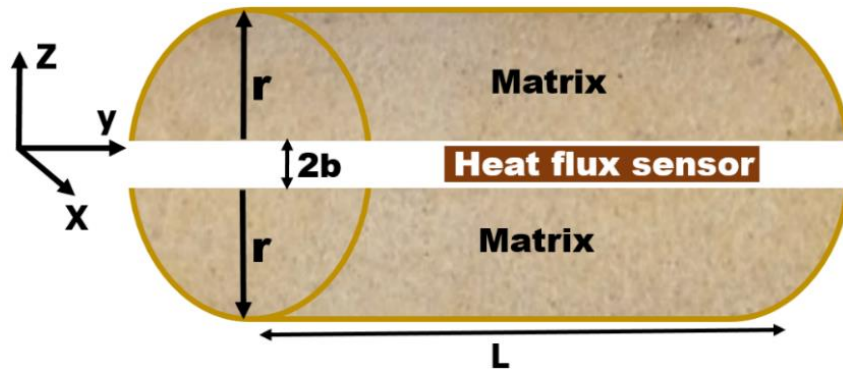
Figure 3.2. The artificial fractured core plug (A single fracture-matrix system)
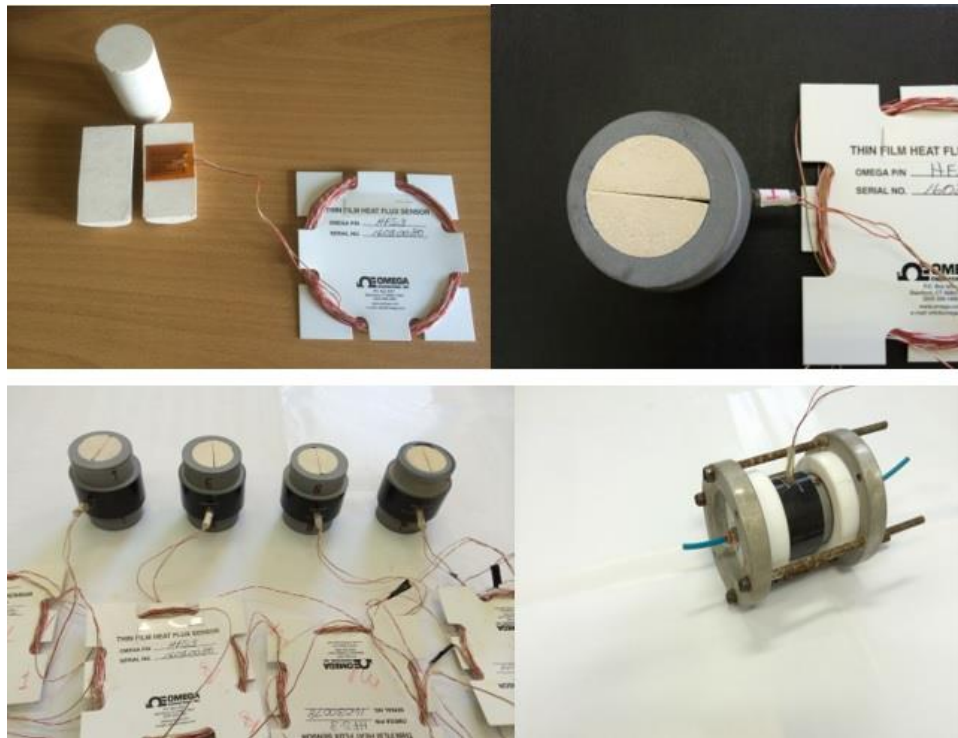
Figure 3.3. Fractured core assembly

3.3. Experimental Setup

This apparatus is made of injection fluid reservoir, pump (ISCO syringe-500D), fractured core assembly, water bath to maintain the temperature of the core sample's outer surface at constant values (70 or 90 °C) by potting core assembly inside it, thermocouples to measure inlet fluid, outlet fluid, and water bath temperatures over cold water and tracer injection , production collector system, data logger (Elimko E-680) to record heat flux along matrix-fracture interface, and inlet, outlet, and fracture temperatures, and injection and production lines involving plastic and metal transmission tubes. This set up was used for flow-through experiments such as cold water injection (matrix-fracture thermal transport), tracer solution injection (matrix-fracture solute transport), micro-particles tracer injection (matrix-fracture particles transport) experiments. The schematic of the experimental apparatus is shown in the following figures;
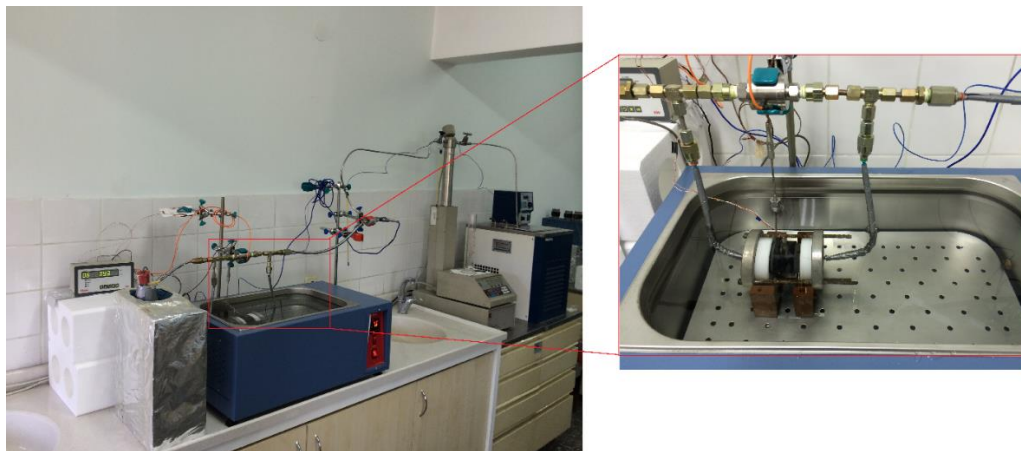
Figure 3.4. The core flooding experiments set-up
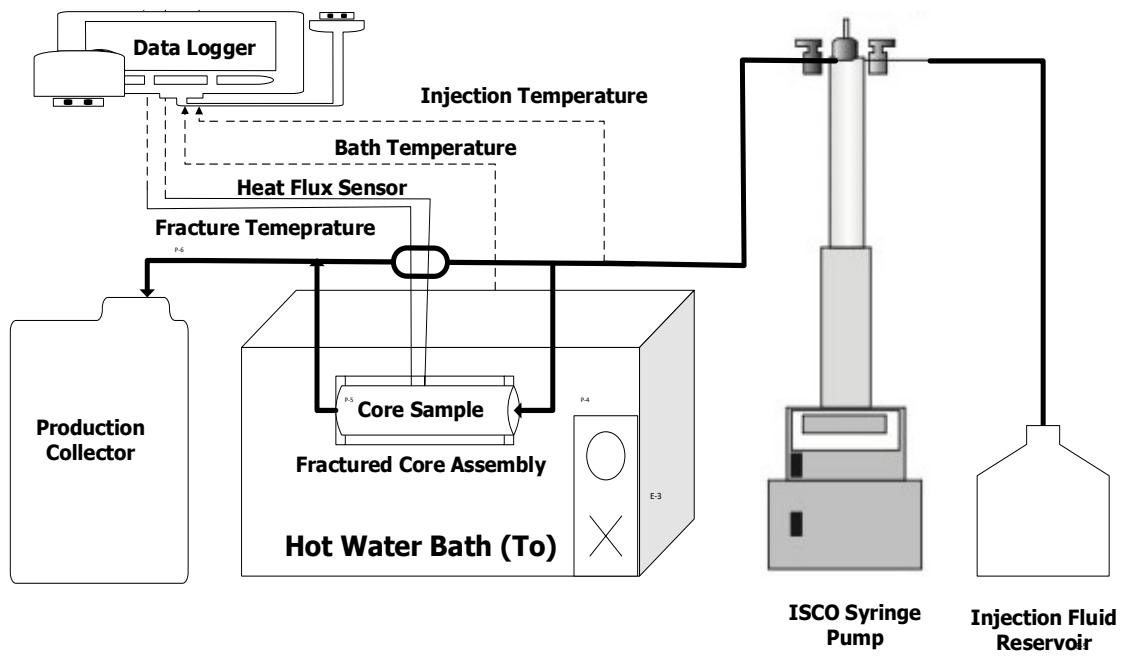
Figure 3.5. Schematic drawing of experimental set-up used in flow-through experiments

CHAPTER 4

NUMERICAL SIMULATION MODEL

4.1. Numerical model description

Numerical simulation is typically an appropriate method to analyze the mechanisms involving the phenomena. In addition, for optimizing the parameters numerical model should be built to predict system functionality and response under different conditions. The aim of numerical simulation is representing of a real system to forecast the capabilities of system in various steps and operations conditions (Heidari et al., 2011).

The numerical simulation is complementary of experimental outcomes in identification of main controlling parameters in studies. The development of numerical model to represent the realistic experimental observations is a useful tool in the understanding of phenomena. It provides considerable and accurate insight into the processes controlling solute flow and transport in fracture-matrix system unlike analytical solution of solute transport equations, which are based on many assumptions and simplifications (Sanaee et al., 2012).

The simulation of experimental data is used to design and optimize for calculation of some decision variables. Therefore, the selection of an appropriate simulator can be important step in modeling laboratory-scale experiments. The most prominent feature of simulator used is the capacity and functionalities that is essential for modeling (Mohammadi et al., 2012).

The three-phase multi-component thermal simulator, STARS by CMG (Computer Modeling Group Ltd.) is used for implicit finite difference numerical simulation of thermal transport and tracer solution transport in the single fracture-matrix systems (CMG STARS Manual). For simplicity a quarter of the fractured core plugs were simulated due to symmetrical shape.
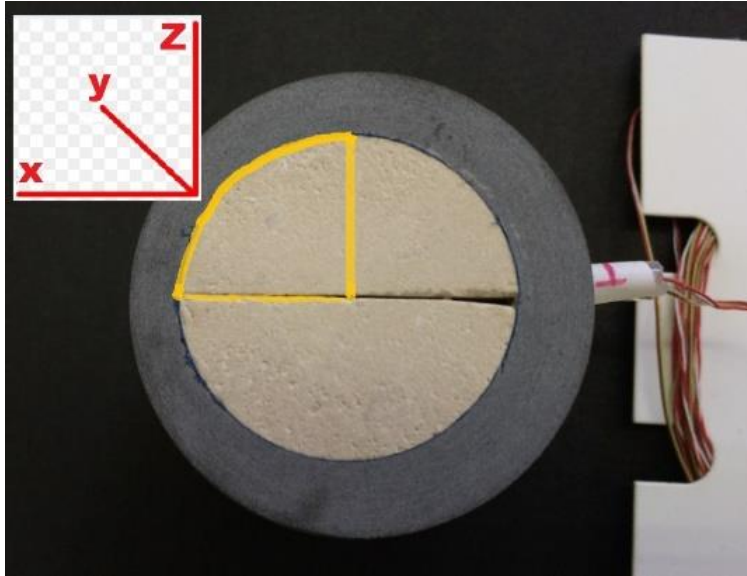
Figure 4.1. A quarter of the fractured core plug

The numerical model with the Cartesian grid system representing a single-matrix system has 15×120×26 grid blocks in x, y, and z directions, respectively. The grid size is variable with respect to space and directions. The grid blocks were set to be finer near matrix-fracture interface to have an accurate analysis of matrix-fracture transfers. The heterogeneities in numerical model were contrasted with respect to different values of porosity and permeability for rock matrix, fracture, and sensor sections.

The numerical simulation of the single fracture-matrix system to model matrix-fracture transfers over non-isothermal processes includes totally 46800 grid numbers with various sizes.

In the current simulation, the ends of single fracture-matrix system were modeled as injection and production wells. The wells were perforated at the fracture inlet and outlet to flow only fluid through fracture over core flooding process. Fluid movement is expected due to high values of permeability and porosity along fracture section.
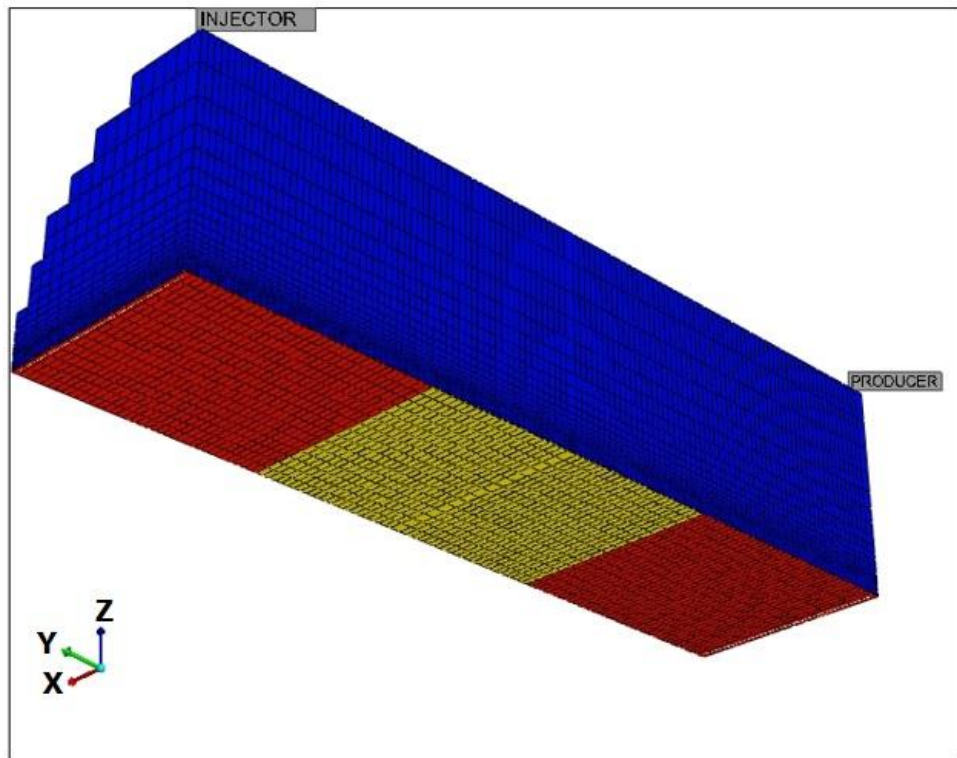
Figure 4.2. Heterogeneities in the 3D view of numerical simulation model

The reason for constructing a Cartesian grid type rather than Radial one of single fracture-matrix system in simulation model is to ensure having 1-D fluid flow along fracture similar to core flooding experiments (Tunnish et al., 2019). The following table shows different section in single fracture-matrix system simulated.

Table 4.1. *Type and dimension of grid system in the numerical simulation model.*

Rock Type	Color	Position		
		X	Y	Z
Matrix	Blue	1:15	1:120	2:26
Fracture	Red	1:15	1:37 -------------------------------- 84:120	1
Sensor	Yellow	1:15	38:83	1

4.2. History matching

The numerical model can only be reliable in the case of good calibration with actual observations. The model is calibrated when it can reproduce the observed data. This calibration process is named history matching (Cavalcante et al., 2017). It is performed by means of a trial and error method of adjusting model parameters until an acceptable match is achieved. Accordingly, history matching is the most time-consuming, expensive, and often frustrating step over numerical simulation of a process. Therefore, the assisted history matching techniques has been introduced. In this approach, the simulated data is verified by measured data through an objective function. History matching is defined as an optimization problem in which objective function is solved based on boundary conditions (Amini and Mohaghegh, 2019; Shahkarami et al., 2015).

A group of parameters are selected for numerical model as the base values and the parameter variations. Over history matching process, the base values are taken fixed, but the parameter variations are modified to achieve a good match numerical results with real data (Klump et al., 2011).

History matching involves the modification of uncertain parameters of model to reproduce the real results. The purpose of history matching process is handling uncertain parameters in the model calibration to reproduce results closer to observed

data. Consequently, it can be used to analyze mechanisms involving in a process and predict performance of a system in different conditions (Rai et al., 2015).

Numerical model is the significant tools for studying thermal transport (heat transfer) over cold water injection and solute transport (mass transfer) over tracer solution injection in a single fractured core plug. The comparison of experimental and simulated data makes it possible to get information about the properties of matrix-fracture transfers, and transport and flow parameters in the single fracture-matrix systems. In general, a numerical simulation model should be calibrated to determine a valid set of parameters providing the model to predict flow and matrix-fracture transfers in fractured porous media for different flooding scenarios (Amini and Mohaghegh, 2019). In addition to model verification, the calibrated model can be used to understand more about the properties of samples.

CHAPTER 5

THERMAL TRANSPORT IN SINGLE FRACTURE-MATRIX SYSTEMS

5.1. Theory

5.1.1. Heat Transfer Mechanisms

Heat transfer can be described as exchange of thermal energy (heat) because of temperature gradient between physical systems while heat flux can be defined as the amount of heat passing through a unit area per unit time. It is a vector quantity that its magnitude is proportional to the magnitude of temperature difference (Bird et al., 2002; Incropera and DeWitt, 2002).

Thermal transport process is classified into three different kinds of modes (Bird et al., 2002; Incropera and DeWitt, 2002):

 (i) Conduction

Heat conduction is transfer of thermal energy due to either random molecular motion or due to the motion of free electrons. The driving force is temperature difference for heat conduction, in fact, energy is transferred from more energetic zone to less energetic zone. Conduction is sometimes also called heat diffusion.

Fourier's law is used to explain the conductive heat flux. It illustrates that heat is transferred from an area with higher temperature to area with lower temperature. This law is stated by

$$q_{conduction} = -k\nabla T \qquad (5.1)$$

where q is the conductive heat flux (J min^{-1} cm^{-2}); k is the thermal conductivity (J min^{-1} cm^{-1} °C^{-1}); T is the temperature (°C).

(ii) Convection

Convective heat transfer is any transfer of thermal energy by the bulk motion of fluid. It involves simultaneous occurrence of advection and diffusion mechanisms. Convection can be categorized into two types: natural and forced based on their driving force.

- Natural convection: It refers to fluid movement which naturally occurs by buoyancy differences (density differences).
- Forced convection: It refers in which the fluid is made to flow by some external agent like pump and fan etc.

The convective heat transfer occurs generally in system involving a solid surface in contact with a flowing fluid. The rate of the convective heat transfer is proportional to temperature difference between solid surface and fluid. The convective heat flux can be described by Newton's law of cooling, writing as

$$q_{convection} = h\,(T_s - T_f)$$

(5.2)

where q is the convective heat flux (J min^{-1} cm^{-2}); h is convective heat transfer coefficient (J min^{-1} cm^{-2} °C^{-1}); T_s and T_f are temperatures of solid surface and flowing fluid (°C).

(iii) Radiation

The radiative heat transfer is caused by electromagnetic radiation. The rate of heat radiation depends mainly on their temperature and surface characteristics.

In radiative heat transfer, objects with differing thermal energies emit or absorb electromagnetic waves/particles (photons). If a photon is absorbed the bodies thermal

energy of the mass increases, if a photon is emitted the thermal energy of the mass decreases. The radiative heat flux can be described by

$$q_{radiation} = \varepsilon F \sigma (T_1^{\ 4} - T_2^{\ 4}) \tag{5.3}$$

where q is the radiative heat flux (J min^{-1} cm^{-2}); σ is Stephan-Boltzmann constant 3.406×10^{-10} (J min^{-1} cm^{-2} °C^{-4}); ϵ is emissivity; F is the view factor; T_1 and T_2 are temperatures of bodies (°C).

5.1.2. Thermal Properties

5.1.2.1. Thermal Conductivity

Thermal conductivity can be defined as the ability of materials to transfer heat. The dimension of thermal conductivity is J S^{-1} m^{-1}K^{-1} in SI system. It is equal to the amount of heat per unit of the area of the surface per unit of time (Incropera and DeWitt, 2002; Lienhard, 2013).

The geologic rocks have a large range of thermal conductivity values because thermal conductivity of rocks depend on temperature, pressure, porosity, composition of rock and pore-filling fluids, namely, the values of thermal conductivity range widely for rocks and pore-filling fluids. In fact, thermal conductivity of all pore-filling fluids is lower than that of rocks. This makes that the overall thermal conductivity decreases with increasing porosity (Narasimhan, 2013). The effect of porosity on thermal conductivity is shown in Figure 5.1.
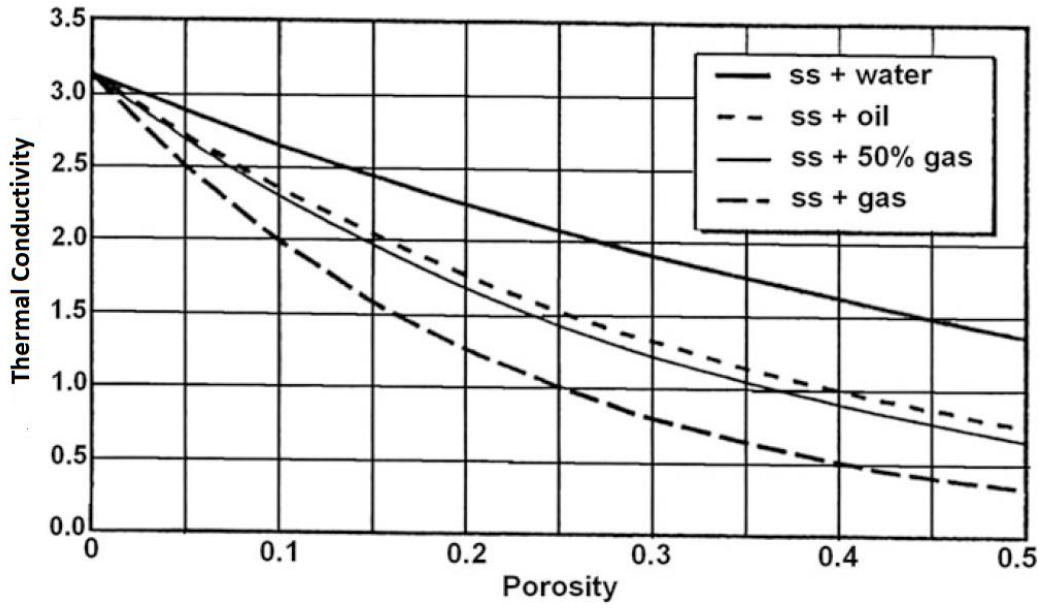
Figure 5.1. The effect of porosity on thermal conductivity of a sandstone with different pore-filling fluids at ambient temperature and pressure (Narasimhan, 2013).

The dependency of thermal conductivity of a porous rock on porosity and fluid saturation was described by a series of "mixing law" equations and given thermal conductivity values of solid rock and pore-filling fluids (Kaviany, 1995; Narasimhan, 2013).

The minimum value of thermal conductivity can be calculated by the weighted harmonic mean of the two conductivities (Nield and Bejan, 2006):

$$k_{\min} = \frac{k_s k_f}{\left[\phi k_s + (1-\phi)k_f\right]} \tag{5.4}$$

Where Ø is rock porosity; k_s and k_f are thermal conductivity of solid rock and pore-filling fluids

The maximum value of thermal conductivity can be expressed as the weighted arithmetic mean of the two conductivities (Nield and Bejan, 2006):

$$k_{\max} = \phi k_f + (1 - \phi) k_s \tag{5.5}$$

Also, the thermal conductivity of porous rock can be described using geometric mean (Nield and Bejan, 2006):

$$k_{geo} = k_f{}^{\phi} k_s{}^{1-\phi} \tag{5.6}$$

In general, the mathematical models proposed indicate the following order of different thermal conductivities:

$$k_{harmonic} < k_{geometric} < k_{arithmetic} \tag{5.7}$$

The extensive studies show that there are many correlations between temperature and thermal conductivity measurements in rocks. Thermal conductivity is mainly influenced by temperature variation in rocks with low porosity. The thermal conductivity of most rocks declines by a factor of 1.5 to 4 when temperature increases from 0 to 800 °C. The dependency of thermal conductivity of sedimentary and metamorphic rocks on temperature variation is larger than that of volcanic rocks. However, there are several exceptions to the general trend of decreasing thermal conductivity with temperature. To illustrate, mineralogical structure and compositions in rocks (i.e. feldspar content) cause that thermal conductivity of rocks increases with rising temperature. Thermal conductivity of many rocks are direction-dependent variation. Thermally anisotropic in rocks is due to a dominant orientation of an anisotropic mineral (Kaviany, 1995; Narasimhan, 2013).

5.1.2.2. Heat Capacity

The specific heat capacity is defined as the amount of energy to raise the temperature of a unit of the mass of a matter by 1 degree. It explains the capability of the materials to store heat with dimension in SI: J/kg K. The specific heat can be measured at constant pressure (c_p) or at constant volume (c_v) (Incropera and DeWitt, 2002; Lienhard, 2013).

When there is no chemical reaction and no change in state, the variation in enthalpy (H) with temperature at constant pressure can be expressed by:

$$\partial H = c_p \partial T \tag{5.8}$$

The heat capacity per unit mass of solids, liquids and gases generally increases with temperature and the effect of temperature can be expressed as:

$$c_p = b + cT + fT^2 \tag{5.9}$$

Where c_P is the specific heat at constant pressure and b, c, and f are coefficients.

In addition, the other form of heat capacity is volumetric heat capacity which can be defined as density and specific heat product (ρc_p) with dimension J/m^3K in SI. It describes the ability of a given volume of a material to store internal energy while undergoing a given temperature change, but without undergoing a phase transition. It is different from specific heat capacity in that the volumetric heat capacity is a 'per unit volume' measure of the relationship between thermal energy and temperature of a material, while the specific heat is a 'per unit mass' measure. Studies indicate that the heat capacity of geologic rocks increases with rising temperature at ambient pressure.

5.1.2.3. Thermal Diffusivity

Thermal diffusivity is the ratio of the thermal conductivity of the material to the volumetric heat capacity of the material. In fact, it describes how fast heat can be transferred across the medium with time in transient conditions. The dimension of thermal diffusivity is m^2 /s in SI (Incropera and DeWitt, 2002; Lienhard, 2013).

$$\alpha = \frac{k}{\rho c_p}$$
(5.10)

Where α, k, ρ, and c_p are thermal diffusivity, thermal conductivity, density, and specific heat capacity respectively.

Greater the value of thermal diffusivity, faster is the propagation of heat through the medium. This will result either due to a high value of conductivity or a low value of volumetric heat capacity (Kaviany, 1995).

5.1.3. Convective Heat Transfer Coefficient

When the fluid circulates over a solid surface, the challenging issue to analyze heat transfer at solid-fluid system is the heat conduction problem within solid coupled with the heat convection problem on the fluid side. The introduction of the convective heat transfer coefficient makes it simple to evaluate the rate of heat transfer between solid surface and flowing fluid (Bird et al., 2002). Therefore, convective heat transfer coefficient can be used to quantify the amount of heat exchange at solid-fluid systems.

Convective heat transfer coefficient is a proportionality constant to correlate convective heat flux and temperature difference between solid surface and flowing fluid that is driving force for heat exchange. It is used to calculate convection heat transfer between solid surface and surrounding fluid. Convective heat transfer

coefficient can be defined as the rate of heat flux between a solid surface and a flowing fluid per unit surface area per unit temperature difference (Zhao, 1992).

$$h = \frac{q}{(T_s - T_f)}$$ (5.11)

where q is convective heat flux (J min^{-1} cm $^{-2}$); h is convective heat transfer coefficient (J min $^{-1}$ cm $^{-2}$ °C); Ts and T_f are temperatures of solid surface and flowing fluid (°C).

In general, convective heat transfer coefficient is an experimentally determined parameter, depending on all the variables involved in convection such as fluid properties, geometry of solid surface, and bulk fluid velocity (Nield and Bejan, 2006).

At solid-fluid interface, the convective heat transfer coefficient depends on the properties of flowing fluid, geometry of solid-fluid interface, and temperature difference between solid surface and surrounding fluid. In practice, the temperature of solid surface can be crucial in assigning temperature difference at solid-fluid interface, in turn, the convective heat transfer coefficient (Zhao, 1992).

5.1.4. Thermal Transport in Fractured Porous Media

The substantial variations in rock properties such as permeability and porosity across matrix and fracture make fractured porous media as a complicated structure for analysis of matrix-fracture transfers. The matrix-fracture system consists of matrix with low permeability acting as a storage and fracture with high permeability providing path for fluid flow (Kaviany, 1995; Narasimhan, 2013).
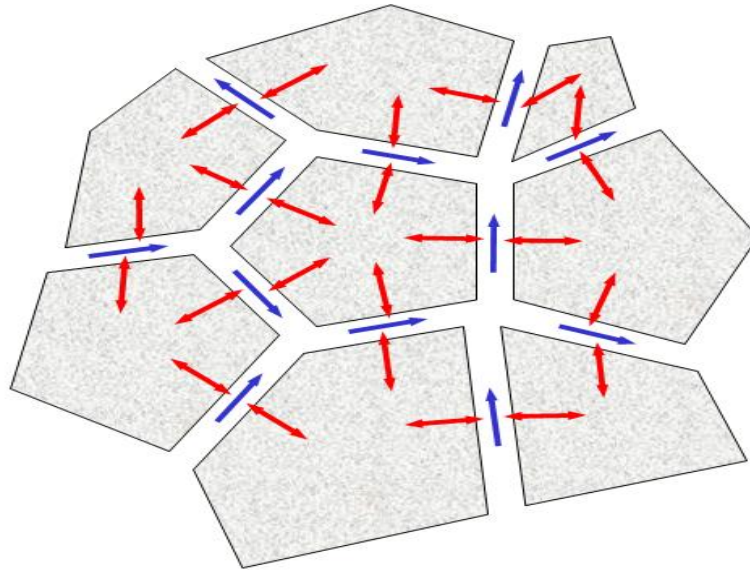
Figure 5.2. Matrix-fracture transfers

In fractured formations, matrix-fracture heat transfer is important in thermal transport processes such as enhanced geothermal systems (EGS) for recovery and extraction thermal energy and enhanced oil recovery (EOR). Matrix-fracture heat transfer has a pivotal role in accomplishing enhanced geothermal systems (thermal transport from hot dry rocks to flowing fluid in fracture by cold water injection) and thermal oil recovery processes (thermal transport from fracture to rock matrix by hot water and steam injection) (Martinez et al., 2014). The analysis of thermal transport in fracture-matrix systems needs a comprehensive understanding of conductive heat transfer within matrix, convective heat transfer along matrix-fracture interface, and fluid flow through fracture (Abbasi et al., 2017; Shaik et al., 2011).

The equations involved in the analysis of thermal transport in fractured porous media are continuity as well as momentum and energy equations, respectively (Bird et al., 2002).

$$\frac{\partial \rho}{\partial t} + \nabla \bullet (\rho u) = 0 \tag{5.12}$$

$$\rho(\frac{\partial u}{\partial t} + u\nabla u) = -\nabla P + \mu \nabla^2 u + F \tag{5.13}$$

$$\rho c_p (\frac{\partial T}{\partial t} + u\nabla T) = k\nabla^2 T + Q \tag{5.14}$$

Where u, T, t, P, F, and Q are velocity, temperature, time, pressure, body force, and heat generation, respectively. The symbols ρ, μ, c_p and k represent the physical properties of density, dynamic viscosity, specific heat capacity and thermal conductivity. In the case of heat flow in a solid, the velocity is neglected, and the equation reduces to the conduction equation.

$$\rho c_p (\frac{\partial T}{\partial t}) = k\nabla^2 T + Q \tag{5.15}$$

Thus, the reasons for the fact that convective heat transfer coefficient is considered as a representative of the amount of heat exchange in matrix-fracture systems are as follow;

Firstly, the analysis of matrix-fracture heat transfer to assess the heat exchange through matrix- fracture interface involves the understanding of convective heat transfer that is the combination of fluid flow in fracture and heat transfer mechanisms in matrix and fracture (Zhao, 1992).

In addition, there exists temperature difference between matrix grains and pore-filling fluids at the pore-scale. Although this temperature difference is relatively small, it can be considered in the case of rapid thermal transients and highly concentrated heat sources in one phase but not the other phase (Narasimhan, 2013).

In homogeneous porous media where fluids move quite slowly, local thermal equilibrium (LTE) between solid and fluid phases makes it simple to determine an effective thermal conductivity without any need for separately examining heat conduction in the solid and fluid although in fractured porous media, fluid in fracture is assumed to be in thermal equilibrium with the fracture surface (matrix-fracture interface) despite the temperature gradient within matrix (Narasimhan, 2013).

At the local thermal non-equilibrium (LTNE), temperature difference between fluid and matrix exists and two energy equations are used to describe heat transfer in matrix-fracture systems. In fact, this theory is an appropriate and real theory to analyze thermal transport in matrix-fracture systems. It makes the convective heat transfer coefficient as a significant parameter for understanding thermal transport in matrix-fracture systems (Jiang and Ren, 2001).

5.1.5. Conceptual and Mathematical Model of Thermal Transport in Fractured Porous Media

Mathematical modelling can be used for effective analysis of matrix-fracture transfer processes. The heat transfer is by vertical conduction in the matrix and by forced convection along the y- axis within the fracture. The heat conduction in the core plug was modelled as 1- dimensional and perpendicular to the fracture surface in z-direction. The fracture is a horizontal plane penetrating the entire length of the core sample (y-axis) (Cheng et al., 2001).

In order to facilitate understanding of thermal transport in fractured porous media, cold water injection through the single fractured core plug was studied. The assumption of local thermal non-equilibrium (LTNE) provides the analysis of matrix-fracture heat transfer by coupling heat transfer mechanisms in matrix and fracture as well as flowing fluid in fracture (Zhao, 2014). In this process the matrix as a heat storage supplies heat source while the fracture provides a pathway to remove heat from rock fracture surface by circulating fluid for transport (Figure5.3).
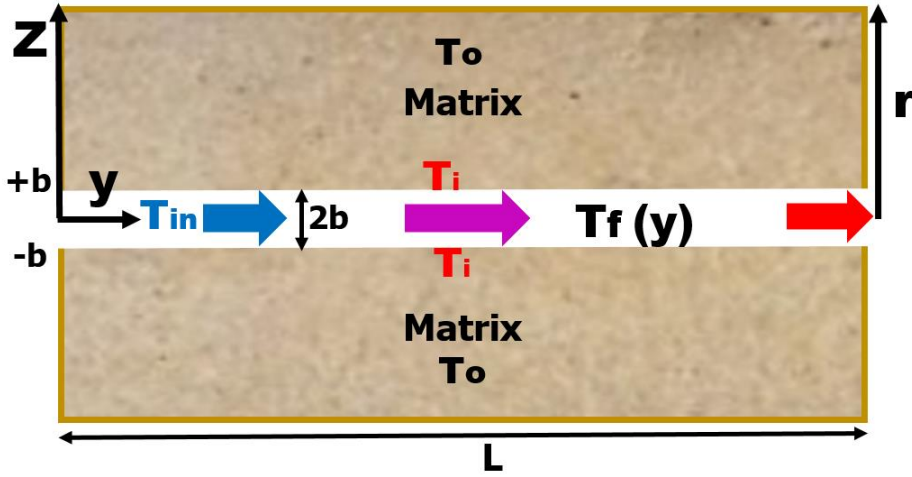
Figure 5.3. A sketch of a single matrix-fracture system in thermal transport process

To quantify thermal front propagation across the single matrix- fracture system as a result of heat transfer along matrix-fracture interface, heat transport in fracture and matrix can be divided by the two PDEs.

The heat transfer mechanisms involving in the fracture are advection, dispersion, conduction and convection from fracture surfaces. The Eq. (5.16) represents the heat transfer in the fracture (Cheng et al., 2001; Zhao, 2014):

$$\frac{\partial T_f(y)}{\partial t} + u\frac{\partial T_f(y)}{\partial y} - D_L\frac{\partial^2 T_f(y)}{\partial y^2} - \alpha_W\frac{\partial^2 T_f(y)}{\partial y^2} - \frac{k_m}{\rho_w c_{p,w} b}\frac{\partial T_m(y,z,)}{\partial z}\Big|_{z=\pm b} = 0 \qquad (5.16)$$

Where D_L is the longitudinal thermal dispersion coefficient; α_W is the water thermal diffusivity; k_w, ρ_W, and $c_{p,w}$ are the water thermal conductivity, water density, and water specific heat capacity respectively; k_m is the matrix thermal conductivity; u is the water velocity in the fracture; b is the half aperture of fracture; T_m and T_f are the temperatures of matrix and bulk water in fracture.

The heat conduction within rock matrix as a dominant heat transfer mechanism can be described by Eq. (5.17):

$$\frac{\partial T_m(y,z)}{\partial t} = \alpha_m\frac{\partial^2 T_m(y,z)}{\partial z^2} \qquad (5.17)$$

32

Where α_m is matrix thermal diffusivity.

The single fractured core plugs including the fracture in y- direction were manufactured to study heat transfer between matrix and fracture fluid. With consideration of small and negligible dispersion effects, energy balance over the fracture in steady state conditions yields

$$u\frac{\partial T_f(y)}{\partial y} - \alpha_W \frac{\partial^2 T_f(y)}{\partial y^2} - \frac{k_m}{\rho_w c_{p,w}\, b}\frac{\partial T_m(y,z,)}{\partial z}\Big|_{z=\pm b} = 0 \tag{5.18}$$

In addition, it was assumed that heat conduction within rock matrix is only carried out in z direction, perpendicular to the fracture plan. The steady thermal conduction is as follows;

$$\frac{\partial^2 T_m(y,z)}{\partial z^2} = 0 \tag{5.19}$$

Analytical solutions to Eqs. (5.18) and (5.19) with regard to the following initial and boundary conditions given between Eq. (5.20) through Eq. (5.23) for single matrix-fracture system under these assumptions that water temperatures in fracture and fracture surface to be in an identical value makes it possible to calculate outlet temperature and have temperature profile along fracture (6.24).

$$T_f(y=0) = T_{in} \tag{5.20}$$

$$T_f(y=\infty) = T_o \tag{5.21}$$

$$T_m(y,r) = T_o \tag{5.22}$$

$$T_m(y,b) = T_f(y) \tag{5.23}$$

An analytical model was used to predict the steady temperature profiles of water in the fracture plane.

$$T_f(y) = T_o + (T_{in} - T_o)\exp\left[\frac{y}{2}\left(\frac{u\rho_w c_{p,w}}{k_W} - \sqrt{\left(\frac{u\rho_w c_{p,w}}{k_W}\right)^2 + \frac{4k_m}{brk_W}}\right)\right] \qquad (5.24)$$

If water thermal diffusion (α_w) is negligible, analytical model for prediction of temperature along fracture in steady state conditions without water thermal diffusivity can be simplified as follow (Zhao, 2014):

$$T_f(y) = T_o + (T_{in} - T_o)\exp\left(-y\frac{k_m}{u\rho_w c_{p,w} br}\right) \qquad (5.25)$$

5.1.6. Calculation of Convective Heat Transfer Coefficient

The analysis of thermal transport in matrix-fracture systems based on local thermal non-equilibrium (LTNE) assumption can be appropriate using Newton's cooling law in Eq. (5.2). Therefore, it seems the convective heat transfer coefficient to be useful to determine overall amount of heat exchange in matrix-fracture systems (Heinze et al., 2017). In the recent studies, the convective heat transfer coefficient was calculated by energy balance and analytical model.

5.1.6.1. Energy Balance

Over cold water injection through the single fractured core plug, heat transfer between hot matrix and flowing cold fluid in fracture causes decrease in temperature of core plug's inner surface (fracture surface temperature). Therefore, the temperature difference between outer surface and fracture surface in core plug contributes to heat conduction within matrix.

While the outer surface of core plug was held at constant temperature (T_o), the average temperature of fracture surface (T_i) due to anisotropy in the fracture surface temperature was taken into account in calculating convective heat transfer coefficient (Zhang et al., 2015).

The average temperature of fracture surface (T_i) can be calculated by analytical solution of heat conduction equation in cylindrical coordinates (Eq. 5.26). An half of the cylindrical core plug is assumed due to symmetry (Figure 5.4) (Bird et al., 2002).

$$k\left[\frac{1}{r}\frac{\partial}{\partial r}(r\frac{\partial T}{\partial r})+\frac{1}{r^2}\frac{\partial^2 T}{\partial \theta^2}+\frac{\partial^2 T}{\partial y^2}\right]=\rho c_p \frac{\partial T}{\partial t} \qquad (5.26)$$

As the boundary conditions are complicated and dynamic, a semi-circle section of model is used to analyze heat conduction and calculate the average temperature of fracture surface (T_i) through the transformation of cylindrical coordinates to rectangular coordinates and integral for temperature field (Zhang et al., 2015):

Assumption: $\dfrac{\partial T}{\partial y}=0$, $\dfrac{\partial T}{\partial t}=0$, $T=T(r,\theta)$ \qquad (5.27)
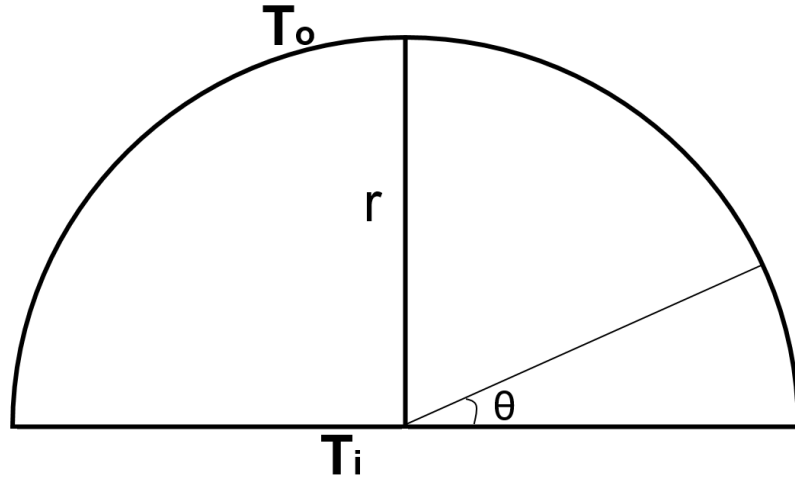
Figure 5.4. Semi-circle section of the model

$$\frac{\partial^2 T}{\partial r^2}+\frac{1}{r}\frac{\partial T}{\partial r}+\frac{1}{r^2}\frac{\partial^2 T}{\partial \theta^2}=0 \qquad (5.28)$$

BC-1: $r = r_\circ$, $T = T\circ$ (5.29)

BC-2: $\theta = 0$, $\theta = \pi$, $T = T_i$ (5.30)

The analytical solution of heat conduction to calculate the average temperature of fracture surface of core plug (T_i) as follow (Zhang et al., 2015):

$$T_i = T_o - \frac{\pi c_{p,w} m^\bullet (T_{out} - T_{in})}{42.32kL}$$ (5.31)

Where $c_{p,w}$ is the specific heat capacity of water (J/Kg °C); $m^\bullet$ is the water mass flow rate (kg/s); T_{in} and T_{out} are water inlet and outlet temperatures (°C); k is thermal conductivity of rock matrix (W/m °C); L is length of core plug (m).

The overall steady energy balance in the single fractured core plug (Zhao and Tso, 1993):

| Heat conduction | = | Heat convection | = | Heat removed by fluid |
| within matrix | | at matrix-fracture interface | | flow through fracture (5.32) |

The heat removed by the water flow, as:

$$q = c_{p,w} m^\bullet (T_{out} - T_{in})$$ (5.33)

Also, the heat convected out of the fractured surfaces can be calculated by:

$$q = h(2A)(T_i - T_f)$$ (5.34)

$$T_f = \frac{T_{in} + T_{out}}{2}$$

(5.35)

The overall energy balance in the single fracture-matrix system can be used to calculate the convective heat transfer coefficient using temperatures of fracture inlet and outlet at steady state conditions (Zhao and Tso, 1993):

$$h = \frac{c_{p,w} m^{\bullet} (T_{out} - T_{in})}{2A(T_i - (\frac{T_{in} + T_{out}}{2}))}$$

(5.36)

where h is the convective heat transfer coefficient (J/min cm^2 °C); T_i and T_f are average temperature of fracture surface of core plug and water mean temperature in fracture (°C), respectively.

5.1.6.2. Analytical Solution of Heat Transfer Equation

With consideration of a constant heat transfer coefficient, steady heat transport in the fracture is governed by Eq. (5.37) (Zhao, 2014):

$$u \frac{\partial T_f(y)}{\partial y} - \alpha_w \frac{\partial^2 T_f(y)}{\partial y^2} - \frac{h}{\rho_w c_{p,w} b} \left[T_m(y,b) - T_f(y) \right] = 0$$

(5.37)

Similarly, analytical solutions to Eqs. (5.19) and (5.37) in boundary conditions of fracture surface Eq. (5.38) with assumption of constant convective heat transfer coefficient and negligible thermal diffusivity of water makes it possible to calculate convective heat transfer coefficient at fracture outlet with known water outlet temperature by Eq. (5.39).

$$- k_m \frac{\partial T_m(y,z)}{\partial z} \Big|_{z=b} = -h \left[T_m(y,b) - T_f(y) \right]$$

(5.38)

$$h = -\frac{u\rho_w c_{p,w} b k_m \ln \dfrac{T_f(y)-T_o}{T_{in}-T_o}}{y k_m + u\rho_w c_{p,w} b r \ln \dfrac{T_f(y)-T_o}{T_{in}-T_o}} \qquad (5.39)$$

5.2. Cold Water Injection Experiments

The cold water injection experiments were carried out to study thermal transport in the single fracture-matrix system. The main objective of cold water injection experiments is measuring the transient values of fracture temperature and heat flux at matrix-fracture interface by heat flux sensor for analysis of thermal transport in single fracture-matrix systems. The experimental measurements of fracture temperature were used to derive thermal properties of matrix by matching the experimental data to the simulation model of thermal transport.

5.2.1. Single Fracture-Matrix System

In present study, four artificial fractured core plugs including heat flux sensor to measure heat flux and fracture temperature were used to conduct cold water injection experiments (Figure 5.5). The physical properties of core plugs were given in the Table 3.1.
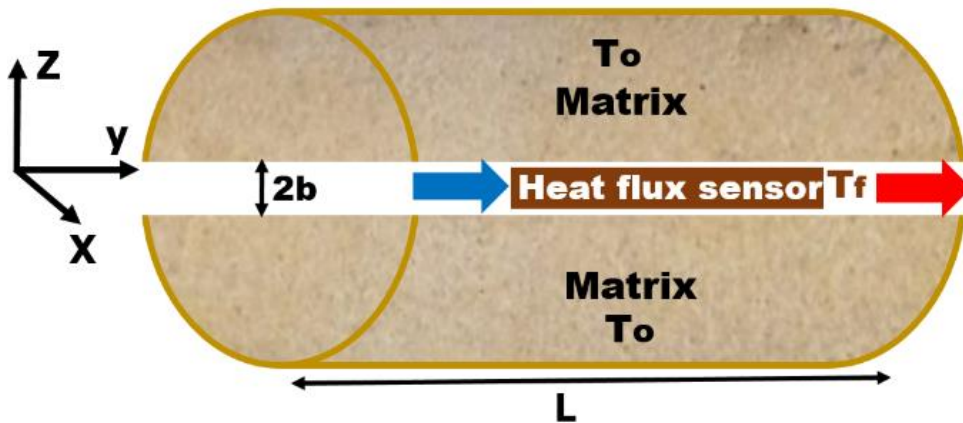
Figure 5.5. Cold water injection experiments

5.2.2. Experimental Procedure

In all experiment runs cold water is injected into fractured core assembly at one end with temperature of (T_{in}) at constant flow rate by a ISCO pump and accumulated from the other end in production collector system. The position of fracture plane and direction of flow is horizontal in all runs.

Over all flooding processes, the temperature of the rock sample's outer surface was maintained at constant temperature of 70 and 90 ºC (T_o) by using a water bath. When the desired initial temperature of core sample of 70 or 90 ºC is measured by heat flux sensor within fracture, this temperature is kept constant for at least an hour to guarantee that the whole core plug is heated up at constant and uniform temperature conditions.

After reaching a steady state temperature within core sample, cold water is injected at different flow rates and injection temperatures for 30 minutes. The inlet cap is connected to a ISCO pump through the injection line. The injection line contains a thermocouple to measure the water inlet temperature(T_{in}) before entering fractured core assembly. On the other hand, the other end of fractured core assembly is connected to production collector system through production line. Water leaves the fractured core, accumulating in the production collector system. Experimental measurement of the fracture temperature and water inlet temperature in addition to heat flux between matrix and fracture are recorded in time interval 1 minutes by means of digital data logger over the experiment runs.

5.3. Results and Discussion

In this current study matrix-fracture thermal transport was analyzed by different methods including experimental measurements, analytical model, and numerical simulation. It is necessary to mention that all flow-through runs were carried out at outer temperatures (T_o) 70 and 90 °C.

5.3.1. Experimental Measurements

The temperature and heat flux in fracture were experimentally measured by the thin film type heat flux sensor for outer temperatures (T_o) 70 and 90 °Cover cold water injection. The experimental measurements of temperature in fracture for core plugs # 1 and # 3 in different flow rates (1,5,10, and 15 cc/min) and outer temperatures were illustrated in the Figures 5.6 and 5.7. The transient temperature decrease in fracture for core plugs # 8 and # 10 over cold water injection are given in appendices section.
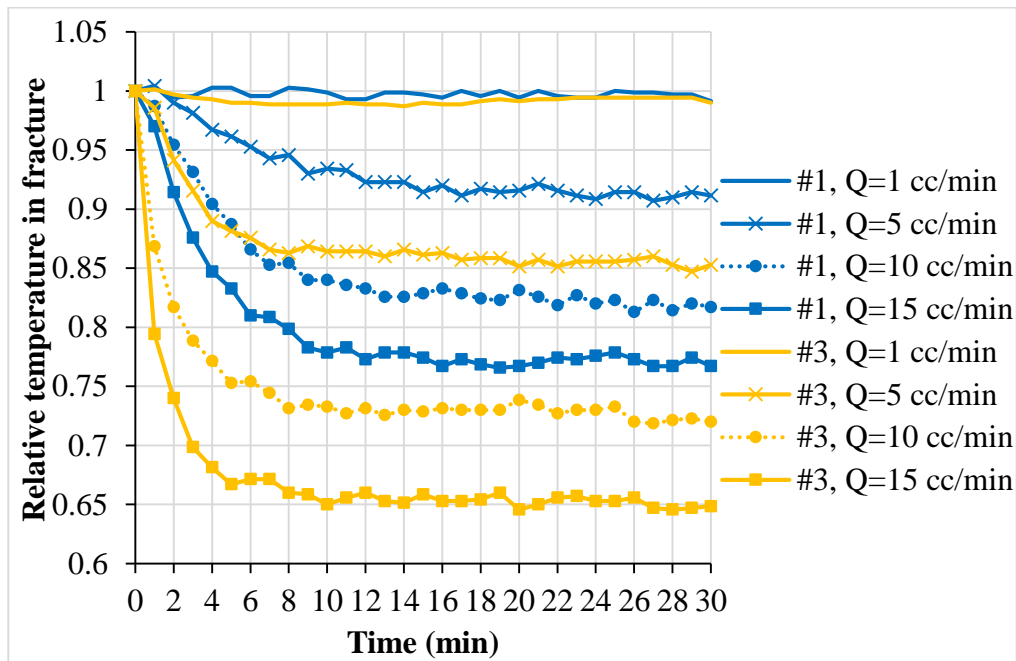
Figure 5.6. Experimental relative temperature decrease in fracture at outer temperature 70 °C

40
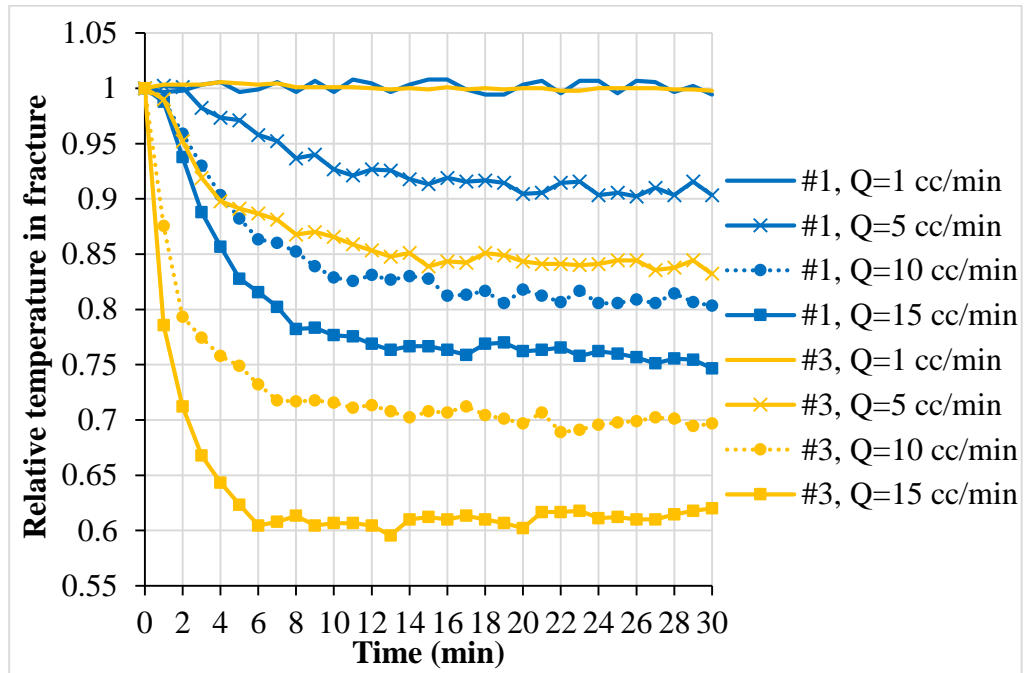
Figure 5.7. Experimental relative temperature decrease in fracture at outer temperature 90 °C

As can be observed from Figures 5.6 and 5.7 that temperature in fracture decreases with increasing flooding duration. This can be as a result of heat swept over fracture surface, contributing to temperature drop in matrix-fracture interface over cold water injection for single fractured core plugs. In spite of the fact that the temperature drop in fracture is considerable in the early time, matrix as a supportive source provides sufficiently heat for fluid within fracture to compensate the heat loss of flowing fluid in fracture by advection at matrix-fracture systems. Therefore, it makes fracture temperature to be constant value in the rest of experiment period. These transient changes in fracture temperature were followed by a period of stability as temperature hovered around a steady state value in fracture for all core plugs. Since heat transfer between matrix and fluid in fracture reaches equilibrium after a certain period of cold water injection. Also, the temperature in fracture declines faster with increasing in injection rate for core plugs # 1,3,8, and 10.

In addition, Figures 5.8 and 5.9 indicate the transient values of heat flux measured experimentally in different injection rates and outer temperature 70 and 90 °C for core plugs # 1 and #3 over cold water injection. The experimental values of heat flux at matrix-fracture interface for core plugs # 8 and # 10 over cold water injection are given in appendices section.
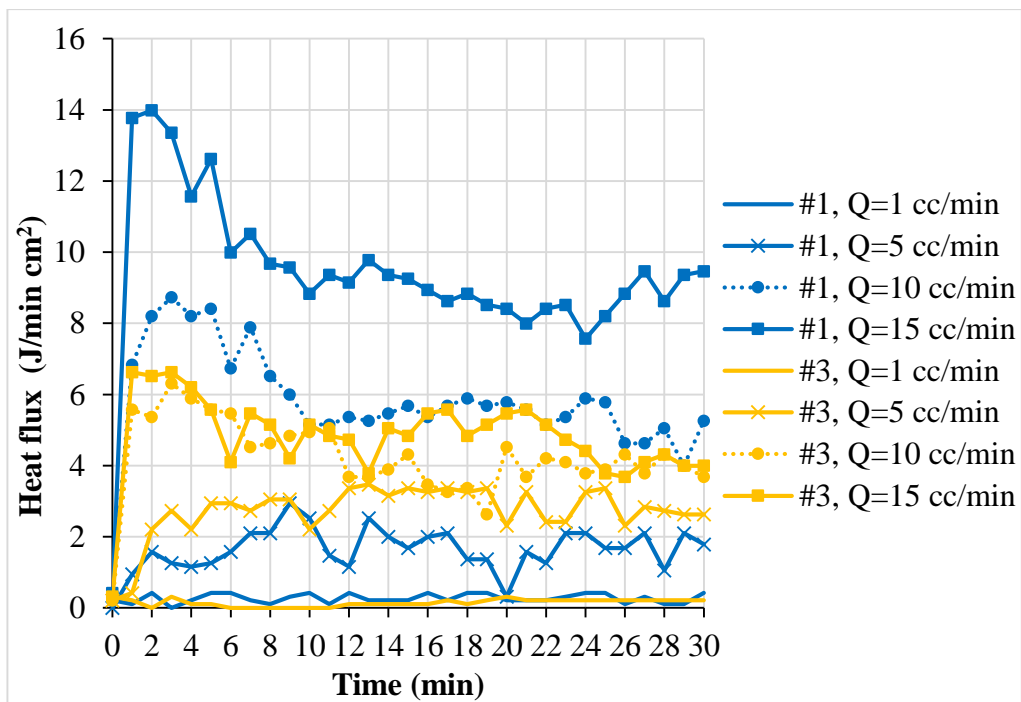
Figure 5.8. Experimental heat flux at matrix-fracture interface at outer temperature 70 °C
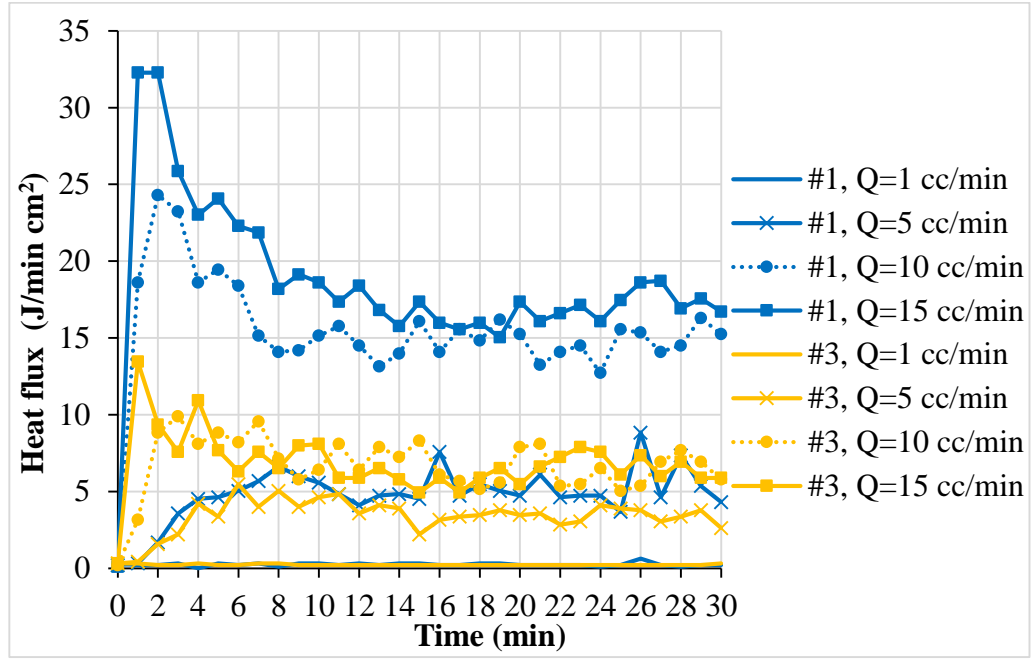
Figure 5.9. Experimental heat flux at matrix-fracture interface at outer temperature 90 °C

As revealed by experimental measurements of heat flux over matrix-fracture interface, the drastic increase in the amount of heat flux in the early time of cold water injection can be due to high temperature difference between fracture surface and fluid in fracture in the first stage. However, with continuing cold water injection, the amount of heat flux experiences a decrease trend. The cold water removes heat over solid-fluid interface, temperature difference decreases and makes fracture surface colder. Therefore, the amount of heat flux declines with reduction in temperature difference over the flooding period.

Moreover, it can clearly be seen that the heat flux increases at the matrix-fracture interface with a rise in flow rate. Because of large volume of cold water contacting fracture at a given time in the case of high injection rate, the temperature increase of flowing water in the fracture declines. In other words, flowing water in fracture is not warmed more, which increases the temperature difference between fluid in fracture and fracture surface as well as the heat flux over matrix-fracture interface.

43

However, there are similar oscillatory trends in heat flux values with increasing flow rate similar to those observed in temperature measurements. Eventually, the amplitude of these oscillations decrease as the injection process progresses.

In fact, the large temperature difference in solid-fluid interface makes a higher heat exchange between rock matrix and fluid in fracture. Figure 5.9 indicates that the extent of heat flux increases with rising matrix temperature at 90 °C due to large temperature difference. The steady experimental values of temperature in fracture and heat flux are given in the Tables 5.1 and 5.2.

Table 5.1. *Experimental thermal values measured in Steady State conditions at outer temperature 70 °C*

Core plug	Volumetric flow rate (Q), cm³/min	Injected pore volume	Injection temperature (T_{in}), °C	Heat flux, J/min cm²	Temperature in fracture (T_f), °C
#1	1	2.14	31.9	0.28	69.7
	5	10.68	31.7	1.80	64.0
	10	21.37	31.6	5.32	57.6
	15	32.05	31.6	8.90	54.1
#3	1	2.04	32.1	0.21	69.5
	5	10.18	31.9	2.94	60.0
	10	20.37	31.6	3.82	51.0
	15	30.55	31.5	4.70	45.7
#8	1	2.42	31.8	0.31	69.7
	5	12.10	31.3	0.69	62.4
	10	24.19	31.4	1.35	53.6
	15	36.29	31.5	1.89	48.6
#10	1	2.17	31.9	0.31	69.6
	5	10.87	31.5	2.05	61.2
	10	21.74	31.4	1.82	53.3
	15	32.61	31.4	2.79	47.4

Table 5.2. *Experimental thermal values measured in Steady State conditions at outer temperature 90 °C*

Core plug	Volumetric flow rate (Q), cm³/min	Injected pore volume	Injection temperature (T in), °C	Heat flux, J/min cm²	Temperature in fracture (Tf), °C
#1	1	2.14	31.6	0.25	89.9
	5	10.68	30.9	5.37	81.7
	10	21.37	31.1	14.73	72.9
	15	32.05	30.8	16.77	68.5
#3	1	2.04	31.2	0.23	89.9
	5	10.18	30.6	3.35	75.8
	10	20.37	30.5	6.53	63.0
	15	30.55	30.5	6.26	55.0
#8	1	2.42	31.4	0.30	89.9
	5	12.10	30.5	2.94	80.3
	10	24.19	30.6	4.25	66.9
	15	36.29	30.6	4.65	59.3
#10	1	2.17	31.3	0.38	89.9
	5	10.87	30.6	8.26	75.8
	10	21.74	30.6	16.97	61.5
	15	32.61	30.6	20.19	55.1

Tables 5.1 and 5.2 indicate the steady state values of temperature in fracture and heat flux at matrix-fracture interface for various pore volumes injected measured experimentally at outer temperatures of 70 and 90 °C. As can clearly be seen that in all core plugs, the amount of heat flux increase with a rise in flow rate while there is a decrease trend in temperature of fracture in both outer temperatures. Even though

this trend is similar in all core plugs, the magnitude of these changes are various in different temperatures and core plugs.

In continue, sensitivity analysis by numerical model makes it possible to describe matrix-fracture heat transfer and clarify the parameters involved in thermal transport with respect to different core plugs (Baston et al., 2010).

5.3.2. Calibration of Numerical Model for Thermal Transport

The experimental measurements of temperature in fracture during cold water injection experiments were taken as the basis for numerical simulation. The history matching of thermal transport simulation model in the single fractured core plugs was carried out using CMG-STARS simulator to reproduce the transient temperatures in fracture similar to the trends measured experimentally. However, the analytical solution of heat transfer equation for the single fracture-matrix systems provides only the steady temperature profiles along fracture rather than the transient temperatures in fracture.

To calibrate numerical model of thermal transport, matrix porosity, matrix permeability, capillary pressure, and initial temperature were assigned to be fixed values. In contrast, fracture porosity, fracture permeability, matrix volumetric heat capacity, and matrix thermal conductivity are the parameter variations for history matching the numerical results with experimental measurements of fracture temperature by iterative modification.

Figs 5.10-5.13 indicate that the transient temperature decrease in fracture were obtained through experimental measurements and matched by numerical simulation for core plugs #1 and #3 to compare at both outer temperatures 70 and 90 °Cover cold water injection. Also, the history matchings of fracture temperatures for core plugs #8 and #10 are given in appendices section.

The figures of transient temperature in fracture at outer temperatures 70 and 90 °C show that there is a decline trend in fracture temperature with a rise in flow rate for

both experimental measurement and numerical model. Namely, the higher flow rate, the more heat can be removed by advection in fracture.
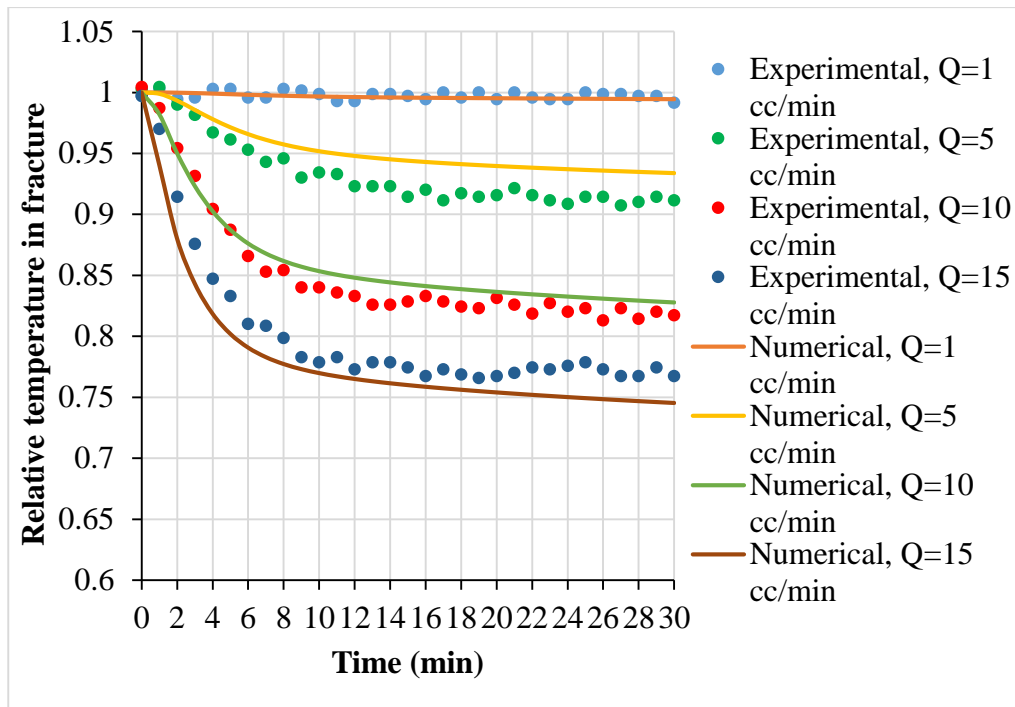
Figure 5.10. History matching of temperature in fracture for core plug #1 at outer temperature 70°C
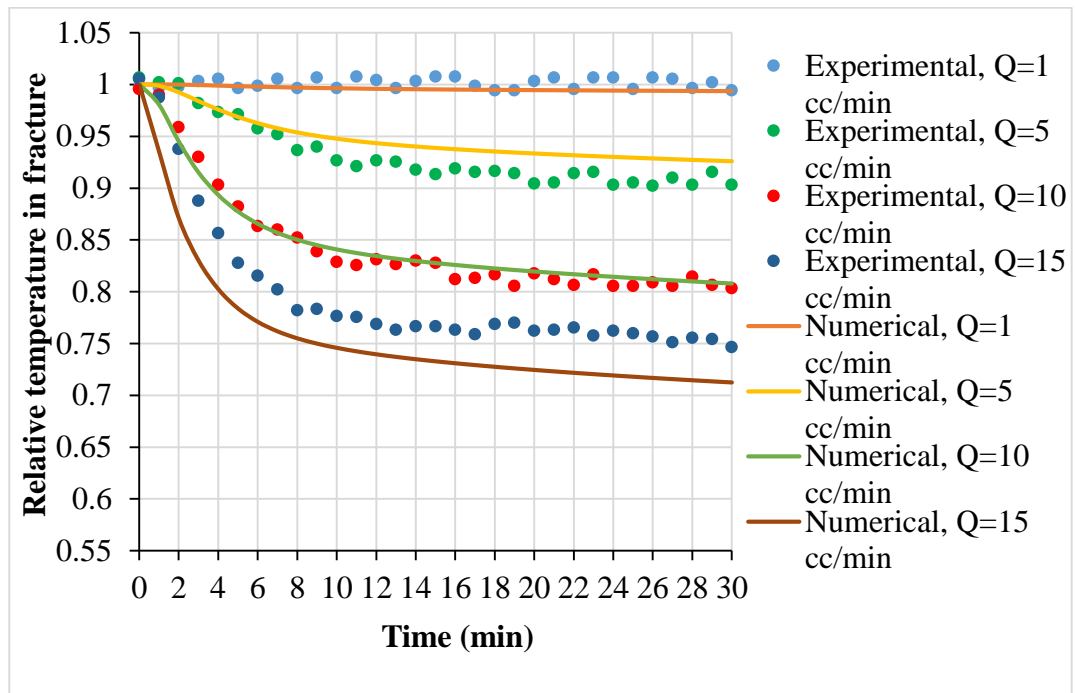
Figure 5.11. History matching of temperature in fracture for core plug #1 at outer temperature 90°C
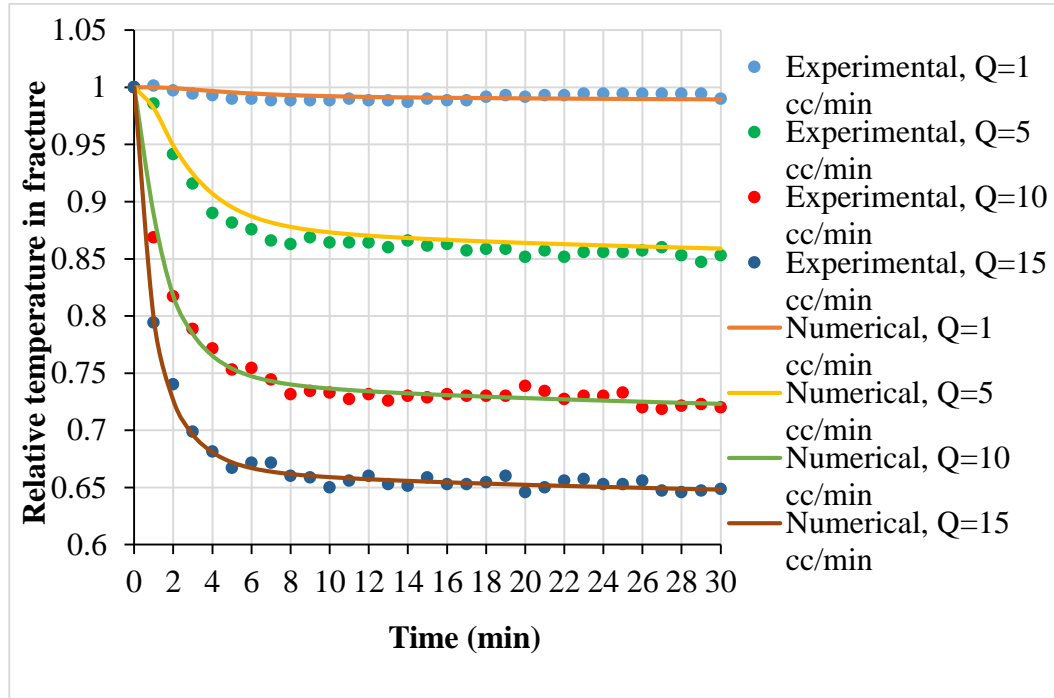
Figure 5.12. History matching of temperature in fracture for core plug #3 at outer temperature 70°C

49
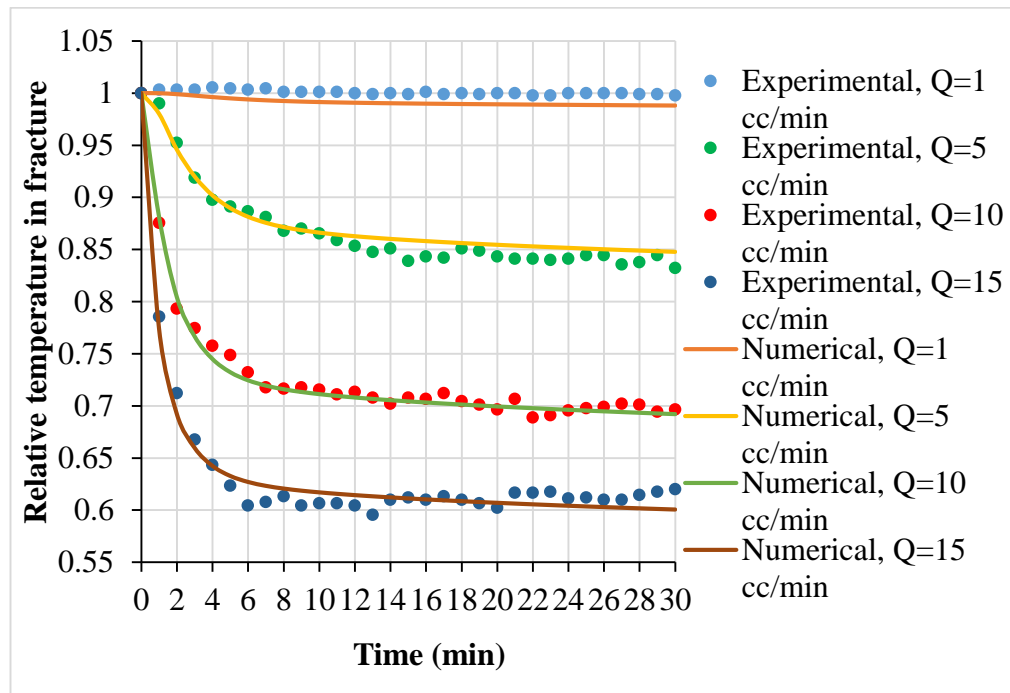
Figure 5.13. History matching of temperature in fracture for core plug #3 at outer temperature 90°C

The graphs illustrate that the simulation results for the fracture temperature coincide very well with the experimental ones at outer temperatures 70 and 90 °C. This proves that our modeling framework is working well. A comparative analysis of measured and simulated results gives information about the properties of matrix-fracture transport and flow in the single fractured core plugs investigated.

The important thermal properties such as volumetric heat capacity and thermal conductivity for matrix were determined by history matching in addition to the porosity and permeability values for fracture and sensor within fracture at outer temperatures 70 and 90 °C. Some important parameters used for calibration of numerical model are given in the Table 5.3. The calibrated model makes it possible to evaluate the major contributing thermal properties of matrix in investigation of matrix-fracture heat transfer and the thermal front propagation along fracture and predict

temperature distribution within rock matrix with various thermal and physical properties.

Table 5.3. *The history matching parameters used for calibration of the numerical simulation model*

	Parameters	Value	
	Fracture porosity (%)	90	
	Fracture permeability (md)	9000	
	Sensor porosity (%)	40	
	Sensor permeability (md)	7000	
	Water density (kg/cm^3)	0.001	
	Water thermal conductivity(J/min cm °C)	0.4	
Core plug	Outer temperature (°C)	70	90
#1	Matrix volumetric heat capacity (J/cm^3 °C)	12	14
	Matrix thermal conductivity (J/min cm °C)	3.5	4.5
#3	Matrix volumetric heat Capacity (J/cm^3 °C)	5	5.8
	Matrix thermal conductivity (J/min cm °C)	1.9	2.5
#8	Matrix volumetric heat Capacity (J/cm^3 °C)	8	13
	Matrix thermal conductivity (J/min cm °C)	2.5	3.5
#10	Matrix volumetric heat Capacity (J/cm^3 °C)	9	9
	Matrix thermal conductivity (J/min cm °C)	2.3	2.4

The results illustrate that thermal properties are temperature dependent parameters, so the thermal behavior of rock matrix will be different in various temperatures. The history matching implies that matrix thermal properties increase with rising outer temperature.

In view of the calibration of numerical model for having fracture temperature closer to experimental measurement, it makes possible to have detailed analysis of matrix-fracture heat transfer using model by numerical simulation.

5.3.3. Sensitivity Analysis by Numerical Model

The numerical model calibrated was used to investigate the effect of thermal properties of matrix on the amount of heat transfer and evaluate thermal transport in matrix-fracture systems in different flow rates and outer temperatures for the core plugs prepared in the present study. The selection of some variables and core plugs contributes to precise investigation of thermal transport. In fact, the core plugs #1and 3 were selected as the representatives for sensitivity analysis of thermal transport through the effect of thermal properties of matrix in addition to the effect of hydraulic parameters on matrix-fracture heat transfer over cold water injection scenarios through the single fractured core plugs.

5.3.3.1. Transient Temperature in Fracture

The transient temperature decrease in fracture during cold water injection is different for two various core plugs, for different flow rates and outer temperatures 70 and 90 °C. The difference in transient temperature can be caused by flow rate in fracture and thermal properties of matrix at various temperatures determining how heat is swept over matrix-fracture interface and transported through matrix to fracture surface from aspects of quantity and rapidity over cold water injection process.

I)   **The Effect of Flow Rate**

Figure 5.14 indicates the transient temperature decrease in fracture during cold water injection in different flow rates for core plug # 3. For two core plugs and all injection

rates, the transient decrease in fracture temperature was followed by a period of stability as fracture temperature stands for a steady value in the rest of cold water injection period.

The results show that the decline of temperature within fracture increases with rising in the flow rate. Namely, the more water is circulated along fracture, the more heat is swept over matrix-fracture interface under high injection rates of cold water that causes the reduced steady value of fracture temperature.
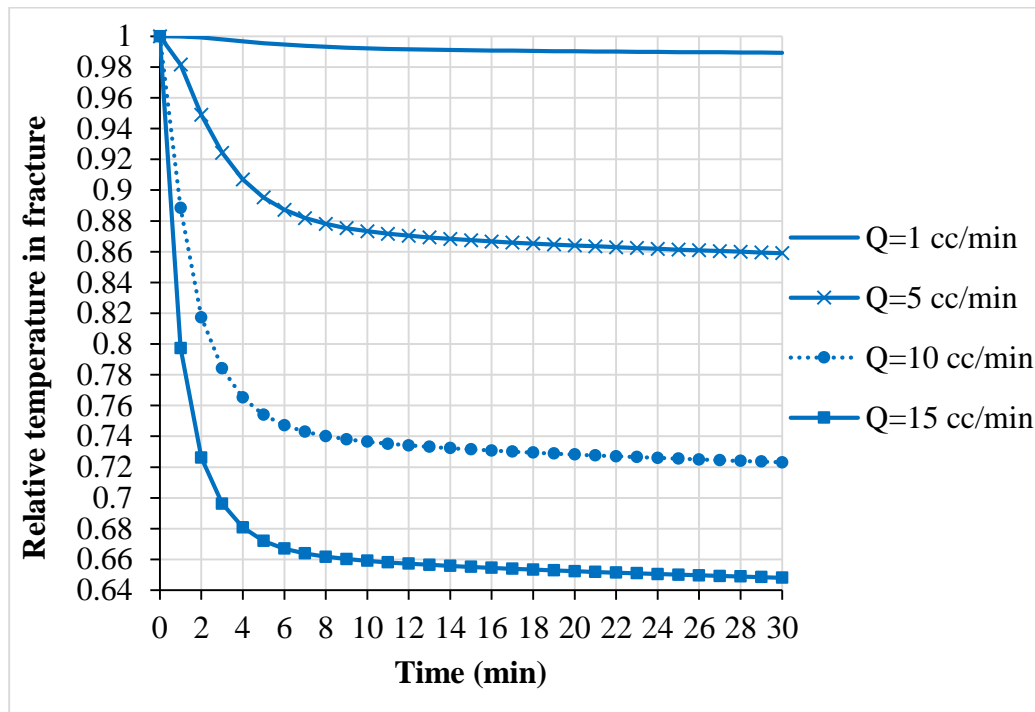
Figure 5.14. Numerical relative temperature in fracture at outer temperature 70 °C for core plug #3

II)   The Effect of Thermal Properties of Matrix

As it was mentioned before that numerical simulation model would give us the useful information about matrix-fracture transport. The analysis of transient temperature decrease in fracture over the cold water injection for core plugs # 1 and #3 at the same

injection rate 10 (cc/min) with outer temperatures 70 and 90 °C indicates that the amount of temperature decrease depends not only on flow operational conditions, but also on thermal properties of core plugs.

Thermal properties of core plugs can be determined by quantifying numerical model to investigate the influence of temperature and thermal properties of matrix on the amount of temperature decrease in fracture for different core plugs during cold water injection (Figure 5.15).
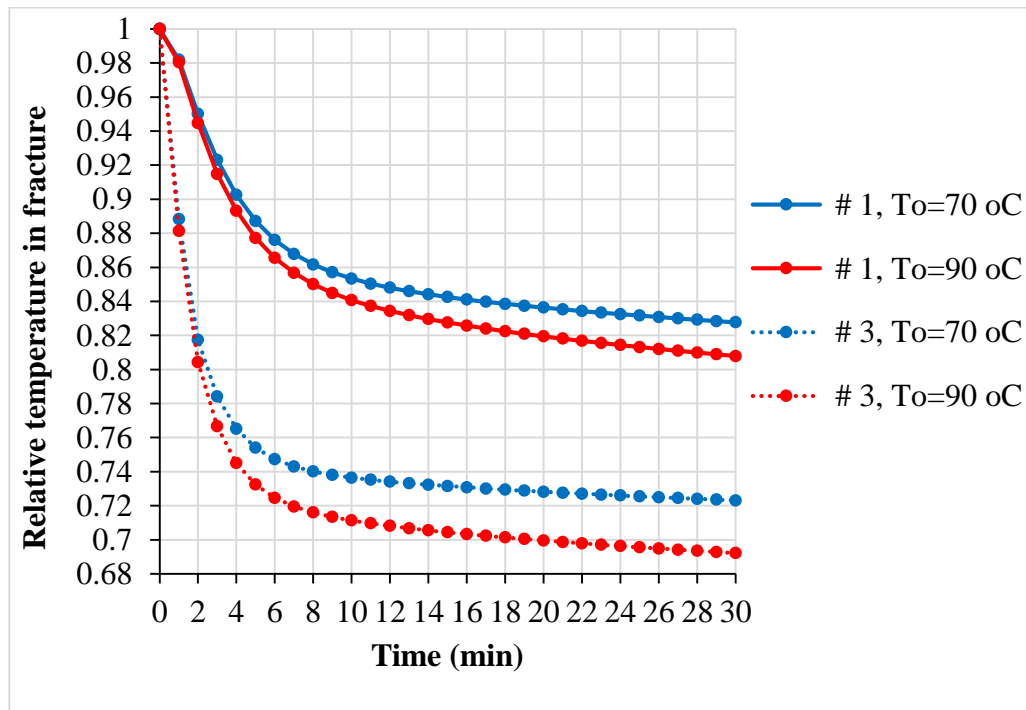
Figure 5.15. Numerical relative temperature in fracture in flow rate 10 (cc/min) for the two core plugs

It can be observed from Figure 5.15 that the amount of temperature decrease in fracture is less in the case of core plug with larger values of thermal properties such as volumetric heat capacity and thermal conductivity for the same flow rate and vice versa. The temperature decrease in fracture is higher in the case of core plug # 3. It

can come from its low values of volumetric heat capacity and thermal conductivity. On the other hand, core plug # 1 with larger values of volumetric heat capacity and thermal conductivity has lower temperature decrease in fracture. Moreover, the amount of temperature decrease in fracture at outer temperature 90 °C is higher than that of at outer temperature 70 °C for both core plugs. This can be described with the fact that by rising outer temperature from 70 to 90 °C volumetric heat capacity of matrix increases, causing less heat transferred from matrix to fracture in which water is circulated.

The quantitative analysis of the plots of transient temperature decrease in fracture for different core plugs at outer temperature of 70 and 90°Cover cold water injection with injection rate of 10 (cc/min) represent that the slope of temperature gradient in transient section of graph is a function of volumetric heat capacity while the duration of this transient period depends on thermal diffusivity of matrix (Figure 5.15). In addition, thermal conductivity has a critical role in the steady state trend. The matrix with lower value of volumetric heat capacity has larger slope in temperature decrease (core plug #3). However, the slope of temperature decrease is smaller in the case of matrix with high value of volumetric heat capacity (core plug # 1).

The values of thermal properties were collected to compare in Table 5.4. It indicates the values of rock thermal diffusivity and transient period in flow rate 10 (cc/min) calculated, in addition to volumetric heat capacity and thermal conductivity of matrix derived by numerical simulation model.

Table 5.4. *The thermal parameters involving in matrix-fracture thermal transport*

Core plug	Outer temperature (°C)	Matrix thermal conductivity (J/min cm °C)	Matrix volumetric heat capacity (J/cm³ °C)	Matrix thermal diffusivity (cm²/min)	Transient period (min)
#1	70	3.5	12	0.29	12
	90	4.5	14	0.32	11
#3	70	1.9	5	0.38	9
	90	2.5	5.8	0.43	8
#8	70	2.5	8	0.31	11
	90	3.5	13	0.27	13
#10	70	2.3	9	0.26	13.5
	90	2.4	9	0.27	13

Because thermal diffusivity is the ratio of the thermal conductivity to the heat storage capacity, the period of transient temperature decrease depends on the value of thermal diffusivity. According to Table 5.4, the larger the value of thermal diffusivity, faster is the propagation of heat through the medium corresponding to smaller transient duration.

In the same way, as can clearly be seen that when value of thermal diffusivity is larger, less heat is stored in matrix and more heat is conducted from matrix to fracture which then will be removed by fluid flow (i.e. advection). In other words, more heat is removed due to high thermal conductivity of matrix, since there is no sufficient heat stored in matrix working as a supportive heat source for fracture fluid (low volumetric heat capacity). Therefore, the slope of temperature decrease in fluid fracture is larger leading to shorter transient period. By contrast, transient temperature decrease period increases in the case of core plugs with low thermal diffusivity.

5.3.3.2. Predicted Temperature Profile of Water along Fracture

The predicted temperature profiles of water along fracture in steady state conditions for the two core plugs for different flow rates and outer temperatures were determined using numerical model. Similar to the transient temperature decrease in fracture, the cold water injection rate and thermal properties of matrix specify the rate of temperature enhancement along fracture.

I)   The Effect of Flow Rate

The influence of flow rate on temperature profile along fracture was investigated at outer temperature 70 °C for core plug #3 (Figure 5.16). The temperature profile of water along fracture represents that the water temperature increases with propagation from fluid inlet to fracture outlet during cold water injection. Nevertheless, the increasing trend involves two different features, firstly, with drastic temperature rise and, secondly, with slight trend. For slower flow rates cooling along the fracture is also slow. As the rate increases temperature along the fracture cools down faster compared to those of the slower rates. The temperature profile becomes almost linear towards the end of the fracture at higher injection rates (Bagalkot and Kumar, 2015).
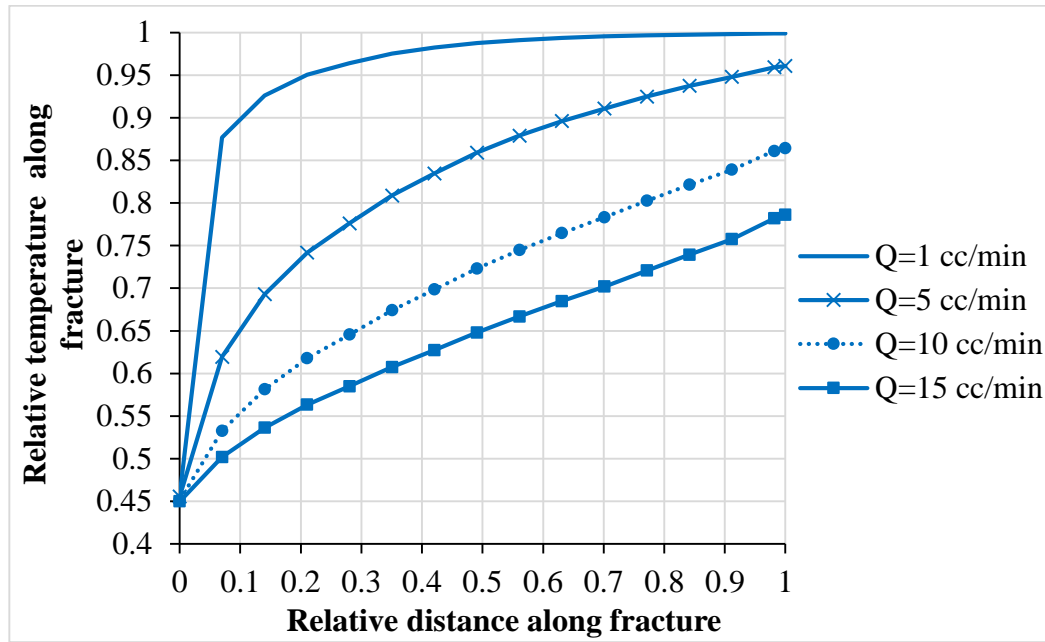
Figure 5.16. Predicted numerical relative temperature profile along fracture at outer temperature 70 °C for core plug # 3

This phenomenon can be attributed to the magnitude of temperature difference and heat exchange between fracture surface and fluid in fracture. At the fluid inlet, the high heat transfer due to the large temperature difference leads to considerable increase in water temperature. Then water becomes warmer with circulation along fracture. Therefore, this results in decreasing temperature difference of matrix-fracture interface causing a slight increase in water temperature through decreasing the rate of heat transfer for the rest of flow path (Luo et al., 2018).

As can be observed that temperature profile is different in various injection rates. The results indicate that temperature profile along fracture decreases with rising cold water injection rate. Since large volume of water flows through fracture space at a given time, matrix cannot sufficiently heat up the water within fracture under high injection rate of cold water. This contributes to decrease in the temperature in outlet fracture with rising injection rate of cold water.

58

II)   The Effect of Thermal Properties of Matrix

In addition to flow operational conditions, thermal properties and temperature of matrix have determinant roles in shaping the behavior of temperature profile along fracture (Luo et al., 2017). The graph illustrates the thermal front propagation for core plugs #1 and #3 in flow rate 10 (cc/min) at outer temperatures of 70 and 90 °C to compare (Figure 5.17).
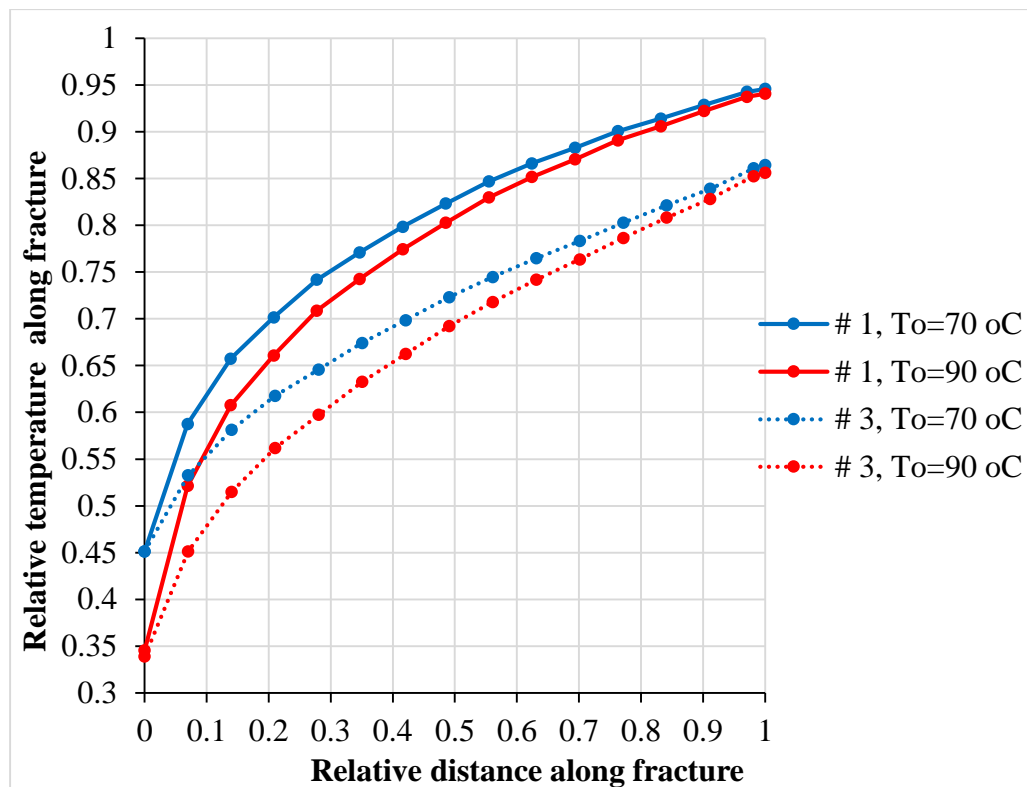
Figure 5.17. Predicted numerical relative temperature profile along fracture in flow rate 10 (cc/min) for the two core plugs

The temperature profile of water along fracture depends on thermal properties of matrix. However, core plug # 1 has higher temperature profile due to its greater volumetric heat capacity and thermal conductivity. The core plug # 3 with lower values of thermal properties has a lower temperature profile along fracture.

In view of larger volumetric heat capacity in the core plugs at 90 °C, temperature profiles along fracture becomes less compared to 70 °C. Because of larger volumetric heat capacity of matrix, heat is prevented to transfer from matrix to fracture regardless of its thermal conductivity.

5.3.4. Convective Heat Transfer Coefficient

The analysis of thermal transport in matrix-fracture system is carried out with quantification of heat exchange between fracture surface and flowing fluid within fracture. The convection over solid-fluid interface as the main thermal transport mechanism in matrix-fracture system can be expressed by convective heat transfer coefficient. Thus, convective heat transfer coefficient can be considered as a representative of the amount of heat exchange in matrix-fracture system.

The convective heat transfer coefficient was calculated by energy balance method (Zhao and Tso, 1993) and analytical solution of heat transfer equation in single fracture-matrix systems (Zhao, 2014) (section 5.1.6). These methods were also used to calculate convective heat transfer coefficient in different pore volume injected (flow rates) and outer temperatures for various core plugs (Figures 5.18 and 5.19).
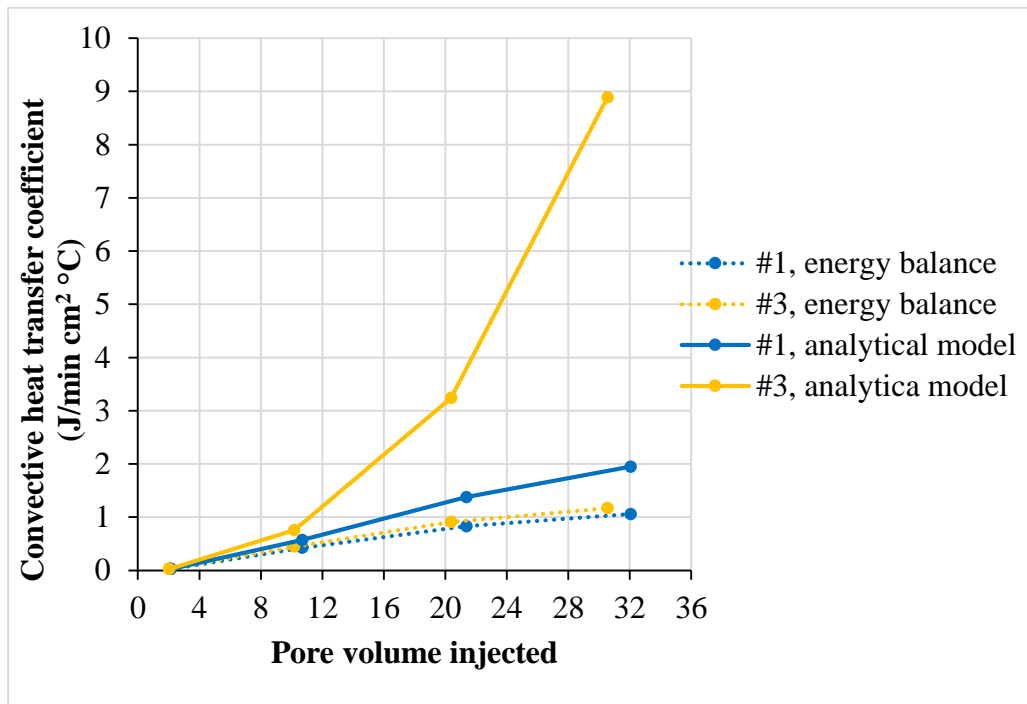
Figure 5.18. Convective heat transfer coefficient for core plugs at outer temperature 70 °C
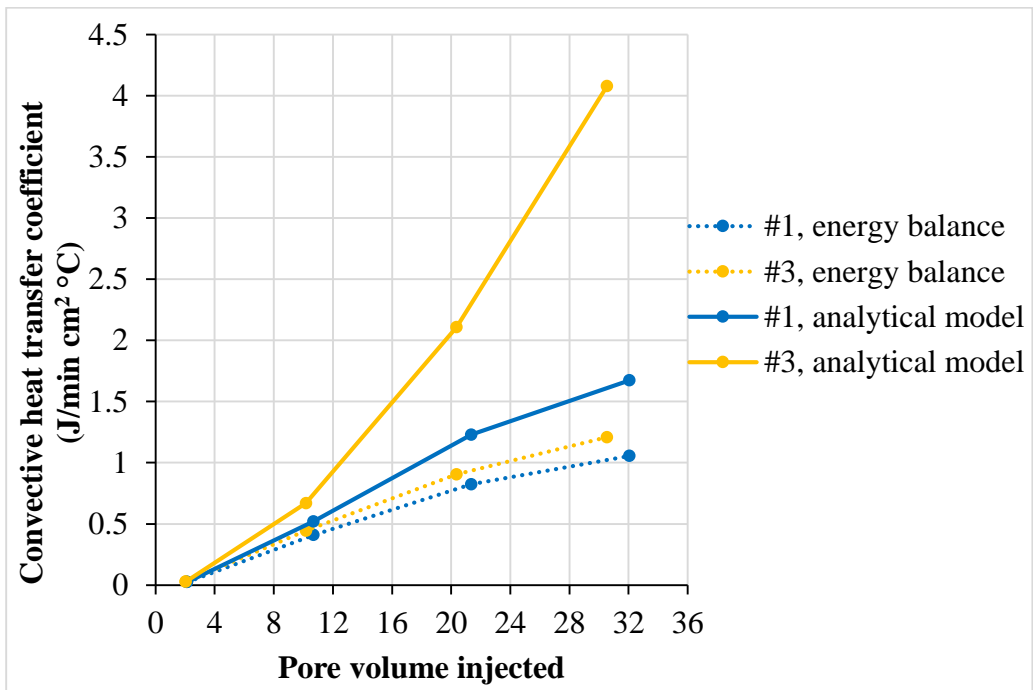
Figure 5.19. Convective heat transfer coefficient for core plugs at outer temperature 90 °C

Figures 5.18 and 5.19 indicate that convective heat transfer coefficient calculated by two methods for core plugs #1 and#3 during cold water injection. In contrast, the plots of relative temperatures in fracture outlet in different pore volume injected are shown at outer temperatures 70 and 90 °C for the two core plugs (Figure 5.20).

Figures 5.18 and 5.19 indicate that the magnitude of convective heat transfer coefficient, calculated by energy balance and analytical methods, increases with increasing flow rate although temperature in fracture outlet decreases during cold water injection (Figure 5.20) which is due to temperature difference between fracture surface and fluid in fracture. In other words, the increase in injection rate increases temperature difference due to larger volume of cold water in fracture at a given time increasing temperature of flowing water. Therefore, high temperature difference causes a decrease in the convective heat transfer coefficient and a decrease of temperature at the fracture outlet.
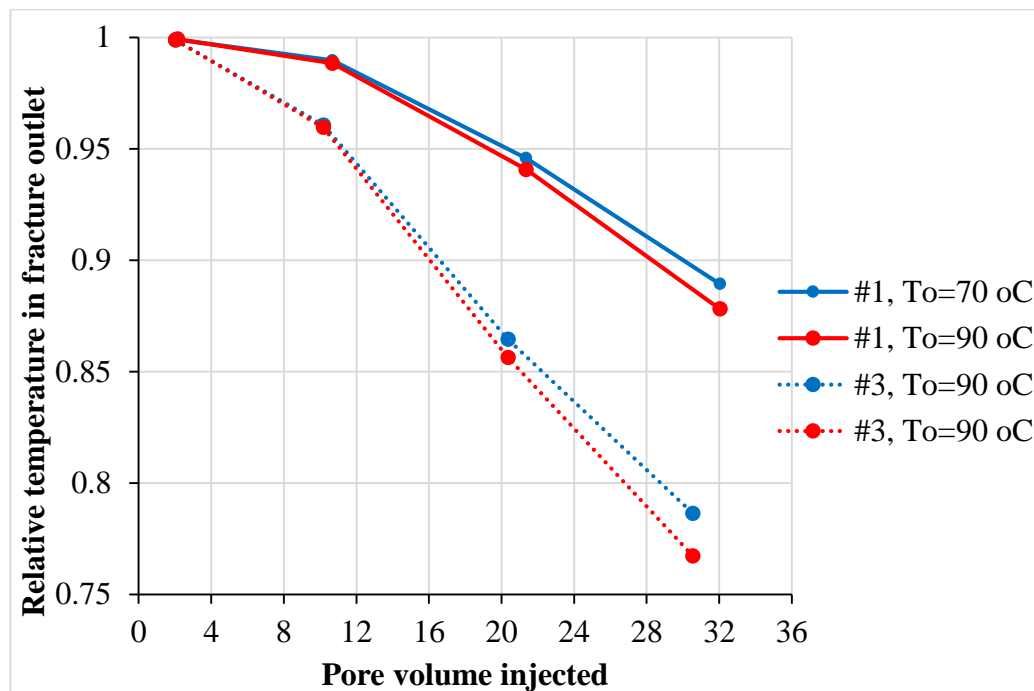
Figure 5.20. Numerical relative temperature in fracture outlet for core plugs at different outer temperatures

As can be observed from figures that the values of convective heat transfer coefficient calculated by energy balance and analytical model (Figures 5.18 and 5.19) cannot verify the decrease of relative temperature in fracture outlet in different pore volume injected over cold water injection (Figure 5.20). Although it was expected that temperature in fracture outlet increases with the rise in injection rate as a result of increment in convective heat transfer coefficient, outlet temperature decreases with rising injection rate.

This drawback may come from some assumptions used to simplify of matrix-fracture heat transfer. These hypotheses include local thermal equilibrium (LTE) assumption representing the same temperature in fracture surface and fluid in fracture and assumption of constant convective heat transfer coefficient along fracture as well.

The convective heat transfer coefficient as an index for quantitative analysis of the amount of heat exchange over matrix-fracture interface is a function of physical and thermal properties of fluid, geometrical shape of the interface, and temperature difference in matrix-fracture interface. In practice, flowing the fluid through fracture provides the temperature difference between fracture surface and fluid in fracture. The rate of temperature difference can be affected by not only flow rate in fracture, but also thermal properties of matrix.

Similar to real- world system, as observed in numerical model, there are temperature distribution rather than uniform temperature in matrix-fracture system and temperature difference in matrix-fracture interface for all core plugs and flow rates. The temperature distribution in various injection rates at outer temperature 90 °C for core plug # 3 during cold water injection are shown in Figure 5.21.
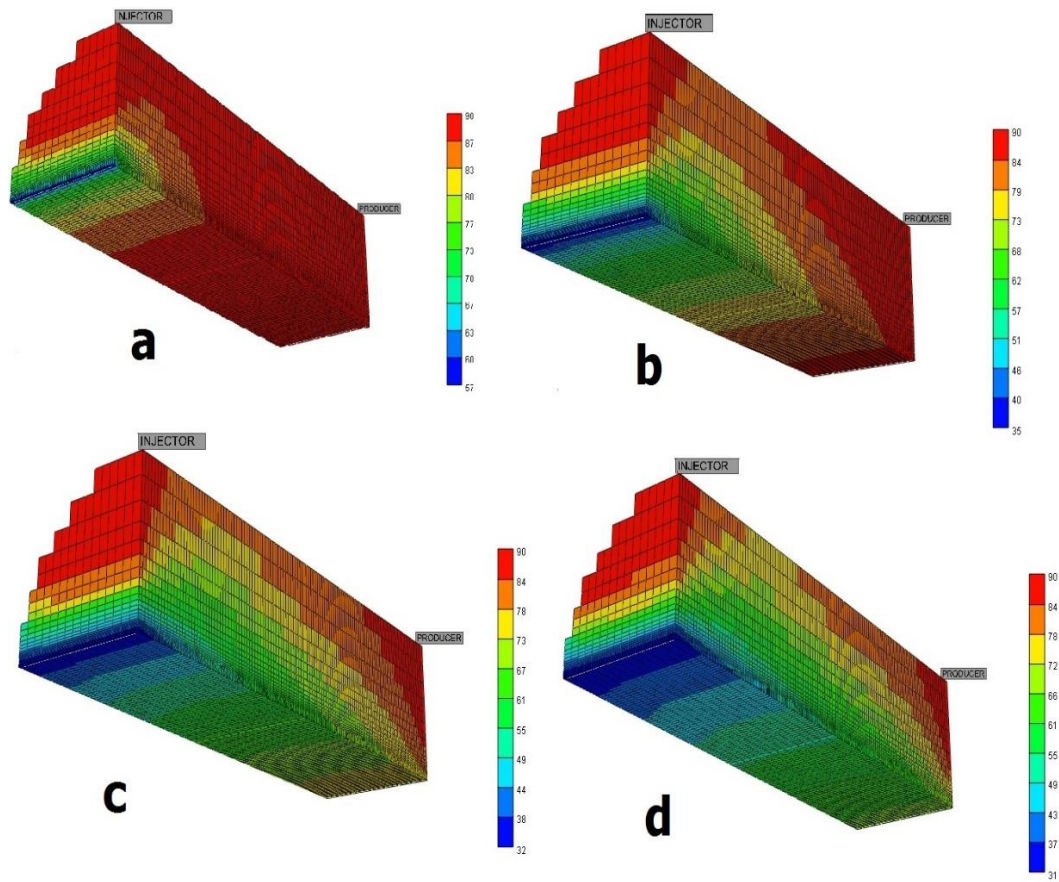
Figure 5.21. Temperature distribution in matrix-fracture system for core plug # 3 at outer surface temperature 90 °C, (**a**) injection rate **1 cc/min**; (**b**) injection rate **5 cc/min**; (**c**) injection rate **10 cc/min**; (**d**) injection arte **15 cc/min**

As mentioned previously, thermal properties of matrix affect the values of fracture surface temperature in steady state heat transfer conditions. In turn the temperature of fracture surface has a significant role in establishing of the temperature difference in matrix-fracture interface and hence the convective heat transfer coefficient. The matrix with larger values of thermal properties provides low temperature difference over matrix-fracture interface, causing larger heat transfer coefficient.

In the current study, experimental heat flux values measured by the thin film type heat flux sensor in fracture and temperature difference between fracture surface and fluid

in fracture determined by using the numerical model in fracture were used to analyze accurately matrix-fracture heat transfer. According to Newton's cooling law at the solid-fluid interface, the convective heat transfer coefficient is proportional to heat flux amount, but inversely proportional with temperature difference between fracture surface and fluid in fracture Eq. (5.11).

The values of convective heat transfer coefficient in different pore volumes injected (flow rates) at outer temperatures 70 and 90 °C for core plugs #1 and #3 are shown in the Figure 5.22.
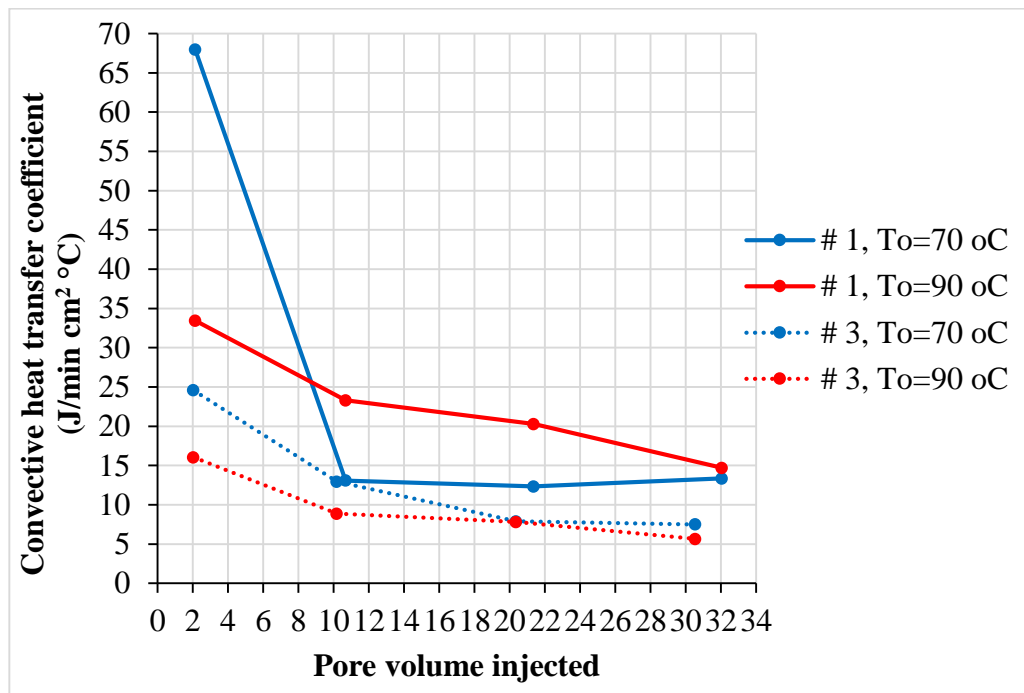
Figure 5.22. Convective heat transfer coefficient for the two core plugs

Figure 5.22 illustrates that the value of convective heat transfer coefficient is high during early times (low pore volume injected). During this period the effect of thermal properties of matrix on temperature difference of matrix-fracture interface is more pronounced over cold water injection.

In other words, the value of convective heat transfer coefficient affected by temperature difference of matrix-fracture interface depends more on thermal properties of matrix than fluid hydrodynamics conditions in low pore volume injected. In contrast, fluid motion conditions in fracture affects considerably on the convective heat transfer coefficient at later stages of flooding (high pore volume injected). For example, core plug #1 with large volumetric heat capacity and thermal conductivity that keeps the temperature difference over solid-fluid interface low, has larger heat transfer coefficient as opposed to core plug #3 involving the low thermal properties in low pore volume injected.

5.3.5. Variable Convective Heat Transfer Coefficient with Respect to Space and Time

Because of the dependency of convective heat transfer coefficient on thermal properties and flowing conditions at the matrix-fracture interface, it can be changed along the fracture during cold water injection as a function of time. Therefore, the determination of convective heat transfer coefficient along solid-fluid interface is challenging to analyze the heat transfer in matrix-fracture system. To cope with the problem, new forms of convective heat transfer coefficients were introduced in the present study. Thus, local and transient convective heat transfer coefficients can be calculated by using Eq. (5.11) with experimental measurement of heat flux values as well as temperature difference of solid-fluid interface determined by numerical simulation model used as inputs. The use of heat flux values measured experimentally over matrix-fracture interface is introduced for calculating of the convective heat transfer coefficients. However, the dynamic heat transfer coefficient with respect to spatial heterogeneity and temporal evolution was only determined by a numerical simulation in the recent study (Heinze et al., 2017).

5.3.5.1. Local Convective Heat Transfer Coefficient

The numerical model makes it possible to calculate temperature difference between fracture surface and fluid in fracture at different cross sections. The numerical model of the single fracture-matrix system, used in the present study, involves 46800 grids with different sizes in x, y, and z directions respectively (chapter 4).

The temperature gradient between fracture surface and fluid in fracture was derived from numerical model along fracture at steady state conditions. Figure 5.23 indicates the steady temperature difference in matrix-fracture interface at different injection rates and outer temperatures 70 and 90 °C for core plug # 3.
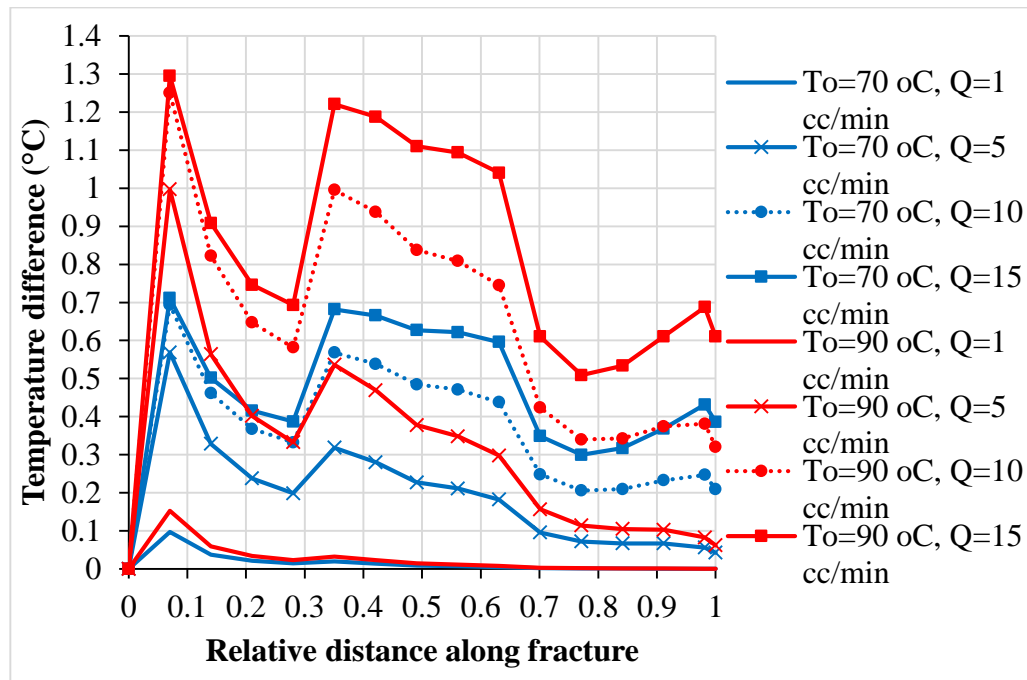
Figure 5.23. The steady temperature difference in matrix-fracture interface for core plug # 3

The plots of steady temperature difference between fracture surface and fluid in fracture along fracture plane indicate that temperature difference in matrix-fracture interface is changing along the fracture. The figures show that the temperature

67

difference at fracture inlet is higher than fracture outlet. The larger temperature difference at the fracture inlet can arise from lower fluid temperature compared to fracture surface at the inlet injection. Because the fluid is heated by the warmer fracture surface (matrix-fracture interface) along the fracture the temperature difference between fracture surface and fluid in fracture experiences a gradual decrease. The slight increase in temperature difference in middle cross section of fracture is due to the thin film heat flux sensor installed in the fracture with less value of permeability. In fact, this section disrupts thermal transport. Near the outlet, the temperature difference is less than that observed near the inlet. Moreover, the rate of temperature difference in matrix-fracture interface increases with rising injection rate and outer temperature of core plug. The low temperature increase of flowing water at high flow rate during cold water injection is due to large volume of water within fracture at a given time that results in large temperature difference along the matrix-fracture interface.

Fig 5.24 shows the other parameters that assign the rate of temperature difference are thermal properties and outer temperature of matrix.
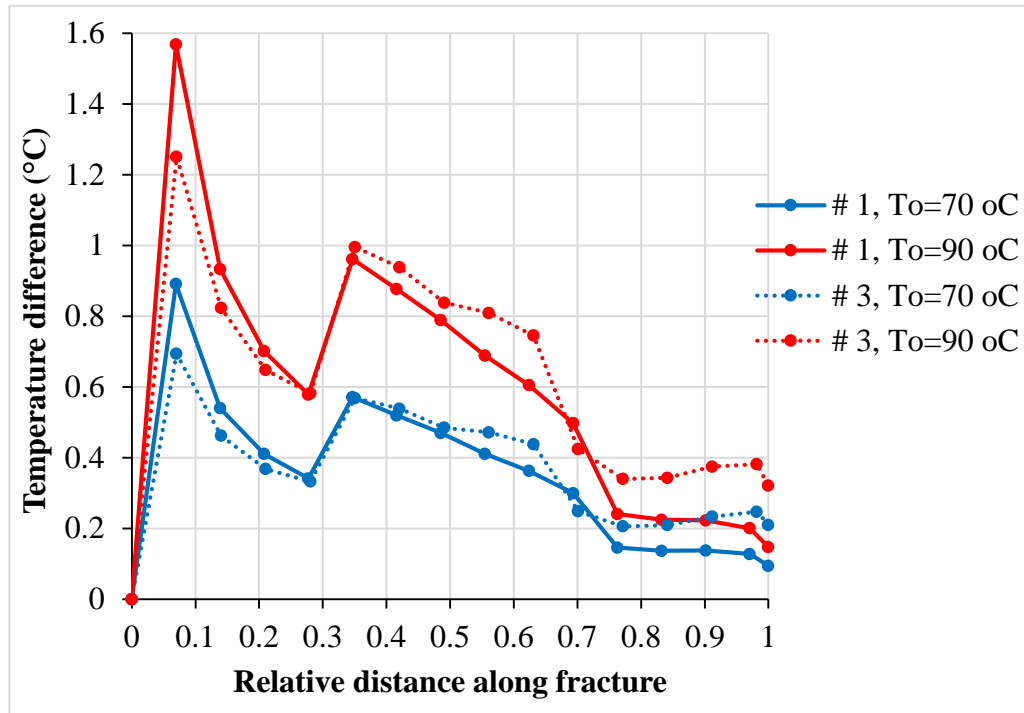
Figure 5.24. The steady temperature difference in matrix-fracture interface in flow rate 10 (cc/min) for the two core plugs

Fig 5.24 indicates that the thermal properties of matrix determine the amount of temperature difference over matrix-fracture interface. It can be seen that qualitative behavior of temperature difference is similar the magnitude of the temperature difference for different core plugs. This is probably due to different thermal properties of the rock matrix. This shows that the thermal properties of rock matrix determine the extent of temperature difference at the matrix-fracture interface. Core plug #1 with higher volumetric heat capacity and thermal conductivity has lower temperature difference by extracting more heat from rock matrix to matrix-fracture interface while core plug #3 with smaller thermal properties has larger temperature difference during cold water injection. The temperature difference at the matrix-fracture interface for 90 °C is higher than that of 70 °C. This can be caused by the higher volumetric heat capacity of rock matrix leading to smaller heat transport from rock matrix to matrix-fracture interface. With regard to dependency of convective heat transfer coefficient

69

on temperature difference of matrix-fracture interface, thermal properties of rock matrix are more effective than flow operational conditions in conductive/diffusive dominant heat transfer mechanism at early times (i.e. low pore volume injected). On the other hand, during late times, fluid hydrodynamic conditions play a crucial role in temperature difference as advective heat transfer mechanism becomes dominant.

In current study, heat flux was experimentally measured at the fracture for various injection rates at outer temperatures 70 and 90 °C for the two core plugs #1 and #3 over cold water injection. As a representative, the transient values of heat flux at injection rate 10 (cc/min) are shown in Figure 5.25.
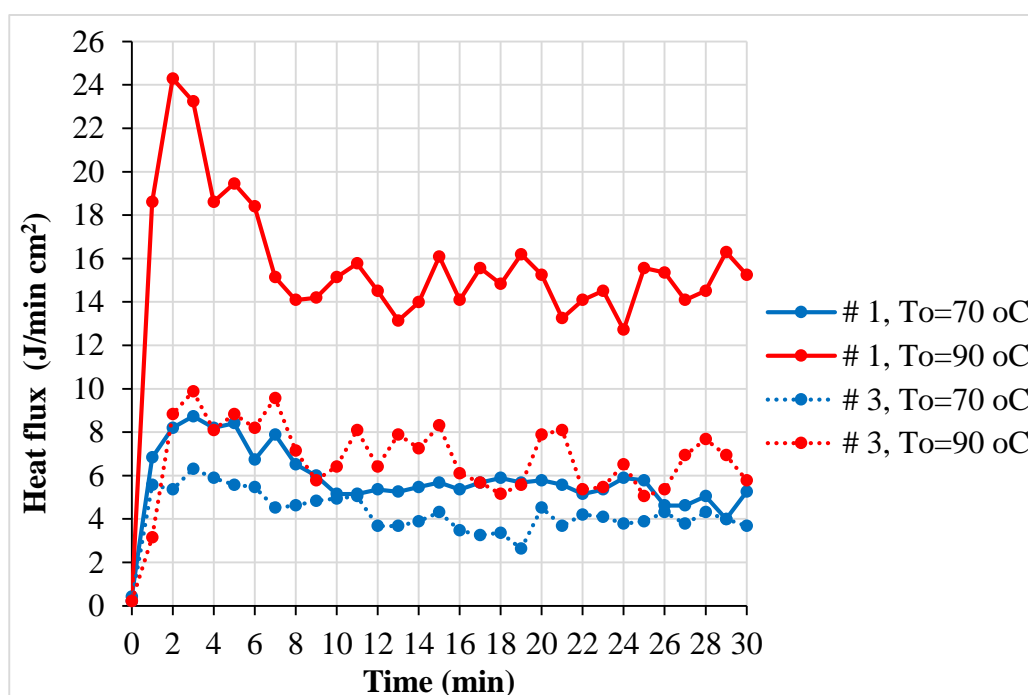
Figure 5.25. The experimental values of heat flux in flow rate 10 cc/min for the two core plugs

The amount of heat flux increases with a rise of injection rate. Also, in each injection rate, similar to temperature difference, heat flux in matrix-fracture interface is high at the early times. In fact, the extent of heat flux between matrix and fluid in fracture is

proportional to temperature difference in solid-fluid interface. Figure 5.25 indicates that the extent of heat flux increases as a result of large temperature difference between the injected fluid and the matrix increases. In this regard, the role of thermal properties of matrix in heat transfer from matrix to matrix-fracture interface is undeniable. As can clearly be seen that heat flux in core plug # 1 is higher than that of in core plug #3 in injection rate 10 (cc/min) over cold water injection. This amount is great in temperature 90 °C compared to 70 °C due to large temperature difference.

The early transient changes in heat flux are followed by a period of stability with small fluctuations around a constant value. This may come from reversible motion of water in matrix-fracture interface. While water with low temperature penetrates into matrix, hot water moves back to fracture trying to reach thermal equilibrium at cold water injection.

In view of temperature difference of matrix-fracture interface along fracture distance, we introduced a new method to determine local convective heat transfer coefficient between matrix and flowing fluid in a matrix-fracture system. The local convective heat transfer coefficient can be calculated by using the steady values of heat flux measured at the fracture over the flow-through experiments and the steady values of temperature difference of matrix-fracture (solid-fluid) interface derived from numerical model for various locations along the fracture for different flow rates and temperatures (Figure 5.26).
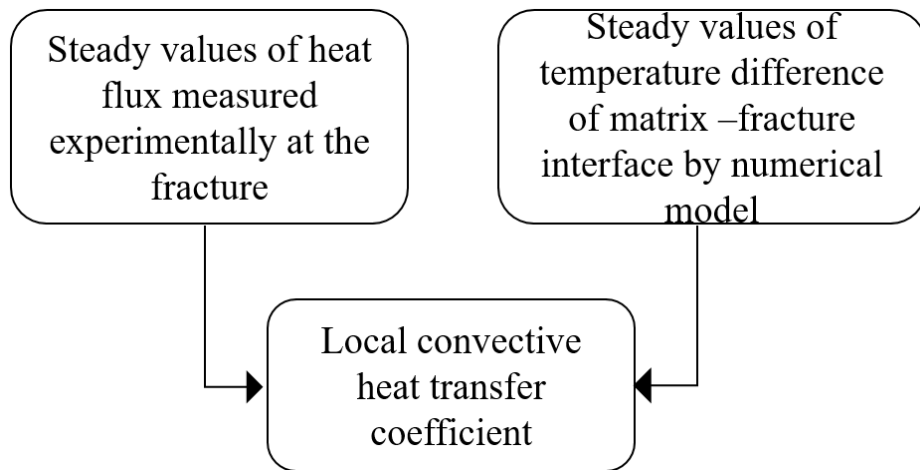
Figure 5.26. Local convective heat transfer coefficient

Fig 5.27 shows the local heat transfer coefficient change along the fracture for different injection rates and outer temperatures 70 and 90 °C for core plug # 3.
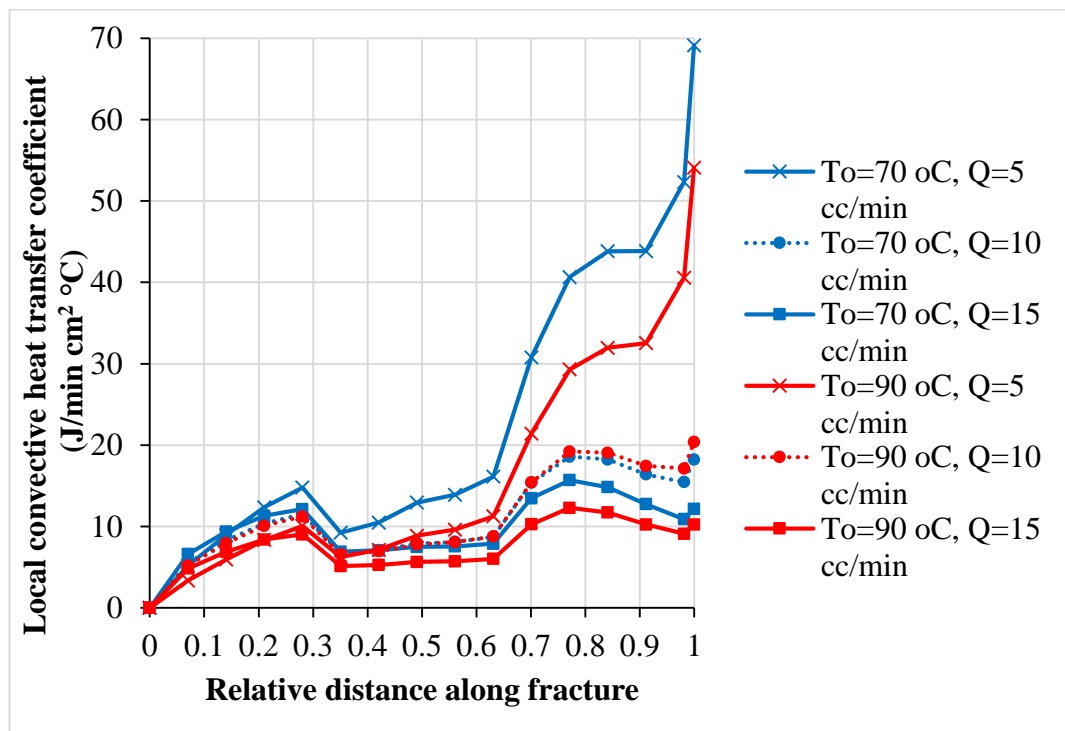
Figure 5.27. Local convective heat transfer coefficient for core plug # 3

It can be observed that the magnitude of local convective heat transfer coefficient increases from fracture inlet to outlet in all flow rates. This can arise from the decrease in temperature difference along the matrix-fracture interface in core plug. As mentioned above, flowing water becomes warmer along fracture that causes the decrease of temperature difference.

Furthermore, the heat transfer coefficient is larger for lower injection rates. Because temperature difference increases with rising flow rates, this results in decreasing convective heat transfer coefficient. As the temperature difference for a flow rate of 1 (cc/min) is extremely small, the values of heat transfer coefficient are very large.

To investigate the effect of temperature and thermal properties of matrix, the values of local heat transfer coefficient along matrix-fracture interface for injection rate 10 (cc/min) for the two core plugs #1 and #3 during cold water injection are shown in Figure 5.28.
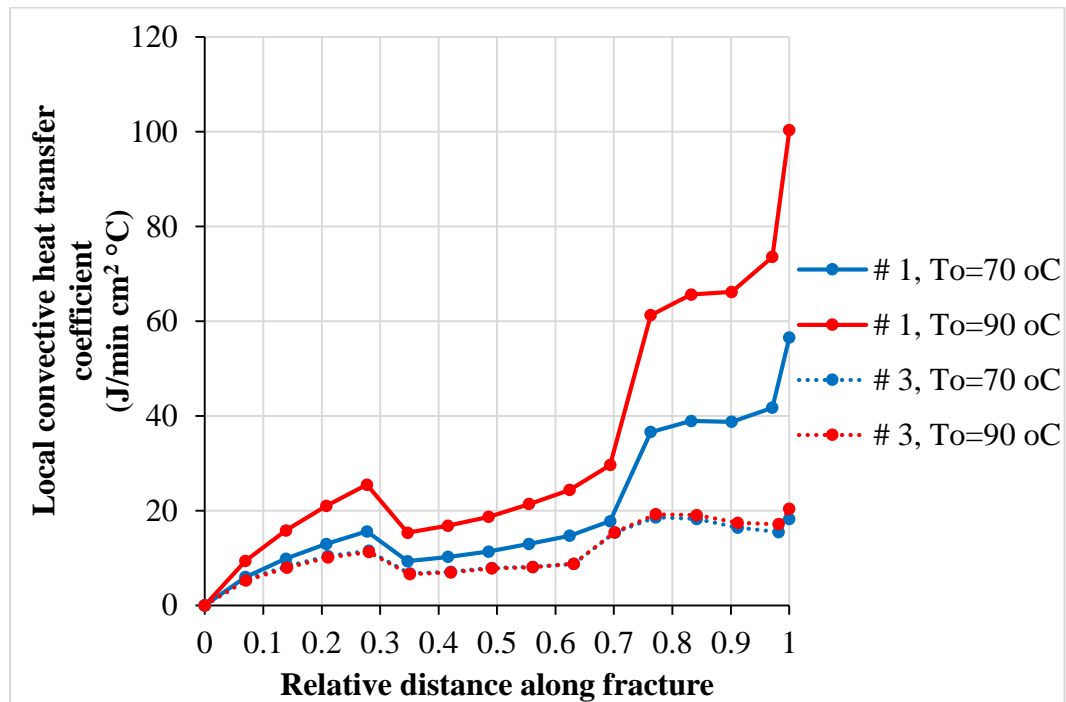
Figure 5.28. Local convective heat transfer coefficient in flow rate 10 cc/min for the two core plugs

It can be observed from Figure 5.28 that the local heat transfer coefficient is larger in core plug #1 due to its high thermal properties. Moreover, the effect of outer temperature of matrix on the local heat transfer coefficient for core plug #1 is more considerable than that of the core plug # 3. In fact, this is due to relatively high increase in the values of matrix thermal properties at outer temperature 90 °C in the case of core plug #1 compared to core plug #3.

5.3.5.2. Transient Convective Heat Transfer Coefficient

In addition to the local convective heat transfer coefficient calculated using steady values of heat flux, fracture surface and fluid in fracture temperatures along the fracture, the transient convective heat transfer coefficient can also be calculated using the transient values of heat flux measured at the fracture over the flow- through experiments and the transient values of temperature difference at the matrix-fracture (solid-fluid) interface derived from numerical model for different flow rates and temperatures (Figure5.29).
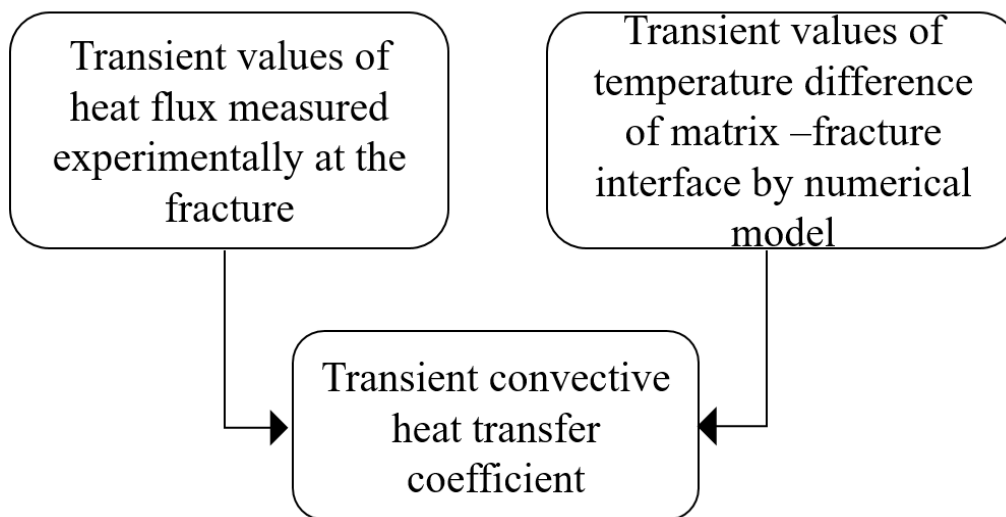
Figure 5.29. Transient convective heat transfer coefficient

Figure 5.30 shows the transient heat transfer coefficient for different injection rates and outer temperatures 70 and 90 °C along the matrix-fracture interface for core plug #3.

Figure 5.30 indicates that transient values of heat transfer coefficients are larger during early times due to larger value of heat flux in the initial stage. When cold water injection continues, the heat flux in matrix-fracture interface decreases, contributing to decrease in convective heat transfer coefficient.
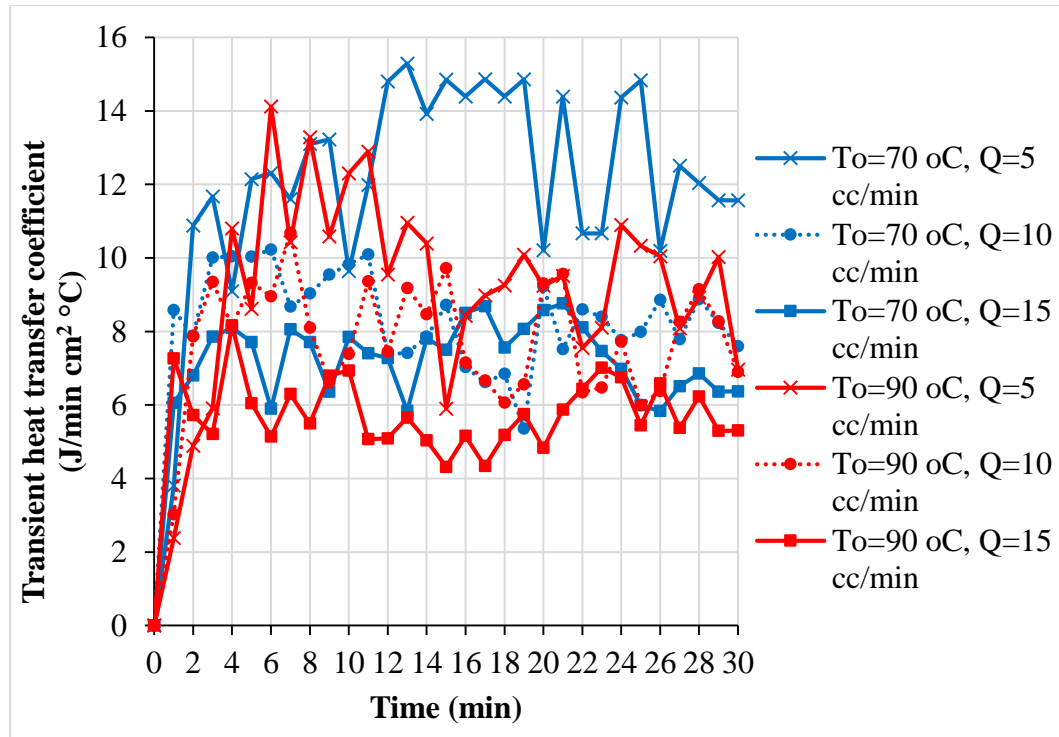
Figure 5.30. Transient convective heat transfer coefficient for core plug # 3

Similar to local heat transfer coefficients, global transient heat transfer coefficients are different for various core plugs with varying thermal properties. Core plug # 1 with high heat flux as a result of its larger thermal properties has larger transient heat

transfer coefficients in comparison with those of core plug #3. As observed in local heat transfer coefficient, temperature effect on transient heat transfer coefficient for core plug #1 is considerably larger than that of core plug #3 as well (Figure 5.31).
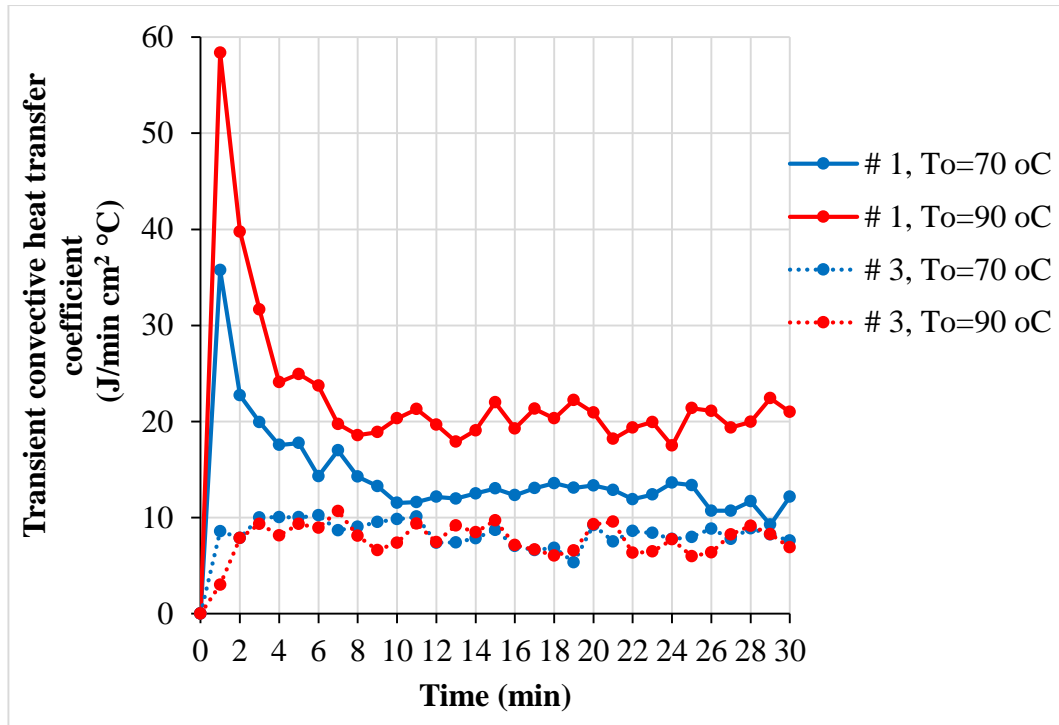
Figure 5.31. Transient convective heat transfer coefficient in flow rate 10 (cc/min) for the two core plugs

Therefore, the trends of convective heat transfer coefficient are relatively compatible with those of heat flux values measured experimentally.

CHAPTER 6

SOLUTE TRANSPORT IN SINGLE FRACTURE-MATRIX SYSTEMS

6.1. Theory

6.1.1. Solute Transport in Fractured Porous Media

A detailed understanding of flow and transport in fractured porous media is more challenging than those of conventional porous media. It can arise from dealing with kinds of heterogeneities in the case of fractured porous media. Fractured porous media comprise high permeability fractures and low permeability matrix, representing heterogeneous systems (Boon et al., 2017).

The spatial variability in physical properties such permeability and storage between fractures and matrix provides heterogeneous distributions in flow and transport properties. The heterogeneities in fractured porous media produce intricate fluid velocity profiles. The large velocity difference between fracture and matrix in which flow velocity in fracture is faster than that of matrix has a profound impact on the nature of flow and transport in fractured porous media (Bijeljic et al., 2011; Kumar, 2012).

Fractured porous media contain two separate flow domains such the high-permeability domain in fracture with advection dominant transport mechanism as opposed to the low-permeability domain of matrix with dispersion and/or diffusion transport mechanism. While fluid flow mainly occurs through fracture, matrix is not effective for flow in fractured porous media. Nevertheless, matrix may have an important role over matrix-fracture transfers. The pore space in matrix provides the storage capacity in transport processes (Schmelling and Ross, 1989). Although solute transport in fractured porous media can be considered as non-Fickian due to early breakthrough

by heterogeneity, the difference of two distinct flow domains leads to considerable solute concentration gradients between fracture and matrix. The solute concentration gradient between matrix and fracture is the main reason for matrix-fracture mass transfer (Geiger et al., 2010).

In addition to velocity difference between fracture and matrix in solute transport by bulk movement of fluid, other chemical and physical processes such dispersion and adsorption within matrix and over matrix-fracture interface can inhibit mass transport in fractured porous media (Werth et al., 2006).

6.1.2. Solute Penetration

An effective parameter involved in matrix-fracture transfers through fractured porous media is penetration process of heat and solute into matrix from fracture contributing to estimation of transfer area in matrix-fracture systems. In fact, the amount of matrix-fracture transfers is proportional to the level of penetration process (Polak et al., 2003; Tachi et al., 2018; Zhu and Zhan, 2018).

Although fractures provide pathways for solute transport due to their high values of permeability in comparison with surrounding matrix in fracture-matrix systems, matrix which is adjacent to the fractures seems to has significant effect on solute transport by penetration process through fractured porous media. Therefore, the main parameters that control the level of solute penetration from fracture into matrix in fractured porous media are (1) flow conditions in fracture, (2) dispersion within matrix (Brouyère et al., 2005; Tang et al., 1981).

Matrix dispersion makes it possible to displace solute from the fracture into the matrix over solute transport in a fracture-matrix system. In other words, the matrix dispersion mechanism acts to reduce the solute concentration profile in fracture and retard breakthrough concentration by removing some of the solute from the fluid in the

fracture and storing it in the matrix (Grisak and Pickens, 1980; Lenormand et al., 1998).

The dispersion in matrix that deals with solute penetration over matrix-fracture transfers can be affected by the pore scale properties of matrix. Although the role of physical properties of matrix (porosity and permeability) in the level of solute penetration in fractured porous media has been identified in many areas of research, in present study the effect of thermal properties of matrix (volumetric heat capacity and conductivity) on solute transport through fractured porous media in different temperatures was investigated in addition to physical properties of matrix.

The solute concentration profile in fracture and breakthrough concentration can be used as a diagnostic tool in the assessment of the level of solute penetration from fracture into matrix. This can be explained by the fact that as penetration level is high, the amount of solute concentration profile in fracture and breakthrough concentration decline. Namely it represents more solutes migrate from fracture into matrix over the duration of flowing tests.

A detailed understanding of the effect of thermal properties of matrix on solute penetration level in different temperatures over solute transport in fractured porous media is essential.

6.1.3. Tracer Testing

Tracer is defined as a non-reactive chemical substance that is added to the fluid to map flow paths, providing information on the flow and transport system heterogeneity in porous media. In fact, tracer testing can be used to determine parameters such as flow velocity, dispersivity, and Peclet number representing dominant transport mechanism. In addition, tracer testing is widely implemented for characterization of spatial distribution of heterogeneities and specification of properties in the porous media in

numerous fields such enhanced oil recovery, enhanced geothermal systems, and hydrological studies (Akin, 2001; Akin and Okandan, 1995).

Tracer testing involves the injection of a chemically inert tracer to flow through porous media and the detection of its recovery through time. The main application of tracer testing is study of flow pattern and quantification of porous media properties. In other words, tracer testing is mostly used to characterize the flow paths and determine transport parameter in porous media (Pruess et al., 2005). Moreover, it provides important information in estimation of solute penetration level and surface area involved in transfers. Tracers can be divided into two general groups: (1) chemical tracers, and (2) radioactive tracers. The most commonly used approach in quantitative measurement of chemical tracers is popular analytical methods. These methods make chemical tracers more convenient than radioactive tracers for characterization of heterogeneities in porous media (Axelsson, 2013).

6.1.4. Conceptual and Mathematical Models of Solute Transport in Porous Media

Reynolds transport theorem is generally used to derive mass conservation, so the continuity equation in a steady flow may be described as (Bird et al., 2002) (Sahimi, 2011);

$$\frac{\partial}{\partial t}\int_{CV}\rho dV + \int_{CS}\rho(u \bullet n)dA = R$$
(6.1)

Where ρ is the density of flowing fluid with velocity u at time t and R is chemical reaction term. The differential form of the continuity equation is given by;

$$\frac{\partial \rho}{\partial t} + \nabla \bullet (\rho u) = R$$
(6.2)

The governing continuity equation in the case of solute that is miscible in the solvent is;

$$\frac{\partial C}{\partial t} + \nabla \bullet j = R \tag{6.3}$$

Where C is the solute concentration and j is total flux of the solute. As total flux of the solute consists of advection flux and diffusion flux, so

$$j = Cu - D_m \nabla C \tag{6.4}$$

Where D_m is the molecular diffusivity of the solute in the solvent. Thus, the continuity equation for the solute with constant velocity (u) and molecular diffusion (D_m) without any chemical reaction (R=0) can be expressed as advection-diffusion equation;

$$\frac{\partial C}{\partial t} + u \bullet \nabla C = D_m \nabla^2 C \tag{6.5}$$

As the advection-diffusion equation cannot describe the dispersion process in porous media, the most commonly proposed equation to govern solute transport over flowing through porous media is advection-dispersion equation;

$$\frac{\partial(\phi C)}{\partial t} + \nabla \bullet (\phi C u) = \nabla \bullet (\phi D \nabla C) \tag{6.6}$$

$$\frac{\partial(\phi C)}{\partial t} + \phi u \bullet \nabla C = \phi D \bullet \nabla^2 C \tag{6.7}$$

Where Ø is porosity of porous media and D is dispersion coefficient. Unlike the thermal transport, the coupling in the solute transport is a function of the pore-scale physical properties of matrix such as porosity and permeability.

The main transport mechanisms involved in the solute transport through porous media are advection and hydrodynamic dispersion (mechanical dispersion along with molecular diffusion). Advection is a mechanism that compound or dissolved solid is

transported by the bulk movement of fluid. However, hydrodynamic dispersion (dispersion) occurs mainly as a result of mixing and spreading. The mixing is caused by variations in velocity field due to the fluid flow conditions, heterogeneities in medium, and the chemical and physical interactions with the solid surface of the medium (Figure 6.1) (Sahimi, 2011).
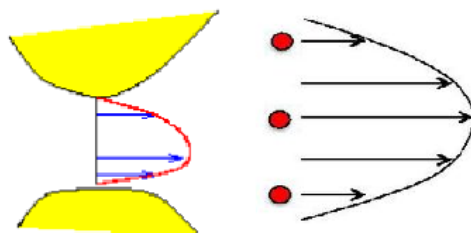
Figure 6.1. Variations in flow velocity caused by heterogeneities

In general, hydrodynamic dispersion (dispersion) includes mechanical dispersion and molecular diffusion;

$$D = au + D_m$$

(6.8)

Where D is hydrodynamic dispersion (cm^2/min); a is dispersivity (cm); u is velocity (cm/min); D_m is molecular diffusion (cm^2/min).

6.1.4.1. Homogeneous Porous Media

Mathematical description of mass balance for the non-reactive solute transport process in homogeneous porous media is advection-dispersion equation. For incompressible fluid, constant porosity, constant fluid velocity, and constant dispersion coefficient the advection-dispersion equation can be written as (Sahimi, 2011):

$$D_L \frac{\partial^2 C}{\partial y^2} + D_T \frac{\partial^2 C}{\partial z^2} - u_y \frac{\partial C}{\partial y} = \frac{\partial C}{\partial t}$$

(6.9)
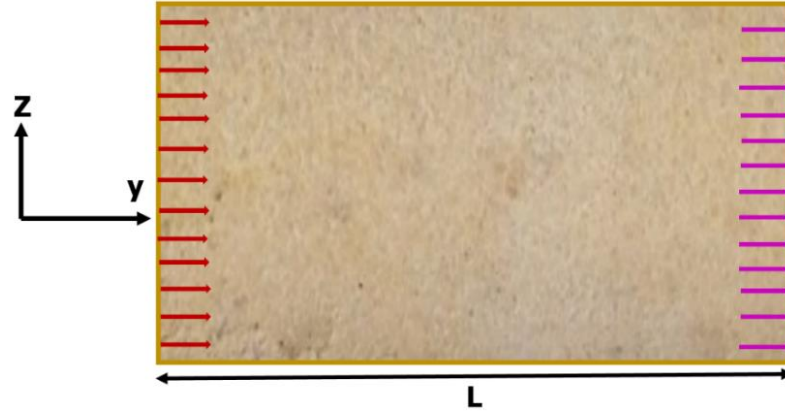
Figure 6.2. A homogeneous porous medium

The advection-dispersion equation in the case of one-dimensional flow (longitudinally) is:

$$D_L \frac{\partial^2 C}{\partial y^2} - u_y \frac{\partial C}{\partial y} = \frac{\partial C}{\partial t} \tag{6.10}$$

Where C: solute concentration, D_L: longitudinal dispersion coefficient, D_T: transverse dispersion coefficient, and u: solute velocity injected

Thus, the spreading of solute by both mechanical dispersion and molecular diffusion in porous media can be illustrated by dispersive part of the advection-dispersion equation. The solution of 1-D advection-dispersion equation with given initial and boundary conditions is obtained by the Laplace transform technique (Coronado et al., 2009):

initial condition: $\qquad C(y \geq 0, t = 0) = 0$ $\qquad\qquad\qquad$ (6.11)

boundary conditions: $\qquad C(y = 0, t > 0) = C_o$ $\qquad\qquad\qquad$ (6.12)

$$C(y \rightarrow \infty, t > 0) = 0 \tag{6.13}$$

$$C(y,t) = \frac{C_\circ}{2\sqrt{\pi D t}} \exp\left[-\frac{(y - ut)^2}{4Dt} \right] \tag{6.14}$$

This can be rewritten to the complementary error function (erfc) in the form of dimensionless parameters. The tracer concentration in continuous injection given by Coats and Smith (1964) and Bear (1972) as follows (Ramírez-Sabag et al., 2005):

$$C_c(y_D, t_D) = \frac{C_\circ}{2}\left[erfc\left(\frac{y_D - t_D}{\sqrt{4t_D / Pe}}\right) + \exp(y_D Pe) erfc\left(\frac{y_D + t_D}{\sqrt{4t_D / Pe}}\right)\right]$$

(6.15)

Where dimensionless space; $y_D = \dfrac{y}{L}$ (6.16)

 L; characteristic length

Dimensionless time; $t_D = \dfrac{tu}{L}$ (6.17)

 Peclet number; $Pe = \dfrac{uL}{D}$ (6.18)

Peclet number is usually used to evaluate the dominance of mass transfer by advection or dispersion/diffusion. The Peclet number is a dimensionless numbers relevant in the study of transport phenomena in a continuum. In mass transfer, it corresponds to the ratio of mass transport by bulk fluid motion (advection) to mass transport by dispersion or and diffusion. A large Peclet number is characteristic of an advective system. On the other hand, the system becomes dispersion when the advective velocity (u) approaches zero.

6.1.4.2. Fractured Porous Media

Fractured porous media are extremely heterogeneous systems. They are different from homogeneous porous media in the sense of spatial distribution of physical heterogeneities. The very large contrast in physical pore-scale properties such as permeability and specific storage between matrix and fracture causes preferential

behavior of flow through fracture in fractured porous media as opposed to homogeneous porous media.

For simplicity in the understand of transport process in fractured porous media, a single fracture-matrix system was used rather than the complex fracture geometries. Figure 6.3 schematically shows solute transport process in a single fracture-matrix system on which the mathematical model is established. A non-reactive solute is injected into the fracture with half-aperture (b) at space y=0 by constant-concentration source (C_o) at constant flow rate. The solute concentration over outer boundary of matrix is assumed to be zero.

The main transport mechanism of solute though fracture is advection while diffusion is predominant mechanism of solute transport within matrix in the z-direction. In addition to solute diffusion within porous matrix, the solute diffusion is possible along matrix-fracture interface as well. It also assumed that diffusion in y-direction within matrix and longitudinal dispersion in fracture are negligible. Even though the fracture with high permeability provides a flow paths to transport solute, the rock matrix adjacent to the fracture is an important part in the overall solute transport process (Bodin et al., 2003).

The physical properties of rock matrix such as porosity and permeability affect on the quantity of solute transport in matrix-fracture systems through dispersion coefficient (Boving and Grathwohl, 2001).
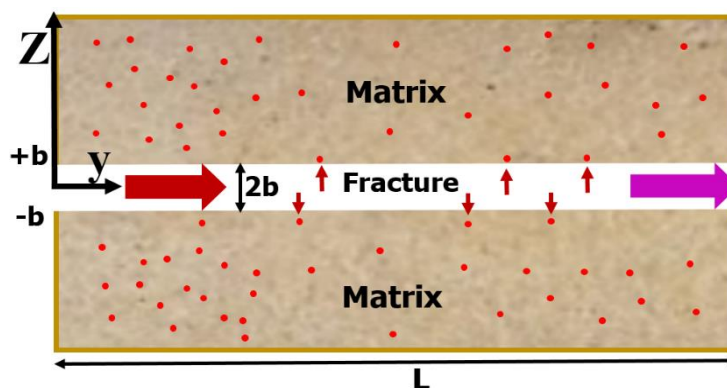
Figure 6.3. A schematic representation of solute transport in a single fracture-matrix system

For the fracture: dispersion coefficient in the fracture (Zou et al., 2016):

$$D = D_f = a_L u_y + D_m$$ (6.19)

Where D_f is dispersion coefficient in fracture; a_L is the longitudinal dispersivity along the fracture; u_y is fluid velocity in fracture; D_m is the molecular diffusion coefficient of solute in the fracture fluid.

For the porous matrix (u=0): dispersion coefficient= effective diffusion coefficient (D_e)

$$D = D_e = \tau D_m$$ (6.20)

Where D_e is effective diffusion coefficient of matrix; τ is the tortuosity of matrix; D_m is the molecular diffusion coefficient of solute.

The governing equation for solute transport in the fracture (Zhu et al., 2016; Zou et al., 2016):

$$\frac{\partial C_f}{\partial t} + u \frac{\partial C_f}{\partial y} - D_f \frac{\partial^2 C_f}{\partial y^2} - \frac{\phi D_e}{b} \frac{\partial C_m}{\partial Z}\Big|_{z=\pm b} = 0$$ (6.21)

Where C_f is solute concentration in the fracture; u is fluid velocity in fracture; D_f is dispersion coefficient in fracture; D_e is effective diffusion coefficient of matrix; b is the fracture half aperture; C_m is solute concentration in the rock matrix.

The equation for non-reactive solute transport and with a constant-concentration source and negligible longitudinal dispersion in the fracture can be described as follow

$$\frac{\partial C_f}{\partial t} + u \frac{\partial C_f}{\partial y} - \frac{\phi D_e}{b} \frac{\partial C_m}{\partial Z}\Big|_{z=\pm b} = 0$$ (6.22)

Moreover, the transverse diffusion within rock matrix as a dominant solute transport can be governed by:

$$\frac{\partial C_m}{\partial t} = D_e \frac{\partial^2 C_m}{\partial Z^2}$$

(6.23)

As solute concentrations in fracture and fracture surface are assumed to be equal over matrix-fracture interface, analytical solution for solute transport in the fracture and within rock matrix with respect to initial and boundary conditions as follows (Grisak and Pickens, 1981; Zhu et al., 2016):

For fracture:

$$C_f(y = 0, t) = C_o$$

(6.24)

$$C_f(y, t = 0) = 0$$

(6.25)

$$\frac{C_f(y,t)}{C_o} = erfc \left[\frac{\dfrac{\phi D_e}{ub} y}{2\sqrt{\dfrac{D_e}{u}(ut - y)}} \right] \quad \text{if} \ \ t > y/u$$

(6.26)

For matrix:

$$C_m(y, z = b, t) = C_f(y, t)$$

(6.27)

$$C_m(y, z = \infty, t) = 0$$

(6.28)

$$C_m(y, z, t = 0) = 0$$

(6.29)

$$\frac{C_m(y,z,t)}{C_o} = erfc \left[\frac{(\dfrac{\phi D_e}{ub} y) + Z - b}{2\sqrt{\dfrac{D_e}{u}(ut - y)}} \right] \quad \text{if} \ \ t > y/u$$

(6.30)

$$C_f(y,t) = C_m(y,z,t) = 0 \quad \text{if} \ \ t \le y/u$$

(6.31)

6.1.5. Breakthrough Curve in Continuous Tracer Injection

Tracer breakthrough curve is the concentration history of tracer with respect to time in a monitoring place. The increase of concentrations is an S-shaped curve rather than a step-function form in homogeneous porous media over continuous tracer injection. Whereas advection is responsible for bulk movement of tracer, the spread of the breakthrough curve is due to dispersion in homogeneous porous media (Crhribi and Chlendi, 2011).

Transport mechanisms of tracer in fractured porous media are advection and dispersion, the same as in homogeneous porous media. In fractured porous media, tracer is mainly transported by advection only through fractures while the predominant mechanism of tracer transport in porous matrix is dispersion. Dispersion in fractured porous media is caused by (1) mixing at fracture intersections, (2) variation in velocity due to variations in opening widths, (3) molecular diffusion and penetration into inter fracture of porous matrix blocks (Bozbiyik et al., 2017).

The shape of the breakthrough curves can be used to analyze matrix-fracture solute transport in fractured porous media. In the case of no-dispersion transport process, advection is only solute transport mechanism, so breakthrough curve is as a form of the plug flow. The dispersion within porous matrix flattens the breakthrough curve from the plug flow shape. The amount of spread in breakthrough curve practically depends on dispersion within porous matrix. Therefore, the high dispersion range results in an extended breakthrough curve over tracer transport process. Figure 6.4 shows the tracer breakthrough curves for different transport systems (Chowdhury et al., 2015; Patel, 2019).
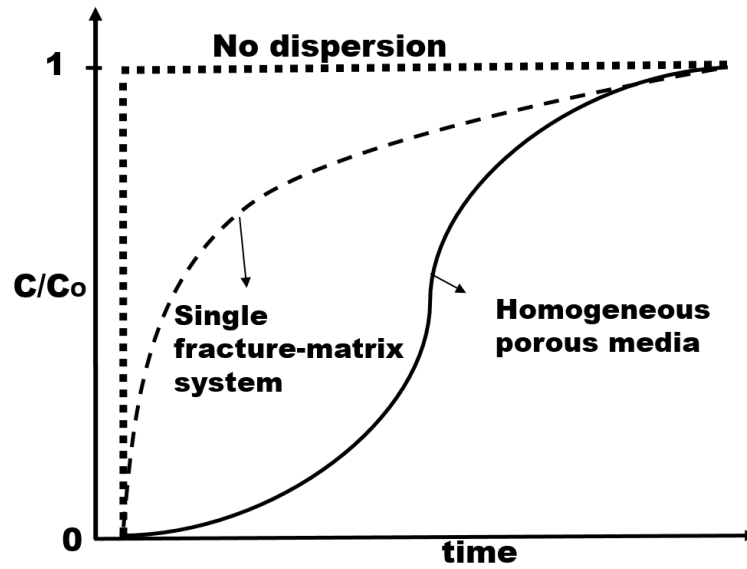
Figure 6.4. The effect of dispersion on the shape of tracer breakthrough curves in different types of porous media

It is observed that the flatness of a breakthrough curve in the single fracture-matrix system is more than that in no dispersion transport process and less than that in homogeneous porous media. It can come from the fracture that is responsible for the main portion of transport by advection, decreasing the effect of dispersion mechanism over solute transport in a single fracture- matrix system. Namely, in single fractured core plugs, tracer penetration into porous matrix blocks and dispersion within rock matrix spreads (flatten) the breakthrough curve from the steeper shape of initial portion of the curve in the case of no dispersion (Biswas and Mishra, 2015; Chowdhury et al., 2015).

6.1.6. Coupled Heat and Mass Transfers in Porous Media

The understanding of flow and transport phenomena (heat and mass transfers) through porous media become essential from view point of their numerous applications in

technological activities and enhanced recovery processes in oil and geothermal reservoirs (Reddy et al., 2010).

Heat transfer is a process by which internal energy from a material transfers to another one while mass transfer is the transport of matter (mass) through flowing media. In the systems involving simultaneous heat and mass transfer processes with concentration variation in different points, there is driving force for mass transport within the system from a point of higher concentration to that of a lower concentration to minimize the concentration difference along with heat transfer (Bird et al., 2002). Thus, it is of increasing interest to incorporate transport processes due to simultaneous occurrence of heat and mass transfers in nature and industries involving fluid flow in non-isothermal conditions (Reddy and Govardhan, 2015).

Coupled heat and mass transfers in the fractured porous media (fracture-matrix systems) over matrix-fracture interface by convection along fracture has many applications in the analysis of processes of practical interest such as enhanced geothermal systems, enhanced oil recovery, well stimulation, and solute/colloid transport in fracture-matrix systems. As the heat flux (energy rate per unit area) and the mass flux (mass flow rate per unit area) can be arisen from concentration gradient and temperature gradient, the relationships between the driven potential and the corresponding fluxes seem to be important. The heat (energy) flux due to mass concentration (composition) gradient is called the Dufour or diffusion-thermo effect. It results from isothermal mass concentration gradient. On the other hand, the temperature gradient can also cause mass flux and this is called "Soret effect" or thermal-diffusion effect (Pal and Chatterjee, 2013; Reddy and Rao, 2012).

In fact, Dufour and Soret effects represent the coupled heat and mass transfers in presence of fluid flow. In general, the Dufour and Soret effects are noticed as smaller-order magnitude than the transport mechanisms described by Fourier's and Fick's laws over transport related processes. Nevertheless, they are taken into account in

areas dealing with geosciences or hydrology such matrix-fracture transfers (Moorthy and Senthilvadivu, 2012).

6.1.7. Soret Effect (Thermophoresis)

As mentioned previously, it can be defined as a kind of mass transport process due to temperature gradient. In addition to the effect of matrix by dispersion or and diffusion mechanism within matrix, the Soret effect, which occurs in form of solute migration in fracture as a result of temperature gradient between fracture fluid and fracture surface ($T_{(Z)}$), can change concentration profile of solute along fracture plane over the duration of the tracer injection experiments in non-isothermal conditions through fracture-matrix systems. Figure 6.5 indicates the schematic representation of Soret effect due to temperature gradient between fracture surface and fluid in fracture in non-isothermal conditions.
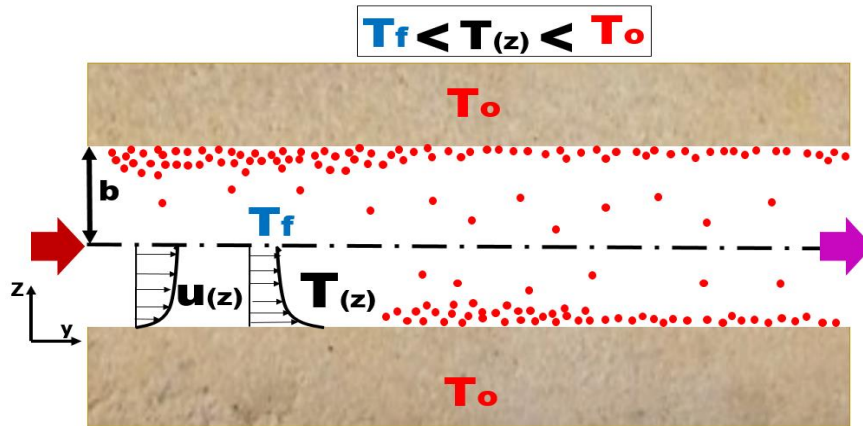
Figure 6.5. The Soret effect (thermophoresis) and temperature gradient in non-isothermal conditions

Along with dispersion/diffusion in fracture, solute particles can be moved in a fluid due to a non-uniform temperature field. The rate of concentration changes for solute due to temperature gradient is given by quantitative description:

$$\frac{\partial C}{\partial t} = \nabla \bullet \left[D\nabla C + \alpha C(1-C)\nabla T \right] \qquad (6.32)$$

Where D is the dispersion/diffusion coefficient; α is the thermal diffusion coefficient; and C is the solute concentration. The first term on the right hand side is the Fick' law of diffusion whereas the second term represents the mass migration because of the temperature gradient named "Soret effect" (Kuiken, 1994; Wiegand, 2004).

In fracture-matrix systems, the temperature gradient between fracture fluid and fracture surface causes the Soret effect involving in mass transfer in addition to advection and dispersion mechanisms along fracture. Because thermal properties of matrix (thermal conductivity and volumetric heat capacity) play a crucial role in establishment of temperature over fracture surface (matrix-fracture interface), in turn, assigning the temperature gradient between fracture fluid and fracture surface, the effect of thermal properties of matrix on mass transfer through Soret effect cannot be underestimated.

This can be explained by the fact that the matrix with high values of thermal properties produces the considerable Soret effect through constituting great temperature gradient in matrix-fracture systems.

In brief, thermal properties of matrix through Soret effect in fracture along with physical properties of matrix by dispersion/diffusion process within matrix lead to changes in the outlet concentration and concentration profile along fracture over non-isothermal tracer injection processes in matrix-fracture systems.

6.1.8. Calculation of Mass (solute) Remained in Matrix

Conservation of mass is usually used for mass balance of conserved quantity (Bergman et al., 2011; Bird et al., 2002):

(input of conserved quantity through the system boundary) -(output of conserved quantity through the system boundary) + (generation of conserved quantity within the system) -(consumption of conserved quantity within the system) = (accumulation of conserved quantity within the system)   (6.33)

Figure 6.6 illustrates the mass balance for a system where the solute transport occurs only in 1-D (y-direction).
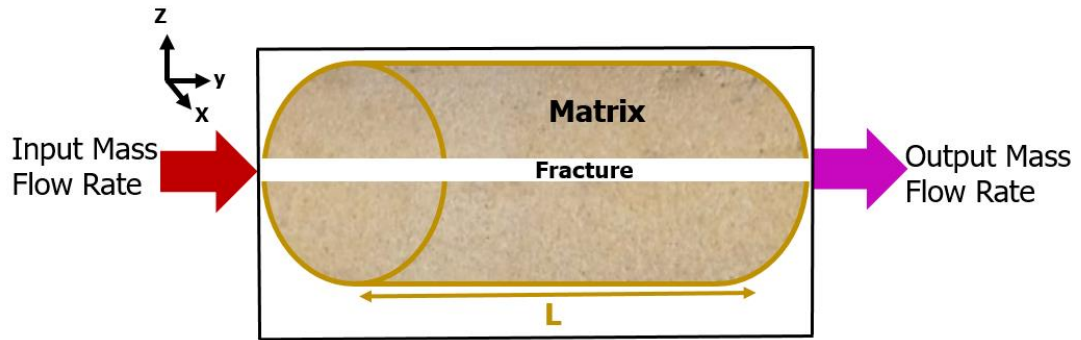
Figure 6.6. The mass balance of solute transport in a single fractured core plug

As the mass per unit time (mass flow rate) that enters or leaves is equal with (A.J) in the system, the mass balance for this case can be written in the following form:

(change of mass in the system in a time interval Δt) = (input mass flow rate) – (output mass flow rate)   (6.34)

$$V \bullet \frac{\partial C}{\partial t} = \left(A \bullet J_1 \right) - \left(A \bullet J_2 \right)$$ (6.35)

Where V is injection volume; C is solute concentration; A is cross section area; J_1 and J_2 are input flux and output flux

$$\frac{\partial C}{\partial t} = \frac{A}{V} \bullet (J_1 - J_2)$$ (6.36)

As the flux is changing in y-direction with gradient of $\dfrac{\partial J}{\partial y}$, so

$$J_2 = J_1 + \frac{\partial J}{\partial y} \bullet L \tag{6.37}$$

Finally, with the consideration of the control volume (A.L) the most general transport equation in y direction is:

$$\frac{\partial C}{\partial t} = -\frac{\partial J}{\partial y} \tag{6.38}$$

Namely, the change of concentration with time $\left(\dfrac{\partial C}{\partial t}\right)$ is simply given by the

difference of what flows in $\left(\dfrac{J_1}{L}\right)$ and minus what flows out $\left(\dfrac{J_2}{L}\right)$.

The mass per unit time remained in the injection volume corresponds to concentration changes as follows,

$$\frac{J}{L} = \frac{AJ}{AL} = \frac{\overset{\bullet}{m}}{V} \equiv \frac{\partial C}{\partial t} \tag{6.39}$$

$$\frac{\partial C}{\partial t} = \frac{C_{in} - C_{out}}{\Delta t} = \frac{\overset{\bullet}{m}}{V} \tag{6.40}$$

As inlet and outlet concentrations, time interval (Δt), and the injection volume (V) involving in flow are known, the mass of solute remained in matrix (m) is given by:

$$\frac{\overset{\bullet}{m}}{V} = \frac{C_{in} - C_{out}}{\Delta t} \tag{6.41}$$

$$m = \sum (\overset{\bullet}{m} \times \Delta t) \tag{6.42}$$

6.2. Solute Tracer Injection Experiments

The main objective of tracer injection experiment is obtaining tracer breakthrough curve as the history of tracer concentration at a detection point. It can typically be used to derive transport parameters by matching the experimental data to a transport model.

6.2.1. Single Fracture-Matrix System

In present study, four artificial fractured core plugs including heat flux sensor to measure heat flux and fracture temperature were used to conduct tracer injection experiments (Figure 6.7). The physical properties of core plugs were given in the Table 3.1.
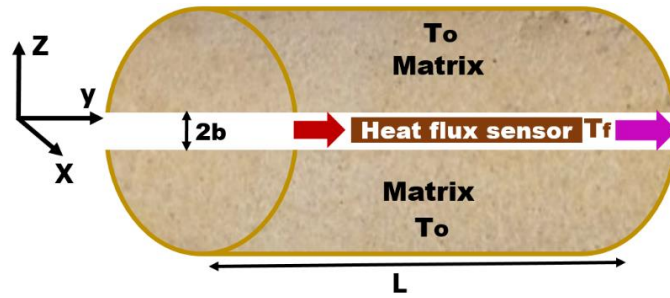
Figure 6.7. Tracer injection experiments

6.2.2. Tracer Solution

In general, fluorescent dyes are simply detected for water tracing even in nominal quantity by fluorometers. Therefore, Rhodamine B with molecular weight of 479.02 (g/gmol) (mark of Carlo Erba Reagenti) was used as a conventional and non-reactive tracer.

6.2.3. Experimental Procedure

The experimental procedure involves continuous injection of rhodamine B as the tracer (solute) with constant injection concentration (C_o) and injection temperature 30

°C (T_{in}) in a steady state flow. In all experiment runs tracer solution is injected into fractured core assembly at one end at constant flow rate 1 cc/min by a ISCO pump and accumulated from the other end with outlet concentration (C_{outlet}) in production collector system. The position of fracture plane and direction of flow is horizontal in all runs. Over the all flooding processes, the temperature of the rock sample's outer surface was maintained constant at temperature (T_o) of 70 ºC. When the desired initial temperature 70 ºC of core plug in the fracture is reached, this temperature is kept constant for at least an hour to guarantee that the whole core sample is heated up at constant and uniform temperature conditions.

After reaching the steady temperature within core plug, tracer solution is injected with constant concentration (C_o) and constant flow rate for 5 hours (300 minutes). The inlet cap is connected to a ISCO pump through the injection line. The injection line contains a thermocouple to measure the water inlet temperature(T_{in}) before entering fractured core assembly. Over tracer injection experiments, temperature in fracture and heat flux over matrix-fracture interface were measured by heat flux sensor, recording in time intervals 5 minutes by means of digital data logger. The tracer effluents were collected in production collector system at regular time intervals 5 minutes to measure their concentrations over the duration of the experiments to obtain tracer breakthrough curves.

6.2.4. Concentration Measurement of Tracer Solution

The most commonly used analytical method to determine the concentration of the solute is spectrometry. The principle of spectrometry is correlating the concentration of a species in solution to the amount of light it absorbs. The fluorescence spectrometry is a common technique in measurement of concentration based on induced fluorescence. The proper calibration procedure is applied to determine dye concentration relative to calibration standards.

After preparing the set of standard solutions with known concentration, the calibration procedure was carried out using Turner Quantech Digital Filter Fluorometer Model NO: FM109510-33 to measure the concentration of unknown samples.

Figure 6.8. Rhodamine B solutions and the fluorescence spectrometry

6.3. Results and Discussion

6.3.1. Experimental Measurements

The outlet Rhodamine B solution over tracer injection experiments through the single fractured core plugs were collected at regular time intervals 5 minutes to measure their concentrations by a digital fluorometer. Figure 6.9 shows tracer breakthrough curves for different core plugs at outer surface temperature 70 °C in flow rate 1 (cc/min) for 5 hours (300 min).
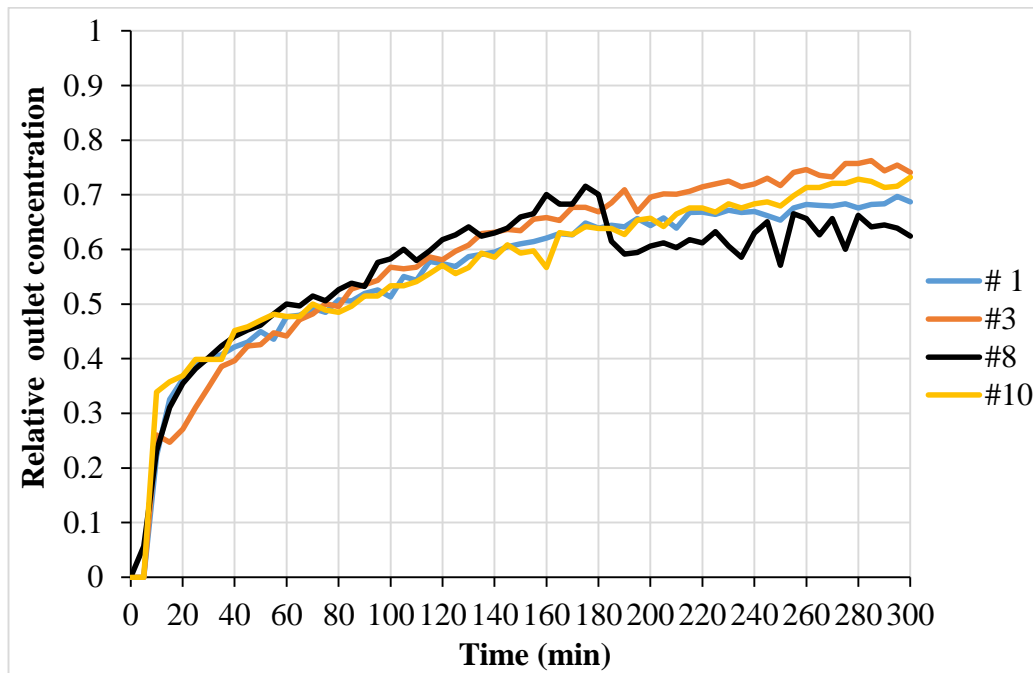
Figure 6.9. Experimental tracer breakthrough curve in flow rate 1 (cc/min) at outer temperature 70 °C for different core plugs

As the tracer is gradually exhausted in four core plugs, a portion of tracer is propagated into porous matrix by dispersion process over the duration of the tracer injection experiments. Consequently, dispersion is a determinant factor in solute transport in single fracture-matrix system.

As can be observed from experimental breakthrough curves that as time goes on, the outlet concentrations increase for all single fractured core plugs. This increase represents that advection is predominant mechanism of solute transport while a small portion of influent tracer is penetrated into rock matrix blocks as a result of dispersion.

As time progresses, the matrix storage capacity (pore volume) is gradually utilized causing large zone of rock matrix is saturated by tracer solution. Then the rise in outlet concentration continues until equilibrium is established between the solute stored in rock matrix and the solute present in fracture. In addition, the tracer effluents hover around a relatively steady value at the rest of tracer injection experiment.

As revealed by the experimental tracer breakthrough curves that steady values of relative outlet concentration depend on physical properties of porous matrix, especially, matrix permeability with the rest parameters fixed. The high value of permeability in porous matrix results in low relative outlet concentration over tracer injection experiments through single fractured core plugs. Figure 6.9 indicates that core plug #3 with lowest matrix permeability has the highest value of relative outlet concentration. In contrast, the lowest effluent concentration is for core plug #8 involving the highest value of matrix permeability. The reason for high outlet concentration over solute transport in single fracture-matrix system for matrix with low permeability is less amount of solute penetration into matrix through dispersion mechanism.

Also, the values of heat flux in matrix-fracture interface and fracture temperature were measured by a heat flux sensor over the duration of the tracer injection experiments at flow rate 1 (cc/min) and outer surface temperature 70 °C (Figures 6.10 and 6.11).
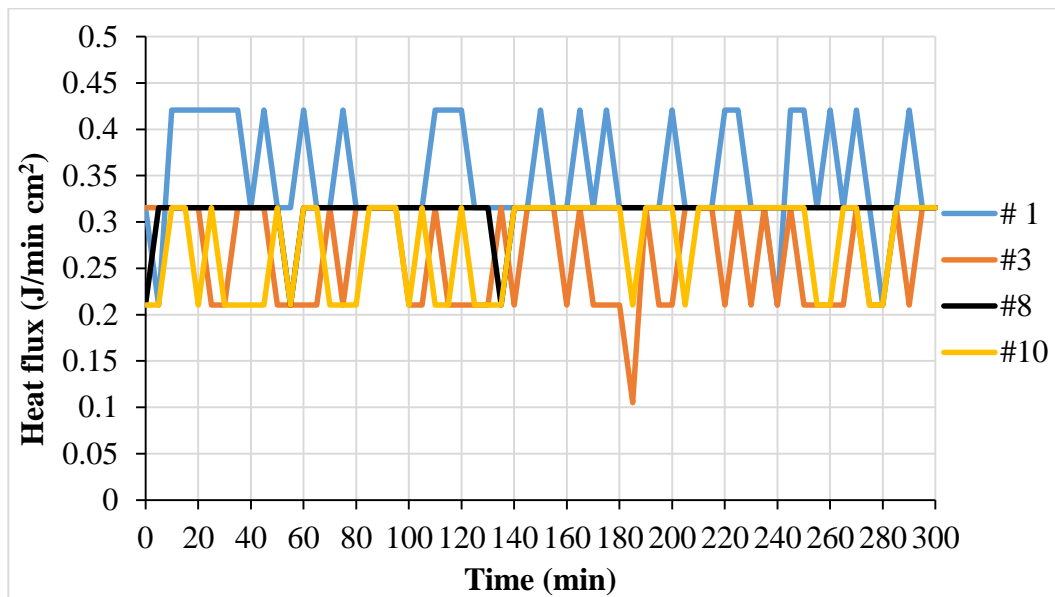
Figure 6.10. Experimental heat flux in flow rate 1 (cc/min) at outer temperature 70 °C for different core plugs

99
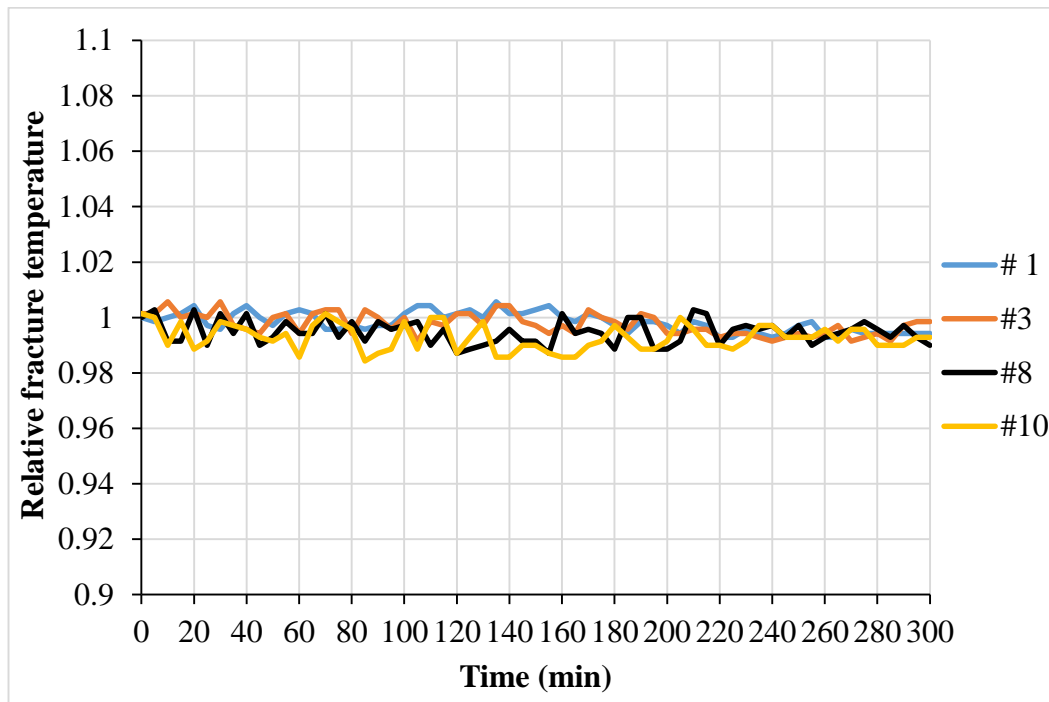
Figure 6.11. Experimental relative fracture temperature in flow rate 1 (cc/min) at outer temperature 70 °C for different core plugs

These figures illustrate that he thermal related values remains comparatively constant at this low flow rate 1 (cc/min) in spite of tracer solution injection for different core plugs. The steady values of experimental measurements are given in Table 6.1.

Table 6.1. *Experimental measurements of tracer injection in steady state conditions in flow rate 1 (cc/min) at outer temperature 70 °C*

Core plug	Matrix permeability (md)	Injection concentration (ppb)	Injection temperature (°C)	Relative outlet concent ration	Heat flux (J/min cm^2)	Relative fracture temperature (°C)
# 1	8.39	39	30	0.69	0.32	0.99
# 3	3.79	34	30	0.75	0.27	0.99
# 8	8.83	32	30	0.64	0.32	0.99
# 10	4.31	32	30	0.72	0.29	0.99

The forward difference in tracer outlet concentration at different time intervals can be used to analyze the matrix-fracture mass transfer (solute transport) over tracer injection through single fractured core plugs (Figure 6.12).
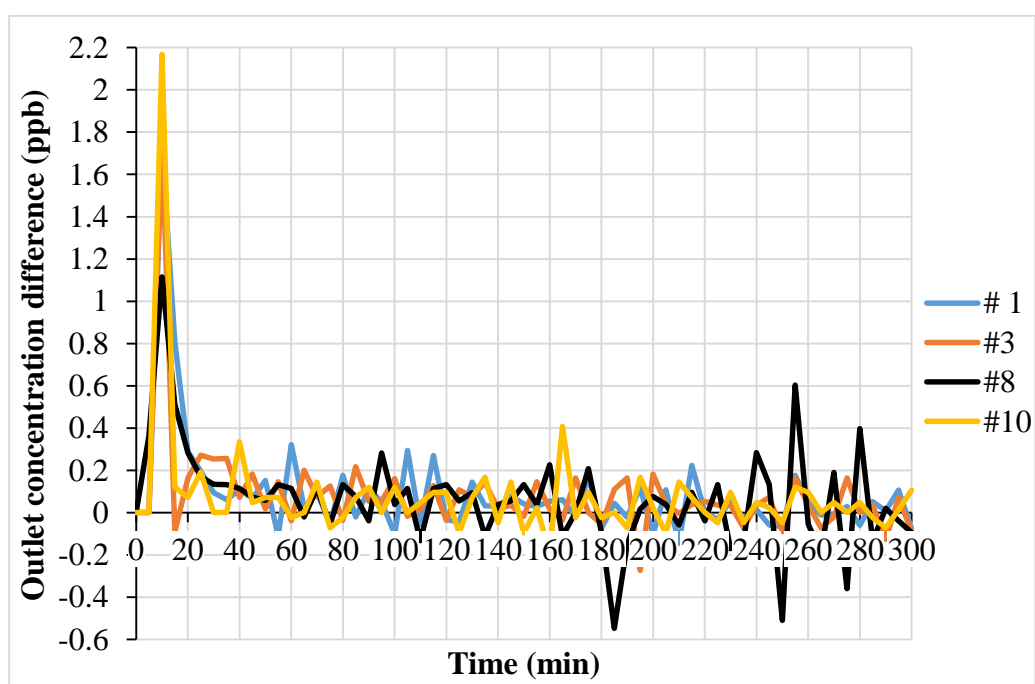
Figure 6.12. Forward difference trends of outlet concentration at flow rate 1 (cc/min) and outer temperature 70 °C for different core plugs

It can be observed in the Figure 6.12 that there are oscillatory trends in the forward difference of outlet concentration with respect to time intervals for all core plugs over tracer injection experiments. The upward and downward trends represent an increase and decrease in outlet concentration relative to preceding time interval, respectively.

The most significant reason behind oscillatory trends is the presence of reversible and reciprocal movements of solute (tracer solution) between porous matrix and fracture. The upward and downward trends in forward difference of outlet concentration can be interpreted as the solute transport from matrix to fracture and from fracture to matrix, respectively.

The amplitude of these oscillations in forward difference of outlet concentration is high in the early time of tracer injection period. The magnitude of fluctuations decreases in the rest of time intervals as a result of achieving an equilibrium in solute transport between porous matrix and fracture.

6.3.2. Calibration of Solute Transport Models

The solute transport through homogeneous and fractured porous media can be modeled then solved analytically and numerically. Tracer test can be used for characterization of porous media achieved by matching mathematical model for tracer transport to experimental data. As the values of porous media properties and transport parameters are the fitting parameters in the model, they are quantified and calculated over matching process.

6.3.2.1. Analytical Models

As there is difference between experimental data and the model's prediction for any given set of model parameters in the form of sums of squared error (SSE), finding the appropriate values of fitting parameters in the models contributes to minimize the sum of the square differences of data sets.

$$\sum (C_e - C_c)^2 \rightarrow Minimum$$

(6.43)

Where C_e is the experimental concentrations measured; C_c is the concentrations calculated by model

The fitting parameters used to fit the tracer concentration model to experimental measurement are peclet number (Pe) and dispersion coefficient (D) in homogeneous porous media Eq. (6.15) and effective diffusion coefficient (D_e) in fractured porous media Eq. (6.26). Practically, the estimation of transport parameters is searched by fitting models to real data in the tracer tests. The values of peclet number, dispersion coefficient, and effective diffusion coefficient for different core plugs were calculated by minimizing the summation of the square of differences by means of Microsoft Excel Solver as follows (Table 6.2):

Table 6.2. *The transport parameters of core plugs determined by analytical models*

| Core Plug | Matrix Permeability (md) | Injection Concentration (ppb) | Homogeneous Porous media | | Fractured Porous Media |
			Dispersion Coefficient (cm^2/min)	Peclet Number	Effective Diffusion Coefficient (cm^2/min)
# 1	8.39	39	2.88	0.23	0.73
# 3	3.79	34	1.74	0.38	0.59
# 8	8.83	32	3.86	0.16	0.90
# 10	4.31	32	3.03	0.22	0.72

In the case of homogeneous porous media, there is a reverse relationship between Peclet number and dispersion coefficient (Table 6.2). The quantity of Peclet number is used to determine the properties of porous media and dominant transport process.

The amount of Peclet number is the representative of the governing transport mechanism. The greater the Peclet number, the less dispersion (Charette et al., 2007).

Mass transfer (solute transport) in the single fracture-matrix system is different from homogeneous porous media in terms of fluid flow distribution. Because main portion of fluid is transported through fracture, velocity within porous matrix is assumed to be zero. That is why matrix dispersion coefficient is considered as the effective diffusion coefficient. It increases with rising the value of matrix permeability. Whereas core plug # 3 has the lowest effective diffusion coefficient 0.59 (cm^2/min) due to less matrix permeability. However, relatively large value of matrix permeability in the case of core plug # 8 causes the highest effective diffusion coefficient 0.90 (cm^2/min) (Table 6.2).

6.3.2.2. Numerical model

The history matching of experimental data was carried out using CMG-STARS simulator. Firstly, the parameters considered as input data for history matching process were investigated. To calibrate the solute transport model, data from tracer injection experiments were assumed as validation data. The main controlling parameter recognized for history matching of solute transport model is dispersion coefficient.

The experimental measurements of Rhodamine B concentrations in the fracture outlet were taken as the basis for numerical simulation. The fracture porosity, fracture permeability, matrix volumetric heat capacity, and matrix thermal conductivity parameters, which are determined in history matching process of thermal transport model, were considered as the fixed values. The values of dispersion coefficient in different directions (anisotropic dispersion coefficients D_x, D_y, D_z) as the parameter variations were iteratively modified until a satisfactory match of the numerical simulation output with the experimental measurements was achieved. Namely, to

align the simulated results with the measured values, the dispersion coefficient is varied (Table 6.3).

Table 6.3. *The dispersion coefficients used for calibration of the numerical model*

		Anisotropic Dispersion Coefficients (D_x, D_y, D_z)
	D_X	**$40 < D_X < 70$**
	D_y	**$50 < D_y < 80$**
Core Plug	Matrix Permeability (md)	**D_Z**
# 1	8.39	**$0.009 < D_Z < 1.3$**
# 3	3.79	**$0.0035 < D_Z < 0.75$**
# 8	8.83	**$0.01 < D_Z < 1.3$**
# 10	4.31	**$0.006 < D_Z < 0.9$**

As opposed to a constant value of dispersion coefficient to fit the analytical models, the anisotropic values of dispersion coefficients were assigned in the calibration of numerical model of solute transport in the single fractured core plugs (Table 6.3). The calibration determines a valid set of model parameters that enables the use of a simulated model for the prediction of flow and/or transport behavior for different scenarios of matrix-fracture solute transport (Dietrich et al., 2005).

The following Figures compare the results of analytical and numerical models calibrated with experimental measurements of tracer outlet concentration that were obtained in section 6.3.2.

Figure 6.13. Comparison of tracer breakthrough curves in flow rate 1 (cc/min) at outer temperature 70 °C for core plug #1
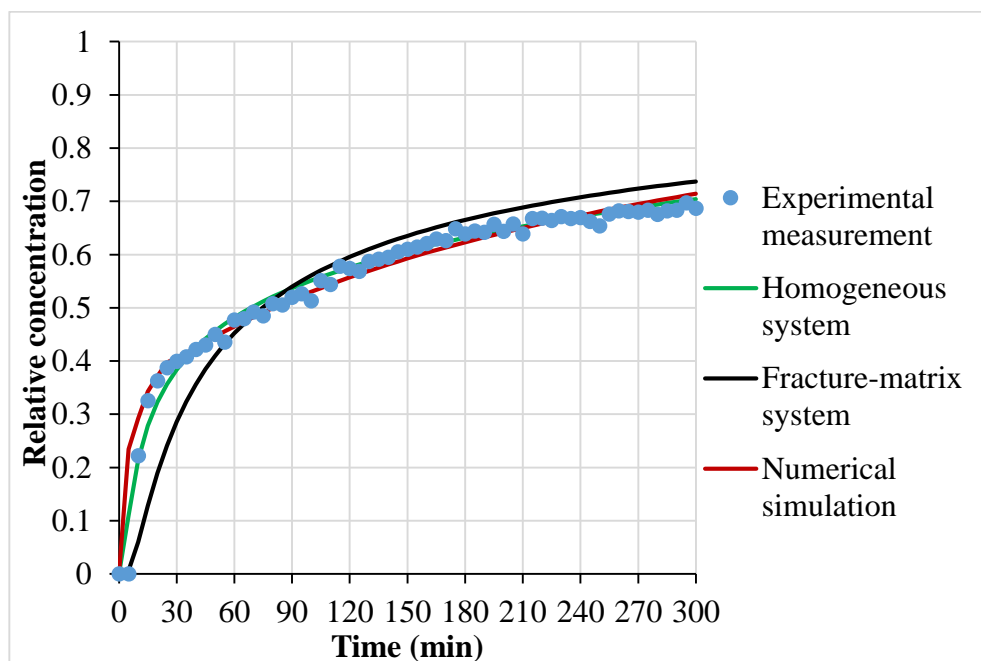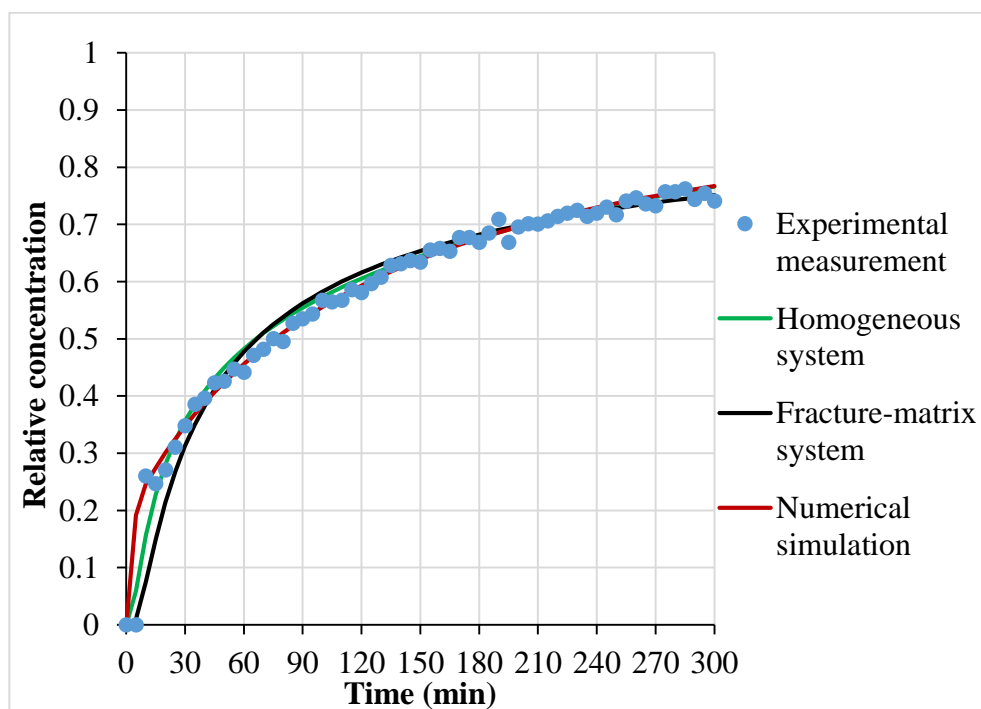

Figure 6.14. Comparison of tracer breakthrough curves in flow rate 1 (cc/min) at outer temperature 70 °C for core plug #3
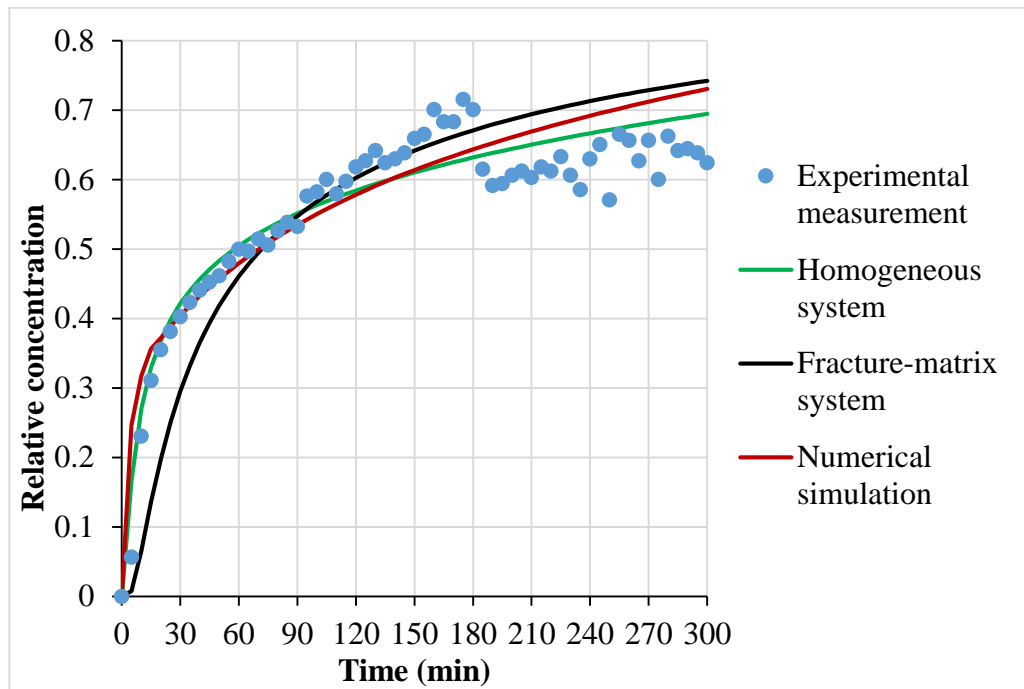
Figure 6.15. Comparison of tracer breakthrough curves in flow rate 1 (cc/min) at outer temperature 70 °C for core plug #8
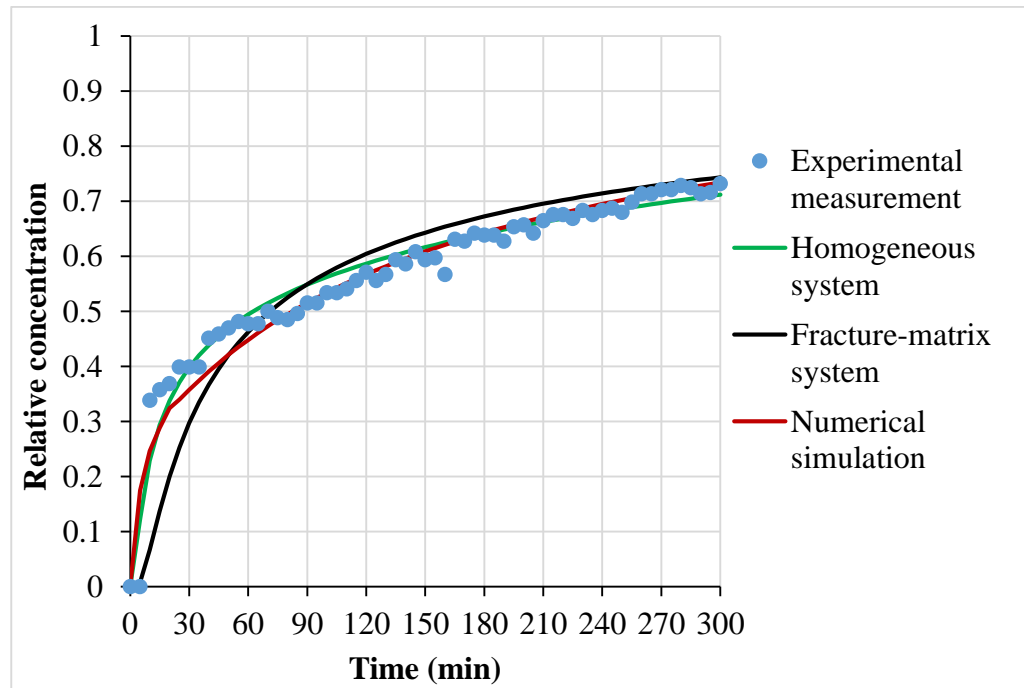
Figure 6.16. Comparison of tracer breakthrough curves in flow rate 1 (cc/min) at outer temperature 70 °C for core plug #10

Figures 6.13-6.16 illustrate that the numerical simulation results for the outlet concentration coincide very well with the experimental ones. This proves that our modeling framework is working well. The good agreement between these simulations and the experimental observations is to be expected because the values of fracture porosity, fracture permeability, and dispersion coefficient are chosen to match the experimental observed outlet concentration.

As single fracture-matrix system can be contrasted with homogeneous porous media in heterogeneity like as fracture providing a pathway for flow and mass transfer. Therefore, the assumptions related to fracture such as negligible longitudinal dispersion in the fracture and equality in concentration between fracture and fracture surface may affect the prediction of outlet concentration by analytical model pertaining to single fracture-matrix system Eq. (6.26).

Figures 6.13-6.16 indicate the noncompliance of outlet concentrations predicted by analytical model of matrix-fracture system with experimental results in the early time of tracer injection. However, as time progresses, this difference becomes less obvious. This trend may be clarified by the fact that solute concentration is not equal over matrix-fracture interface despite assumptions for analytical model in addition to the presence of dispersion in fracture. The numerical models will show the presence of difference in solute concentration between fracture and fracture surface and solute dispersion along fracture.

6.3.3. Sensitivity Analysis by Numerical Model

Since the numerical simulation of solute transport allows the best approximation of the model to the experimental outlet concentrations, the simulated outlet concentrations are in good agreement with values measured in fracture outlet. This represents the capabilities of CMG STARS to simulate these processes, and the calibration of the numerical model with experimental measurements.

The tracer breakthrough concentration, steady concentration profile in fracture, steady concentration difference of fracture and fracture surface (matrix-fracture interface), and mass remained in matrix can be used as a diagnostic tool in the assessment of the level of solute penetration from fracture into matrix.

As can clearly be seen an excellent agreement was achieved for both tracer breakthrough curve between numerical model and experimental results, the calibrated numerical models of core plugs were used to have a sensitivity analysis for investigation of the effect of flow rate and physical and thermal properties of matrix at outer temperatures 70 and 90 °C on solute transport and penetration into matrix.

The focus on some variables and core plugs makes it possible to investigate accurately and easily the solute transport. Thus, the core plugs # 1and # 3 and flow rates 0.25, 1.5, 5 (cc/min) were selected as the representatives for sensitivity analysis of solute transport over tracer injection scenarios.

6.3.3.1. Predicted Tracer Breakthrough Curve

The tracer breakthrough curves are various for two different core plugs with different physical and thermal properties. The difference in outlet concentration history for core plugs # 1and # 3 can be as a result of changes in flow rates of tracer injection and various outer temperatures 70 and 90 °C.

I)   The Effect of Flow Rate

Figure 6.17 shows the predicted tracer breakthrough curves in different flow rates of tracer injection at outer temperature 70 °C for core plug #3. For all core samples, the outlet concentration increases with increasing injection rate. The tracer breakthrough curve is hyperbolic character that represents a relatively lesser solute penetration from fracture into porous matrix for flow rate 5 (cc/min). On the other hand, it changes to parabolic in nature due to greater solute penetration into porous matrix in flow rate 1.5 (cc/min). At flow rate 0.25 (cc/min) the tracer breakthrough curve is almost linear indicating the highest solute penetration into matrix.
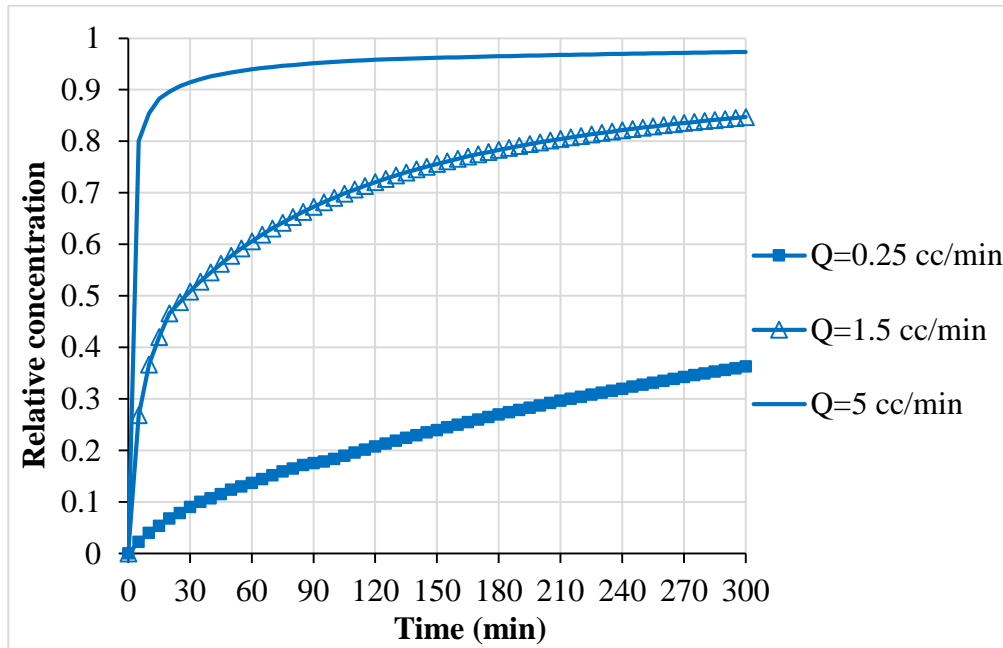
Figure 6.17. Predicted numerical tracer breakthrough curves in different flow rates at outer temperature 70 °C for core plug #3

The high injection rate decreases the contact time of the solute in fracture and fracture surface (matrix-fracture interface) contributing to a decline in solute penetration and an increase in relative outlet concentration. Therefore, the tracer breakthrough is appeared as a steeper curve. However, the tracer breakthrough curves become comparatively less steep with decreasing flow rate, reflecting an extended breakthrough curves as a result of high solute penetration into porous matrix at longer contact time.

II)   The Effect of Thermal Properties of Matrix

Figure 6.18 indicates the predicted breakthrough curves in flow rate 1.5 (cc/min) for core plugs #1 and #3 with different values of thermal properties of matrix at outer temperature 70 and 90 °C. It can clearly be seen that relative outlet concentration of core plug #3 is higher than that of core plug #1. Because of low value of dispersion coefficient in matrix, the core plug #3 has higher relative outlet concentration

compared to core plug #1 with high values of matrix permeability and dispersion coefficient.

Although physical properties of matrix (i.e. matrix permeability) control solute transport by dispersion within matrix in single fractured core plugs over tracer injection processes, as revealed by numerical models calibrated that the tracer breakthrough curves change with increasing outer temperature from 70 to 90 °C. Figure 6.18 illustrates that relative outlet concentration increases with rising outer temperature to 90 °C for core plug #3 while the relative outlet concentration decreases at high temperature for core plug #1.

Figure 6.18. Predicted numerical tracer breakthrough curves in flow rate 1.5 (cc/min) at outer temperatures 70 and 90 °C for core plugs

The main reason why the outlet concentration changes over tracer injection in the fixed flow rate and the same core plug in different outer temperatures of matrix can be attributed to Soret effect (section 6.1.7). As stated before that the Soret effect causes

solute or particle migration (mass flux) in fracture as a result of temperature gradient between fracture and fracture surface in matrix-fracture systems in the non-isothermal flowing tests.

The most important parameter in the formation of temperature gradient between fracture and fracture surface (matrix-fracture interface) in the matrix-fracture systems in the non-isothermal flow- through tests is thermal properties of matrix. Namely, the thermal properties of matrix through establishment of temperature gradient that causes Soret effect have a pivotal role on solute transport in matrix-fracture systems.

In fact, the trend of changes in tracer breakthrough curves is different for non-isothermal tracer testing at different temperatures. It is evident that there is a trend of rise in breakthrough curve for core plug # 3 as opposed to core plug # 1 that has a decreasing trend with increasing outer temperature from 70 to 90 °C (Figure 6.18). The reason behind this issue can be explained as follow.

III)   The Soret Effect and Thermal Properties of Matrix

As seen previously in chapter 5 (Thermal Transport in Single Fracture-Matrix Systems), the thermal properties of matrix are temperature dependent variables, and the values of thermal properties of rock matrix increase with rising outer temperature from 70 to 90 °C in all single fractured core plugs. However, the amount of increase in the values of thermal properties over outer temperature rise from 70 to 90 °C is various from a rock matrix to other ones. Table 6.4 indicates the amount of increase in the values of thermal properties over outer temperature rise from 70 to 90 °C for all core plugs. As can be observed from Table 6.4 that increase in the values of thermal properties in core plugs # 1 and # 8 are higher than that of core plugs # 3 and # 10.

Table 6.4. *The difference of thermal properties values of rock matrix at outer temperature 70 and 90 °C*

Core plug	Thermal Properties of Matrix	70 (°C)	90 (°C)	Increase Rate
#1	Thermal Conductivity (J/min cm °C)	3.5	4.5	1.0
	Volumetric Heat Capacity (J/cm³ °C)	12	14	2.0
#3	Thermal Conductivity (J/min cm °C)	1.9	2.5	0.6
	Volumetric Heat Capacity (J/cm³ °C)	5	5.8	0.8
#8	Thermal Conductivity (J/min cm °C)	2.5	3.5	1.0
	Volumetric Heat Capacity (J/cm³ °C)	8	13	5.0
#10	Thermal Conductivity (J/min cm °C)	2.3	2.4	0.1
	Volumetric Heat Capacity (J/cm³ °C)	9	9	0

In core plugs #1 and # 8 with relatively high increase in the values of matrix thermal properties over outer temperature rise from 70 to 90 °C, heat storage of rock matrix increases, becoming more hot. Thus, the establishment of high temperature over fracture surface (matrix-fracture interface) contributes to high temperature gradient between fracture fluid and fracture surface. This causes that more tracer solute migrates toward fracture surface (matrix-fracture interface) due to Soret effect over non-isothermal tracer injection processes in the single fracture-matrix systems. For

this reason, the amount of outlet concentration of solute decrease in the case of core plugs # 1 and # 8 at temperature 90 °C (Figure 6.19).
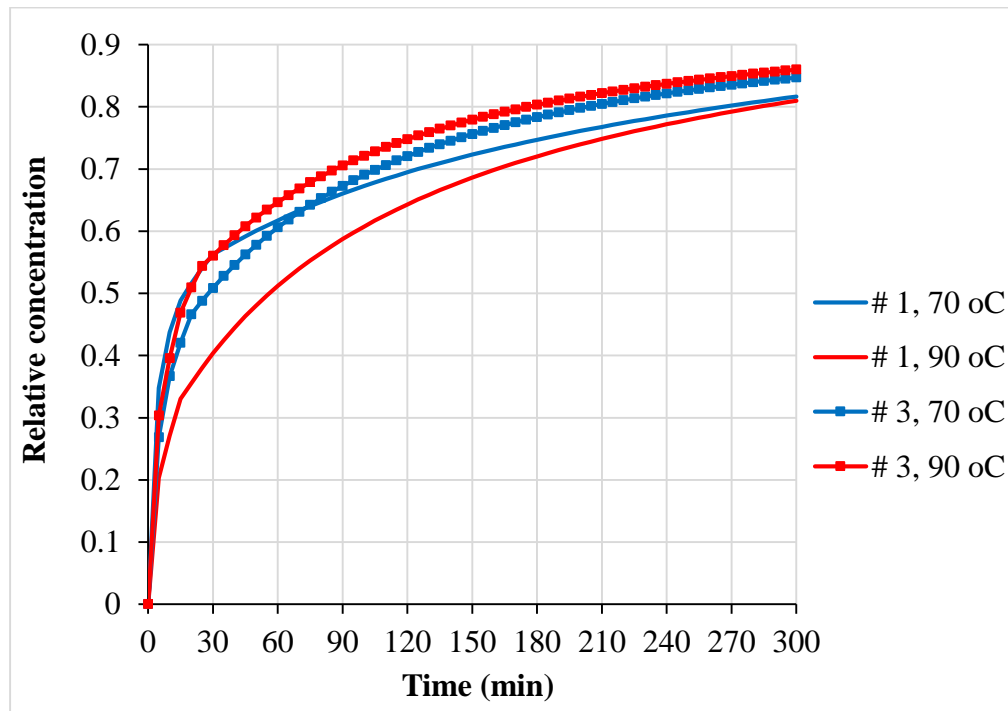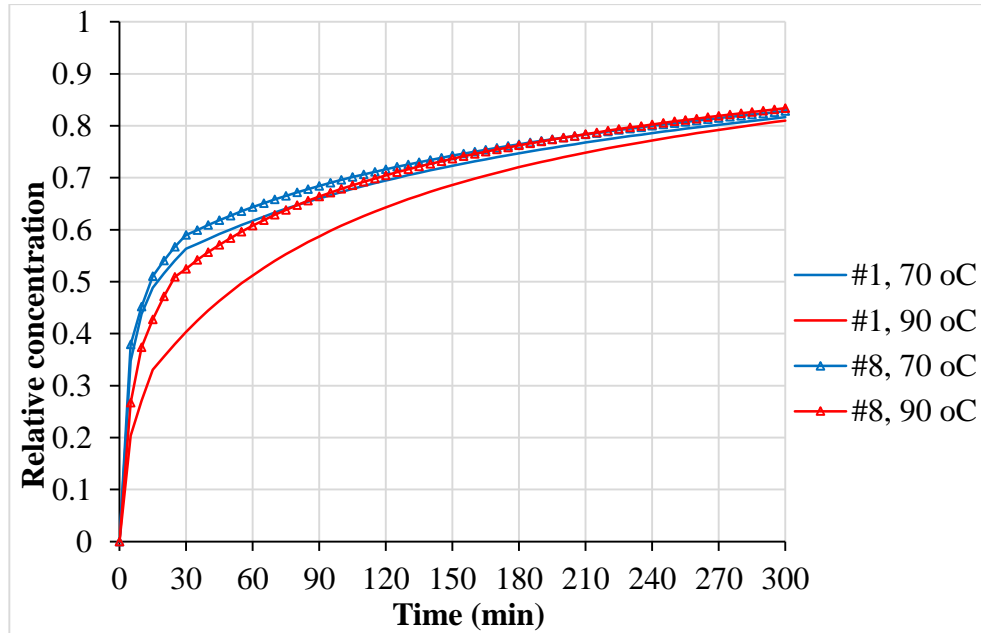

Figure 6.19. Predicted numerical tracer breakthrough curves in flow rate 1.5 (cc/min) at outer temperatures 70 and 90 °C for core plugs

On the other hand, in the case of core plugs # 3 and # 10 with relatively low increase in the values of matrix thermal properties over outer temperature rise from 70 to 90 °C, heat storage of rock matrix and temperature of fracture surface is low. Therefore, the Soret effect is less as a result of low temperature gradient between fracture fluid and fracture surface. Accordingly, the amount of outlet concentration of solute becomes increase in the case of core plugs # 3 and # 10 at temperature 90 °C (Figure 6.20).
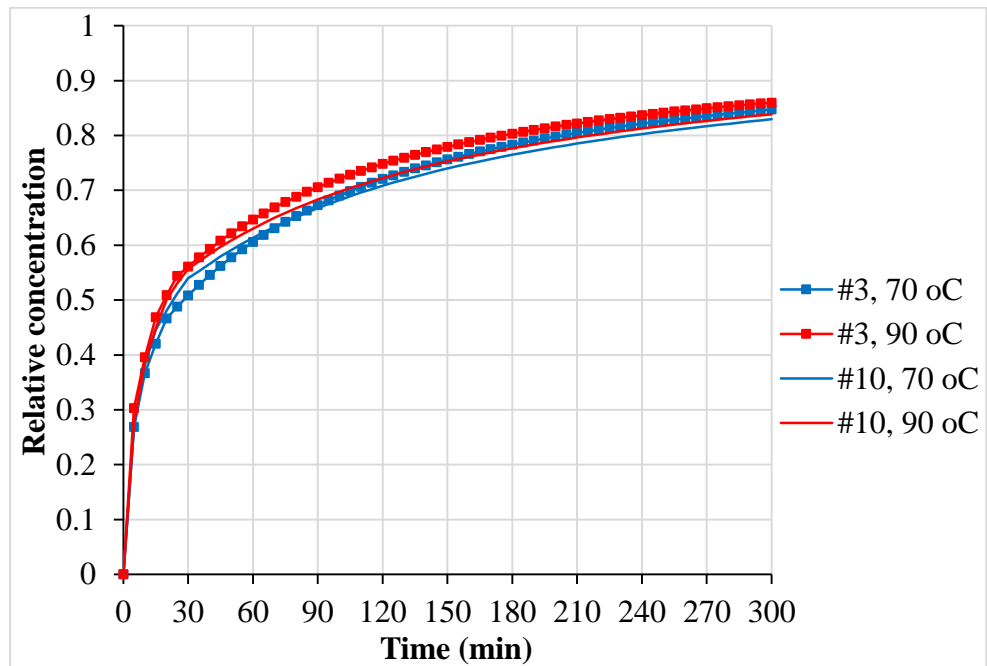
Figure 6.20. Predicted numerical tracer breakthrough curves in flow rate 1.5 (cc/min) at outer temperatures 70 and 90 °C for core plugs

6.3.3.2. Predicted Steady Tracer Concentration Difference in Matrix-Fracture Interface

I)   The Effect of Flow Rate

Figure 6.21 illustrates the steady concentration difference between fracture and fracture surface in different tracer injection rates at outer temperature 70 °C for core plug # 3. The various quantities of concentration difference along matrix-fracture in different flow rates represent that the concentration difference at inlet zone is higher than the rest of fracture length. In fact, it decreases exponentially, approaching to about zero at fracture outlet for all fractured core plugs.

Figure 6.21. Predicted numerical tracer concentration difference of matrix-fracture interface in different flow rates at outer temperature 70 °C for core plug #3

The large difference in tracer concentration between fracture fluid and fracture surface in near to fracture inlet of core plug can arise from more penetration of solute into porous matrix in this section compared to the other parts of fracture length. As the rate of solute penetration into matrix decreases, the difference of tracer concentration experiences a gradual decline in matrix-fracture interface.

As revealed by sensitivity analysis, the amount of concentration difference increases with rising injection rate, achieving the maximum difference at flow rate 1.5 (cc/min) for all core plugs. This trend starts to reduce with increasing in flow rate from 1.5 (cc/min) to higher rates. It can clearly be seen for core plug #3 as a representative core plug. This can be explained by the fact that the increase in flow rate causes large concentration difference along matrix-fracture interface due to more penetration of tracer into porous matrix by dispersion until flow rate 1.5 (cc/min). In continue of rise in flow rate, however, the short contact time of the solute in fracture and fracture

116

surface (matrix-fracture interface) in higher flow rate leads to decrease in solute penetration into matrix. Accordingly, this causes a decline in concentration difference (Fig 6.21).

II)   The Effect of Thermal Properties of Matrix

Figure 6.22 demonstrates the concentration difference along matrix-fracture interface in flow rate 1.5 (cc/min) for core plugs # 1and # 3 at different outer temperature 70 and 90 °C.

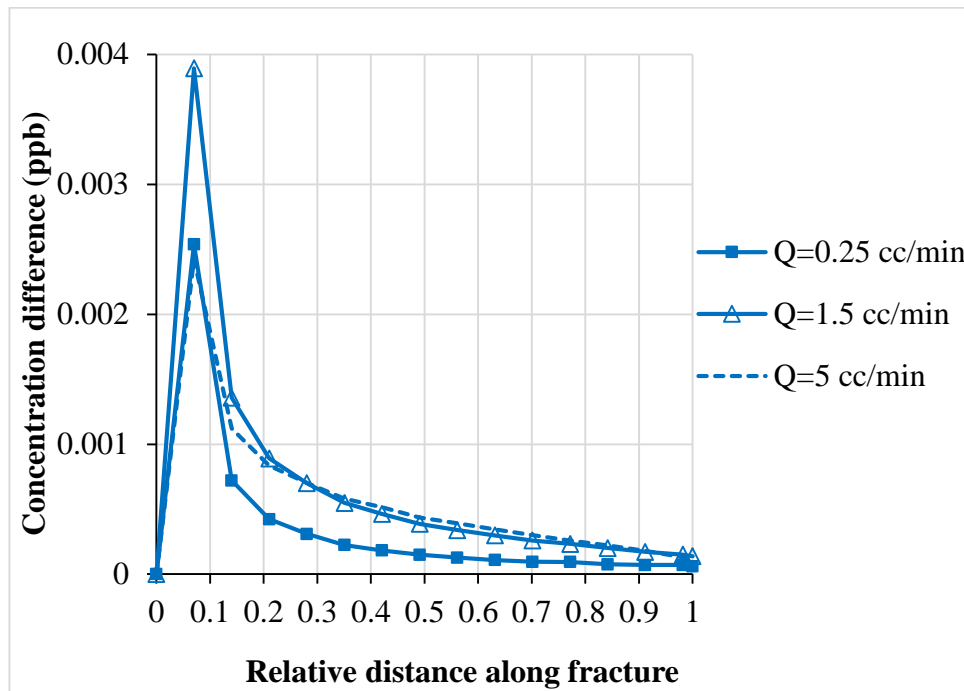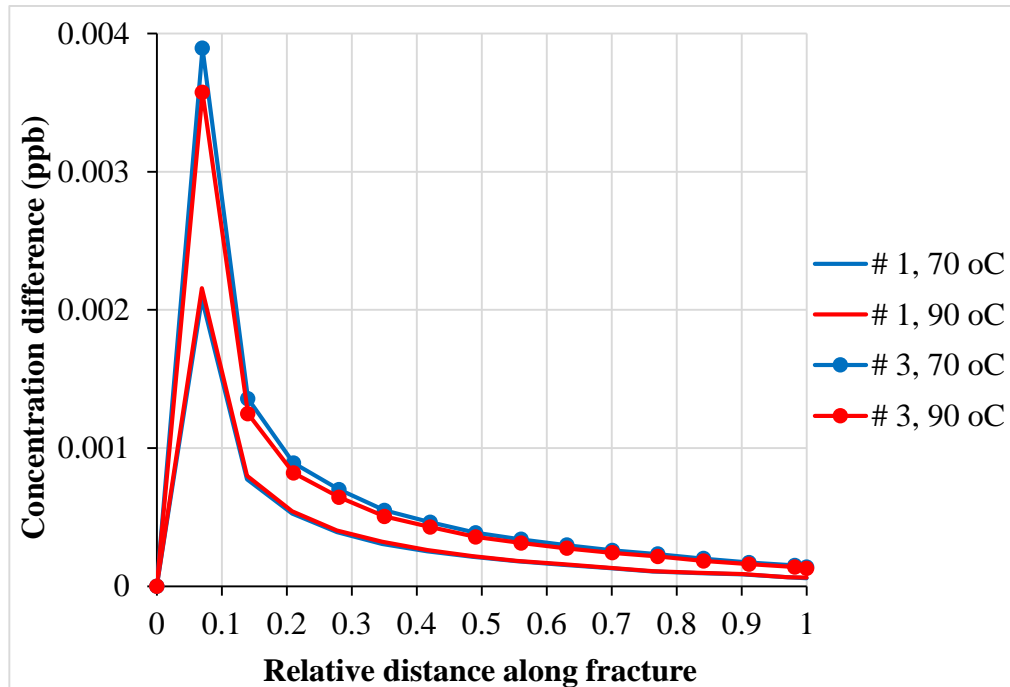*Figure 6.22.* Predicted numerical tracer concentration difference of matrix-fracture interface in flow rate 1.5 (cc/min) at outer temperatures 70 and 90 °C for core plugs

Furthermore, the various trends of changes in concentration difference in matrix-fracture interface for core plugs # 1 and # 3 as a result of increase in outer temperature from 70 to 90 °C can be revealed from Figure 6.22. This can come from thermal properties of matrix that is responsible for temperature gradient between fracture and

fracture surface. In the case of core plug # 3 the less Soret effect through low temperature gradient between fracture fluid and fracture surface is the reason for decrease in solute migration and concentration difference at 90 °C. In contrast, the concentration difference increases slightly at 90 °C for core plug # 1 as a result of large Soret effect through high rate of solute migration in great temperature gradient over non-isothermal tracer injection processes.

6.3.3.3. Predicted Steady Tracer Relative Concentration Profile along Fracture

I) The Effect of Flow Rate

The influence of tracer injection rate on tracer concentration profile along fracture was investigated at outer temperature 70 °C for core plug # 3 (Figure 6.23). The relative concentration undergoes a substantial decrease along fracture plane in low flow rate 0.25 (cc/min) while it increases, approaching to around 1.0 with rising tracer injection rate to 5 (cc/min). Figure 6.23 indicates that the large decrease in relative concentration in the case of low flow rates can come from longer contact time of solute in fracture with porous matrix causing more solute penetration into porous matrix. However, the relative concentration along fracture increases with a decrease in the rate of solute penetration in shorter contact time over high injection rate of tracer through fracture-matrix systems.

Figure 6.23. Predicted numerical tracer concentration profile along fracture in different flow rates at outer temperature 70 °C for core plug #3

It was observed that the decrease in the relative concentration at the fluid inlet zone is higher in comparison with the rest of fracture length in all flow rates. As seen in concentration difference along matrix-fracture interface (section 6.3.3.2), the high solute transport into matrix due to the relatively large concentration difference at the fluid inlet zone: This results in a considerable decrease in relative concentration at the fluid inlet zone compared to other zones of fracture length (Figure 6.23).

II)   The Effect of Thermal Properties of Matrix

The tracer relative concentration profiles along fracture in flow rate 1.5 (cc/min) for core plugs #1 and #3 with various thermal properties of matrix at outer temperature 70 and 90 °C were shown in Figure 6.24. As can be observed that the core plug # 1 has less relative concentration along fracture compared to core plug# 3 in the same

119

conditions as a result of high rate of solute dispersion from fracture into porous matrix with respect to great permeability in its matrix.

Similar to tracer breakthrough curves, the different trends of changes in steady tracer relative concentration along fracture for core plugs # 1 and # 3 in outer temperatures 70 and 90 °C can be seen over non-isothermal tracer injection processes (Figure 6.24). As stated previously in section (6.3.3.1), the high intensity of Soret effect in core plug # 1 because of high temperature gradient between fracture fluid and fracture surface results in decrease in the relative concentration along fracture for core plug # 1 over outer temperature rise from 70 and 90 °C.
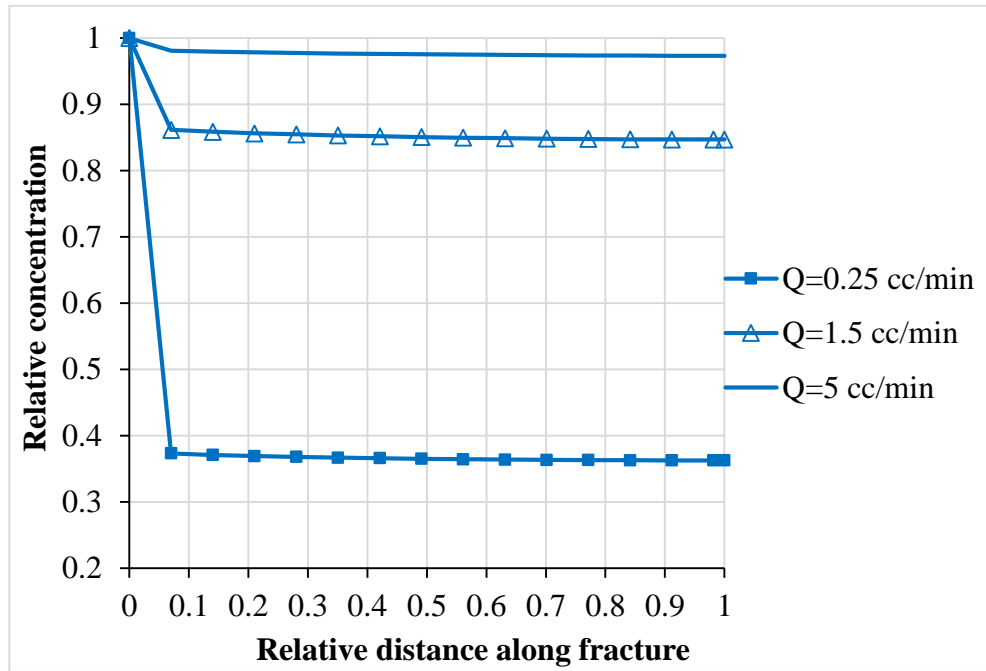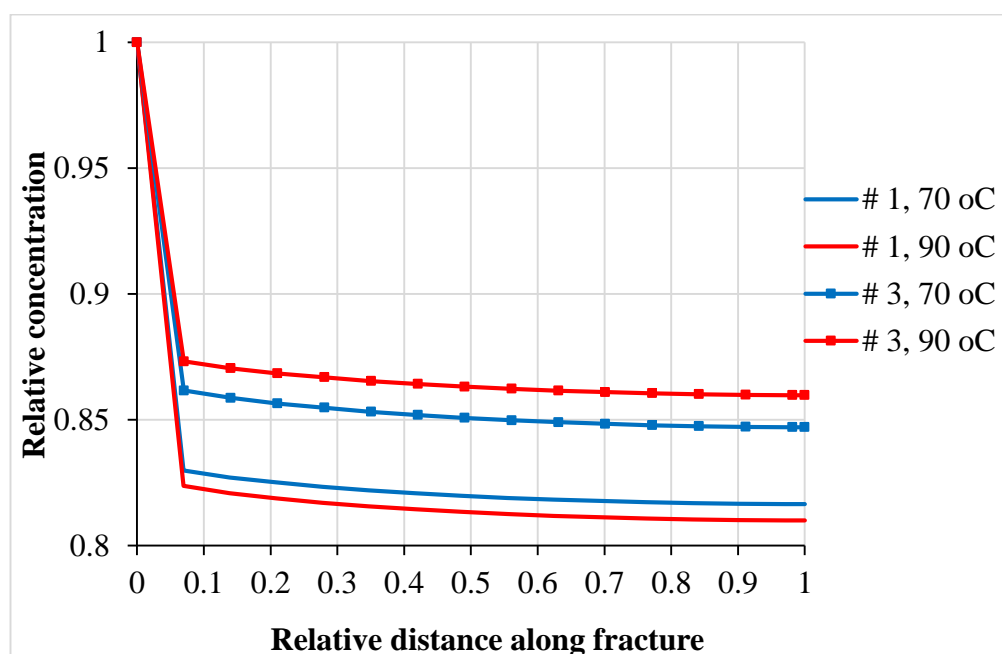

Figure 6.24. Predicted numerical tracer concentration profile along fracture in flow rate 1.5 (cc/min) at outer temperatures 70 and 90°C for core plugs

However, the low temperature gradient over matrix-fracture interface in the case of core plug # 3 due to its thermal properties of matrix makes a decrease in Soret effect over outer temperature rise. In fact, the decrease in the rate of solute migration from fracture fluid to fracture surface causes an increasing trend in the relative

concentration along fracture for core plug # 3 in non-isothermal tracer injection processes (Figure 6.24).

6.3.3.4. Predicted Relative Mass Remained in Matrix

As the amount of mass remained in porous matrix blocks represents the rate of mass transfer in matrix-fracture systems, it can be used to investigate the effect of different parameters involved in solute transport during non-isothermal tracer injection processes. The amount of solute remained in matrix blocks was calculated by mass balance at different pore volumes injected (flow rates) at outer temperatures 70 and 90 °Cover tracer injection processes (section 6.1.8). The trend of mass remained in porous matrix for different single fractured core plugs are shown in Figures 6.25-6.28.

I) The Effect of Flow Rate

Figures 6.25-6.28 indicate that the quantity of solute remained in matrix declines exponentially with rising pore volume injected (flow rate) at outer temperatures 70 and 90 °C for all fracture-matrix systems. As mentioned before the decline in contact time of tracer in fracture and fracture surface is responsible for less solute transport in fracture-matrix systems with an increase in injection rate. Consequently, the decrease in the amount of mass remained in matrix can be attributable to less solute transport process with rising flow rate.

II) The Effect of Thermal Properties of Matrix

Similar to tracer breakthrough curves and tracer concentration profiles, the Figures 6.25-6.28 show that the trend changes in the quantity of mass remained in matrix are different for various core plugs over outer temperature rise from 70 to 90 °C in non-isothermal tracer injection processes.

121

As illustrated previously in Table 6.4, temperature gradient between fracture fluid and fracture surface is large for core plugs # 1 and # 8 that causes an increase in the rate of Soret effect. Thus, the amount of mass remained in matrix increases through more migration of solute toward matrix at outer temperature rise to 90 °C (Figures 6.25 and 6.26).

Figure 6.25. Predicted numerical mass remained in matrix in different pore volumes injected and outer temperatures 70 and 90 °C for core plug #1

Figure 6.26. Predicted numerical mass remained in matrix in different pore volumes injected and outer temperatures 70 and 90 °C for core plug #8

In the case of core plugs # 3 and # 10 with relatively low temperature gradient between fracture fluid and fracture surface, however, the solute migration into porous matrix decreases over outer temperature rise from 70 to 90 °C. Therefore, the less Soret effect is main responsible for decline in amount of mass remained in matrix at outer temperature 90 °C (Figures 6.27 and 6.28).
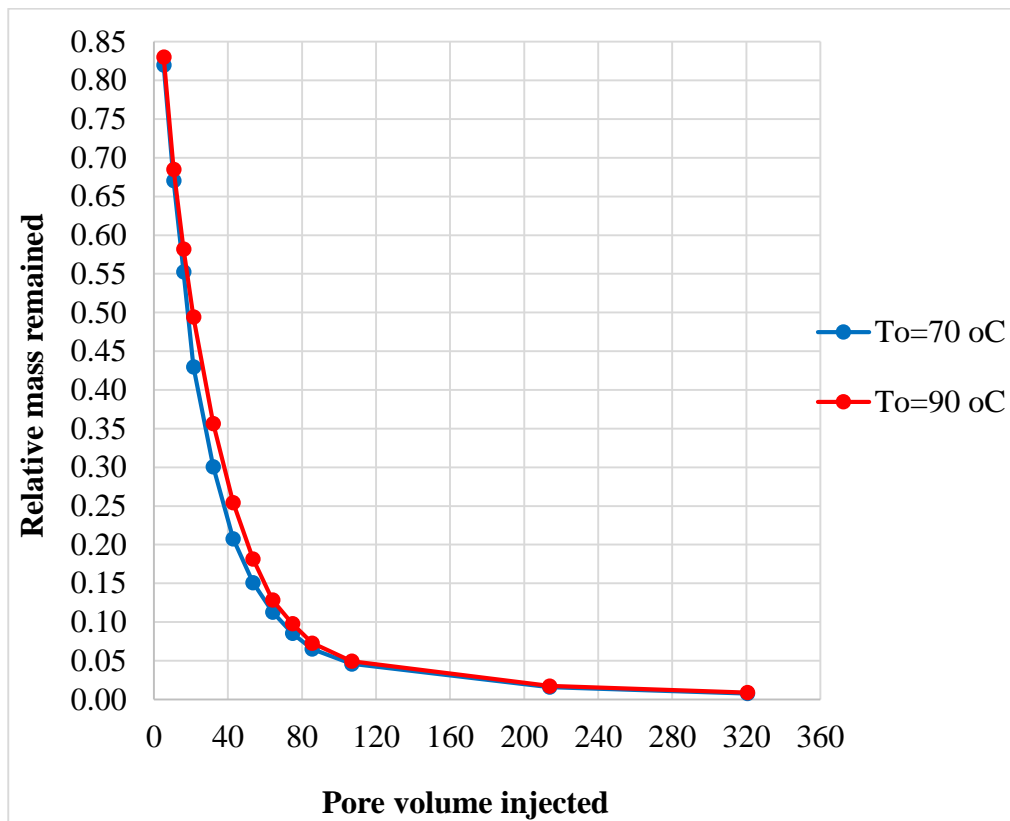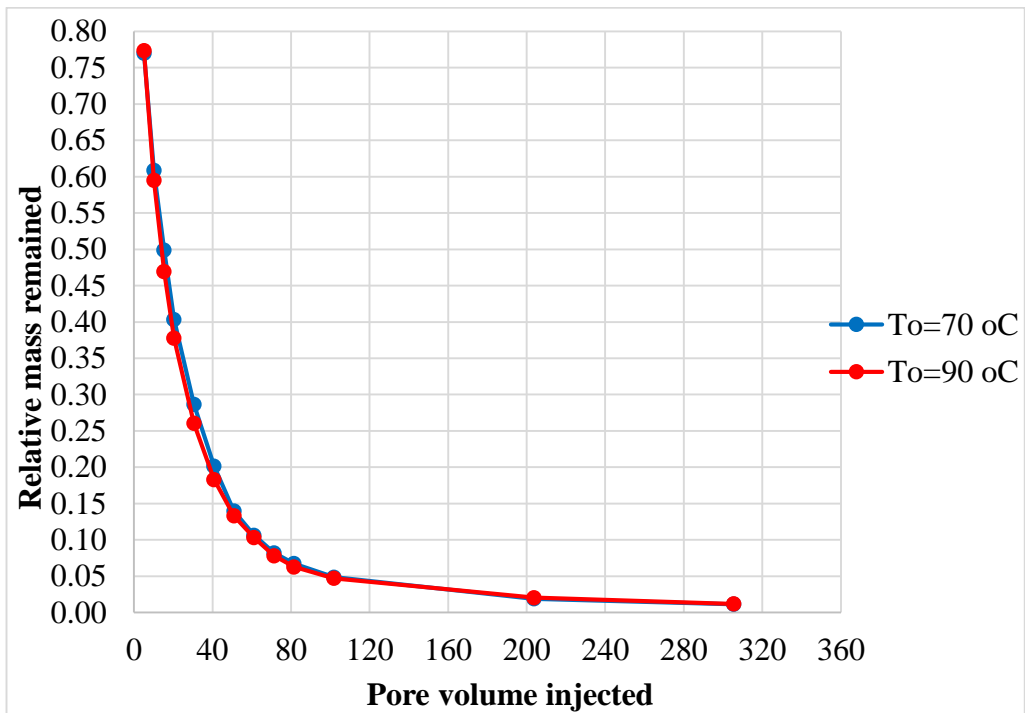
Figure 6.27. Predicted numerical mass remained in matrix in different pore volumes injected and outer temperatures 70 and 90 °C for core plug #3
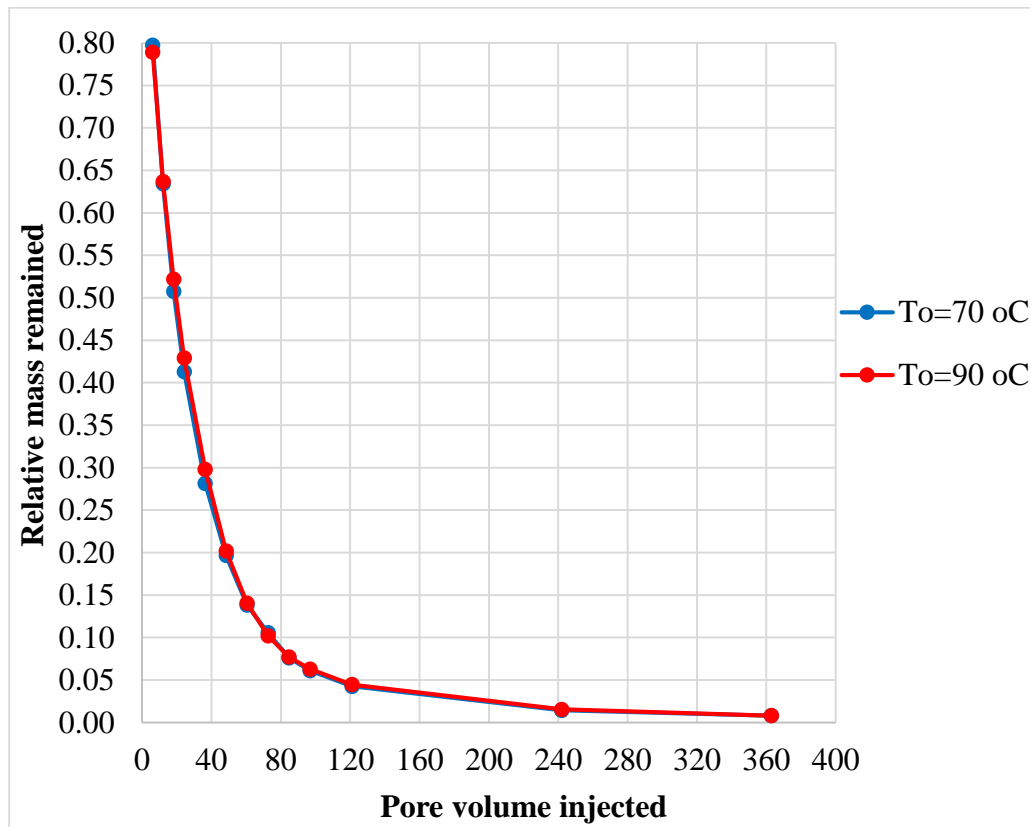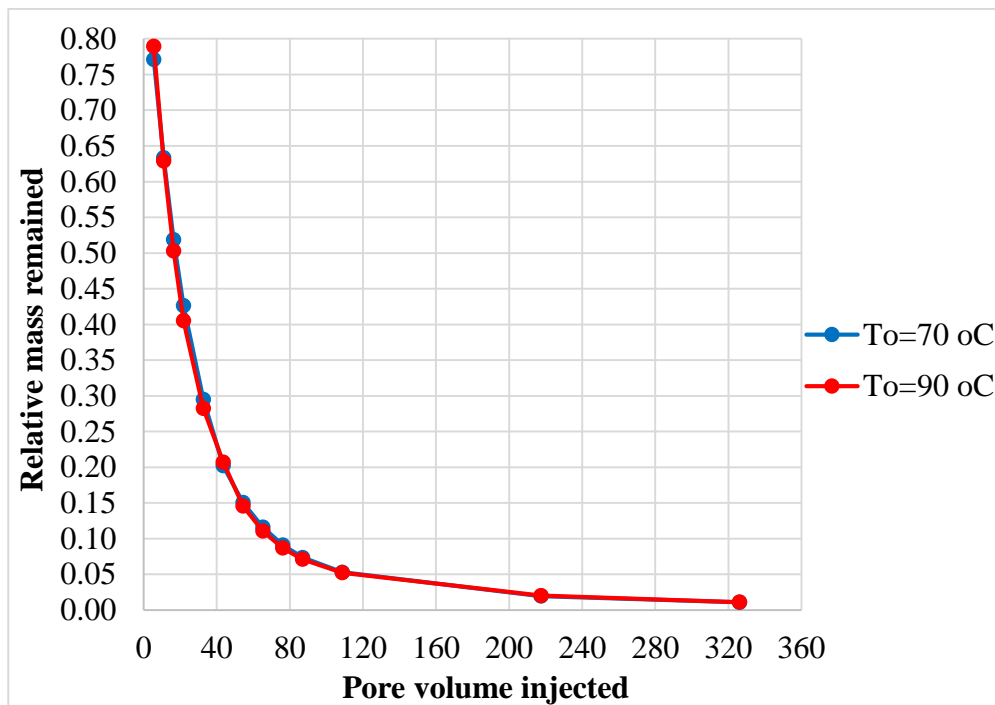

Figure 6.28. Predicted numerical mass remained in matrix in different pore volumes injected and outer temperatures 70 and 90 °C for core plug #10

A precise observation of the Figures 6.25-6.28 indicates that the difference in the amount of mass remained in matrix at outer temperatures 70 and 90 °C is appeared only in the low pore volumes injected (low flow rates) as a result of Soret effect while this difference comes to disappear at high pore volumes injected (high flow rates) over non-isothermal tracer injection through fractured core plugs.

Where pore volume injected (flow rate) is relatively low, the Soret effect has an overwhelming influence on the amount of mass remained in porous matrix through matrix-fracture mass transfer in non-isothermal conditions. Thus, the dependency of the Soret effect upon flow rate was investigated by tracer breakthrough curves of numerical model.

III)   The Soret Effect and Flow Rate

Figures 6.29 and 6.30 illustrate the tracer breakthrough curves in different flow rates at outer temperature 70 and 90 °Cover tracer injection process. They show that the difference in tracer breakthrough curve at high flow rates is negligible compared to low flow rates. This can come back to Soret effect in non-isothermal tracer testing. Namely, Soret effect can be considered as an effective parameter in solute transport at a particular flow rate interval over non-isothermal tracer injection processes.

Figure 6.29. Predicted numerical tracer breakthrough curve in different flow rates and outer temperatures 70 and 90 °C for core plug #1
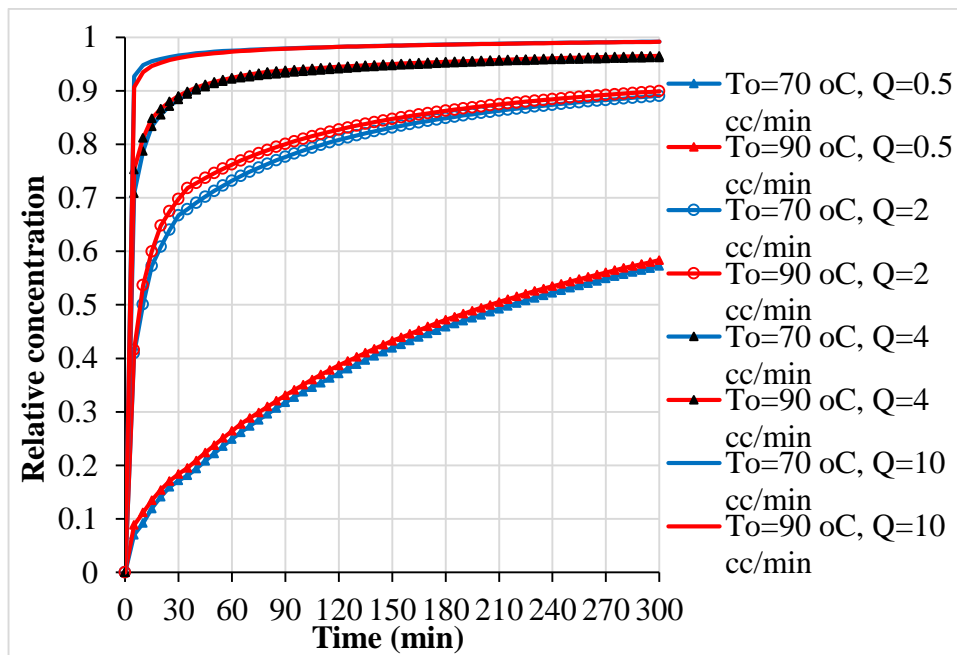
Figure 6.30. Predicted numerical tracer breakthrough curve in different flow rates and outer temperatures 70 and 90 °C for core plug #3

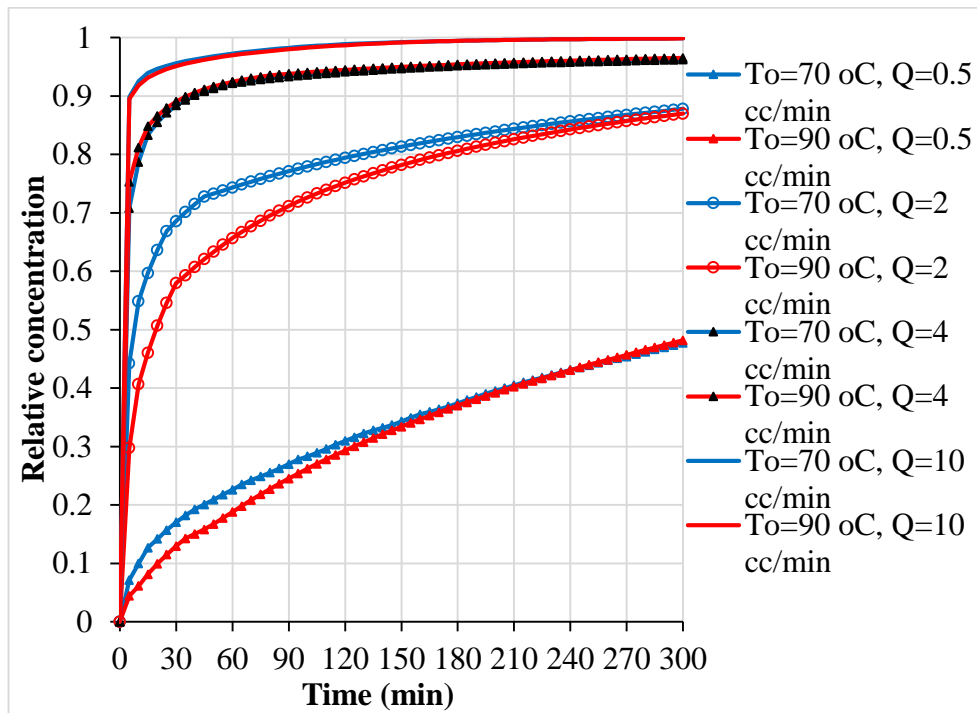Thus, Figures 6.29 and 6.30 represent the reason for dependency of the difference in mass remained in matrix at outer temperature 70 and 90 °C in a particular range of pore volumes injected in non-isothermal tracer injection through fracture-matrix systems.

CHAPTER 7

PARTICLES TRANSPORT IN SINGLE FRACTURE-MATRIX SYSTEMS

7.1. Theory

Micro/Nano-fluids can be defined as the dispersion of Micro/Nano particles in a solution liquid like water. The flow of suspended particles through porous media mainly takes place in different areas such as environmental, chemical, civil, and petroleum engineering (Malgaresi et al., 2019). The migration of particles in Nano and Micro scales has attracted many attentions in the large number of applications pertaining to contamination treatment and areas of energy extraction. Micro/Nano fluids have taken a wide interest in the energy sector such as fixing processes to prevent formation damage, enhanced oil recovery, enhanced geothermal systems, and well stimulation processes (Abdelfatah et al., 2017).

Despite the fact that the advancements in Nano-science contributes oil and gas industry for exploration and production, the complicated local conditions such as salinity, permeability, reservoir heterogeneities provide serious challenges in the case of application for Micro/Nano particles (Abdelfatah et al., 2017).

The irreversible attachment to the rock grain surface provides the primary retention mechanism in transport of colloidal particles through porous media. To predict flow, advection is predominant transport mechanism in particle transport through porous media, in addition to confined hydrodynamic dispersion and Darcy's law (Yu et al., 2012).

Making functional Micro/Nano fluids involves novel material syntheses and new reservoir engineering approaches to determine reservoir parameters based on their transport properties (Alaskar et al., 2012). In other applications of suspended particle tracers, they are developed to be Micro/Nano sensors to acquire reservoir pressure and

temperature at formation and near to wellbore. Fines migration are controlled using hydraulic fracture proppant with nanocrystals without decreasing productivity (Yu et al., 2012).

The conventional solution tracers provide insufficient information about characterization of fractured porous media, in contrast to suspended Micro/Nano particle tracers which are able to evaluate pore-scale properties of the fracture and matrix. As a portion of conventional solution tracers tends to penetrate into matrix by dispersion\ diffusion that is responsible for retardation and problem in characterization. However, the Micro/ Nano particles tracers are useful to characterize fractured porous media due to their physically and chemically-modified properties. (Li et al., 2014).

The transport of suspended Micro/Nano particle through fractured porous media is used to understand the controlling transport mechanisms, improving the analysis of transport process at the molecular level. In fact, the transport behavior can be used to characterize the size, shape, and connectivity of fracture network (Yu et al., 2012).

There are many factors involved in the particle transport such interstitial fluid velocity, solution properties, temperature, and other particles interactions. Therefore, particles should be stable in suspension and disperse in solution. The transport behavior of particle in fracture can be influenced by advection, dispersion, adsorption, desorption, physical straining and air-water interface capturing (Alaskar et al., 2014).

In the case of particle transport, Micro/Nano particles have to be safe to handle and environmentally friendly matter in porous media. The stability of particles suspension and dispersion in solution are crucial conditions during suspended tracer testing processes. In addition, the cohesion of Micro/Nano particles to matrix grains and non-reactivity with matrix grains should be verified (Alaskar et al., 2012).

The transport of Micro/Nano particles suspension in fractured porous media is commonly faster than that of solution tracers. The kind of shape in breakthrough curve of Micro/Nano particles tracer can be attributable to the collision of Micro/Nano

particles with matrix grains. In fact, the rate of particle-matrix attachment determines the breakthrough time of Micro/Nano particles. The absence of particles penetration into surrounding matrix in matrix-fracture systems provides fast-moving flow in fracture and thus faster breakthrough of suspended particle tracer (Alaskar et al., 2014).

The enhanced particles transport through fracture-matrix systems can arise from particles sizes, charge expulsion, and Taylor dispersion. The large size of particles compared to pores throat size in porous matrix can cause such size exclusion at inlet grains that particles circulate through fracture. When both particles and grain surfaces have similar charge, an electrostatic repulsive barrier forces makes the particles away from grain surfaces into flow streamlines within fracture. In addition, Taylor dispersion can be caused by increase in particle size, enhancing particles transport by preventing particles migration from high velocity streamline in fracture, in turn, and the lack of dispersion/diffusion into porous matrix in the fractured porous media (Alaskar et al., 2014).

The size and shape of particles and flow channel are the main factors for physical straining of particles. Particles are physically trapped in the fracture with small aperture. Also, particles with larger size than surrounding pore throat prevent the rest of particles from further penetration. On the other hand, particles with smaller size than surrounding pores throat may diffuse into the porous matrix increasing the rate of collision with matrix grains and thus further particles filtration. In fact, matrix diffusion is proportional to matrix porosity and inversely proportional to flow rate in fracture and particle size (Alaskar et al., 2014).

While Micro/Nano particles are expected to migrate in high velocity streamlines, gravity force is an important factor providing the conditions for particle filtration in porous matrix. Similar to diffusion mechanism for particles transport, the fluid velocity determines gravitational sedimentation (Bagalkot and Kumar, 2018).

In general, the fluid advection and gravity settling as well as matrix diffusion govern the particles transport over particle suspension injection through fractured porous media. The gravity settling makes particles breakthrough time slower. In fact, the rate of settling is proportional to the square of the particles diameter while diffusion is inversely proportional to particles sizes (Bagalkot and Kumar, 2018).

7.2. Micro Particles Tracer Injection Experiments

In our study the suspension of micro particles based on melamine resin, Rhodamine B-marked size 1µm was applied in tracer injection experiments. Then the results were compared with those of Rhodamine B solution to evaluate their performance in the fractured porous media characterization. The injection process and sampling strategies in all experiments are similar to the solute tracer injection experiments in the four single fractured core plugs (section 6.2).

7.2.1. Micro Particles Tracer Suspension

In order to investigate particle transport in matrix-fracture system, micro particles based on melamine resin, Rhodamine B-marked size 1µm (mark of Sigma- Aldrich) was used as a micro particles tracer. This micro particles tracer is made up of an aqueous polycondensation of methylol melamine without surfactants and the micro particles of Rhodamine B. The density of micro particles is 1.5 (g/cm^3) with thermal stability up to 300 °C. While surfaces of particles are hydrophilic, they are stable in acidic and basic solutions.
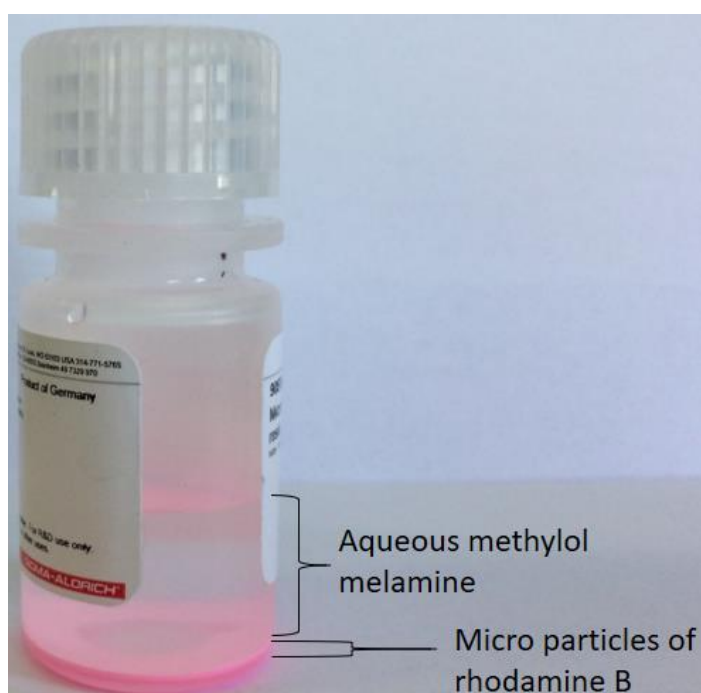
Figure 7.1. Micro particles based on melamine resin, Rhodamine B-marked size 1µm.

7.2.2. Concentration Measurement of Micro Particles Tracer Suspension

As the micro particles of Rhodamine B in tracer suspension are induced fluorescence, the concentration measurements of micro particle suspensions were carried out by the fluorescence spectrometry similar to Rhodamine B solutions (section 6.2). Thus, Turner Quantech Digital Filter Fluorometer Model NO: FM109510-33 was used to measure the concentration of unknown samples.

7.3. Results and Discussion

7.3.1. Experimental Measurements

The outlet Rhodamine B suspensions over tracer injection experiments through the single fractured core plugs were collected at regular time intervals 5 minutes to measure their concentrations by a digital fluorometer. Figure 7.2 shows tracer breakthrough curves for different core plugs at outer surface temperature 70 °C in injection rate 1 (cc/min) of micro particles suspension for 5 hours (300 min).
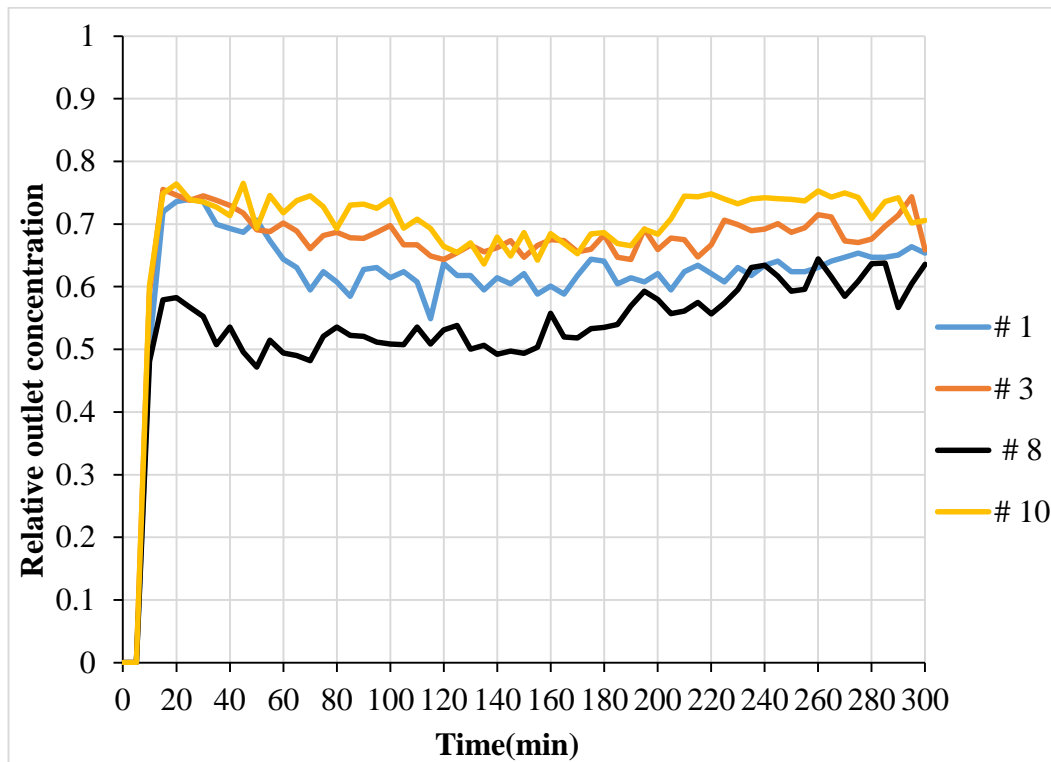
Figure 7.2. Experimental micro particle rhodamine-B tracer breakthrough curve in flow rate 1 (cc/min) at outer temperature 70 °C for different core plugs

As can clearly be observed that the breakthrough curves of micro particles of Rhodamine B suspension (Figure 7.2) differ from those of Rhodamine B solution (Figure 6.9). It is evident that the breakthrough of micro particles suspension is faster than that of solute in all fractured core plugs.

The shape of micro particles breakthrough curve gives detailed information about matrix-fracture transfers and mechanisms involved in particle transport through fractured porous media. As the fracture provides large transport pathway for micro particles compared to the surrounding matrix, advection as predominant mechanism causes the early breakthrough for micro particles transport through a single fracture-matrix system.

134

In fact, the lack of micro particles penetration into the surrounding matrix due to low permeability of matrix, smaller pore throat size of matrix relative to particle size, and similar charge of particles can be considered as a main reason for decreasing in collision with matrix grains and fast-moving streamlines in fracture and thus faster breakthrough for micro particles. No spread in breakthrough curve because of lower attachment of micro particles to matrix grains results in the plug flow form in breakthrough curve.

Similar to tracer testing by Rhodamine B solution injection, the values of heat flux in matrix-fracture interface and fracture temperature were measured by a heat flux sensor over the duration of the micro particles suspension injection at flow rate 1 (cc/min) and outer temperature 70 °C (Figures 7.3 and 7.4).
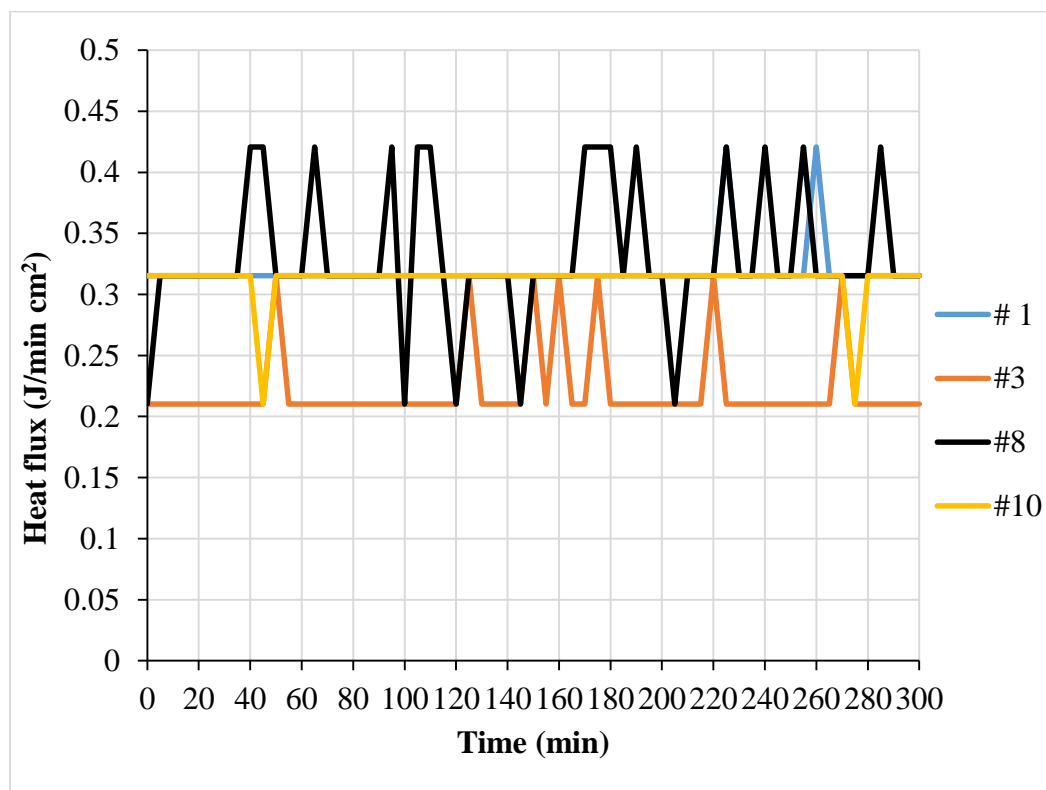
Figure 7.3. Experimental heat flux in flow rate 1 (cc/min) at outer temperature 70 °C for different core plugs
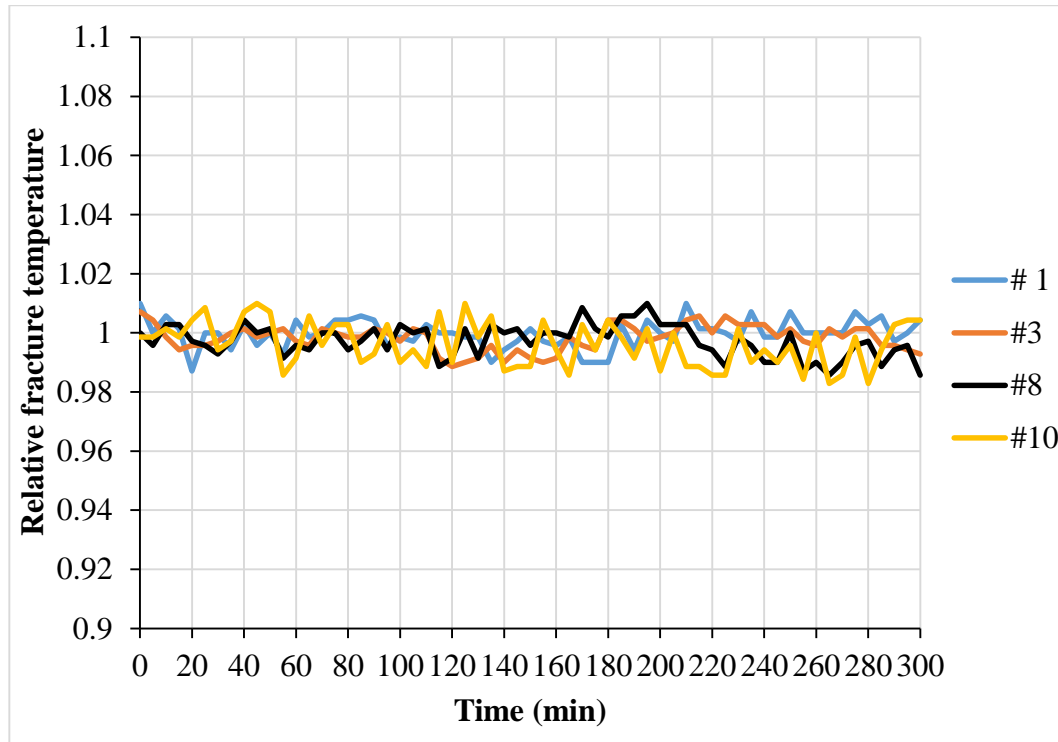
Figure 7.4. Experimental relative fracture temperature in flow rate 1 (cc/min) at outer temperature 70 °C for different core plugs

In view of low injection rate 1 (cc/min) of micro particles suspension, the values of heat flux and temperature in fracture were hovered around the same level in all single fractured core plugs.

7.3.2. Sensitivity Analysis

Although micro particles suspensions may offer some advantages in the characterization of matrix-fracture systems, some problems involved in the application of micro particles of Rhodamine B suspension make it challenging for characterization of fractured porous media.

136

Firstly, whereas suspension flow through the fractured core plugs is mainly dominated by the flow through fracture, the micro particles of Rhodamine B are aggregated within fracture. The aggregation of micro particles of Rhodamine B within fracture may be as a result of adsorbing or sticking of micro particles on fracture wall (matrix-fracture interface) and surface of the heat flux sensor as well as gravity settling of particles in the fracture over micro particles suspension injection through the single fractured core plugs.

In addition, the micro particles suspension used in particle transport study have to ensure that particles are stable and in dispersion form in suspension over the duration of the tracer testing processes. As revealed by observations, micro particles of Rhodamine B suspension tend to be precipitated with progress in time, plugging flow pathway (Figure7.5).
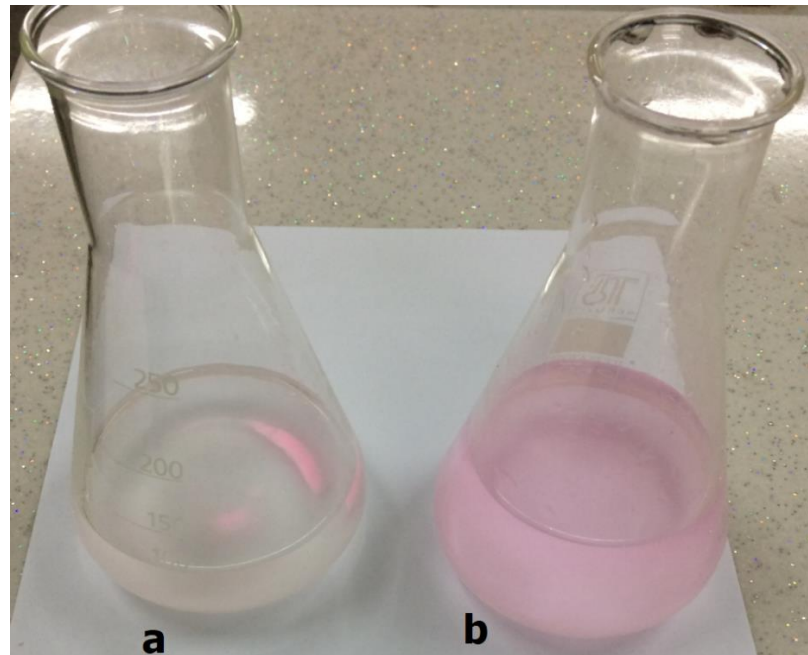
Figure 7.5. Micro particles of Rhodamine B: **a)** settlement **b)** suspension

The above-mentioned reasons make it difficult to model the transport of micro particles, having a sensitivity analysis of transport parameters in different transport scenarios of micro particles in the single fracture-matrix systems.

CHAPTER 8

CONCLUSIONS

8.1. Matrix-Fracture Thermal Transport

- The numerical model of cold water injection through single fractured core plug was built using CMG STARS simulator to analyze matrix-fracture heat transfer. The numerical model calibrated with experimental values of fracture temperature was used to determine temperature difference along matrix-fracture interface and some properties of matrix and fracture. Also, it makes investigation of the effect of flow rate in fracture and thermal properties of matrix on matrix-fracture heat transfer in different core plugs. The model gives an accurate insight into the thermal front propagation along fracture, temperature difference along matrix-fracture interface in different times, and temperature distribution within matrix.

- The experimental measurements of heat flux and temperature in fracture indicate that the values of both heat flux and temperature in fracture decrease with rising cold water injection period. The former is due to decrease in the temperature difference between fracture surface and fluid in fracture while the latter is due to heat swept over fracture surface that causes temperature drop in matrix-fracture interface over cold water injection which were followed by a period of stability, reaching a relatively steady values.

- The rise in injection rate results in more decrease in fracture temperature whereas more increase in heat flux values over cold water injection. They can come from large volume of water contacting fracture at a given time. The large volume of water in fracture in high flow rate causes more temperature drop at matrix-fracture interface, decreasing more fracture temperature. However, the large volume of water in fracture in high flow rate makes that flowing water in fracture is not warmed more. Thus, heat flux increases due to high temperature difference between fracture surface and fluid in fracture.

- The numerical simulation model reveals that matrix-fracture heat transfer depends on not only flow characteristics in fracture, but also thermal properties of matrix with establishment of fracture surface temperature. The rate of heat transfer in matrix-fracture interface is high in matrix with large values of thermal properties as opposed to matrix with low values of thermal properties at outer temperatures 70 and 90 °C. Also, numerical model determined that the thermal properties of matrix are dependent on the outer temperature. To illustrate, the amount of temperature decrease in fracture is less while temperature profile increase along fracture is high in core plug # 1 with large values of thermal properties compared to core plug # 3 with low values of thermal properties over cold water injection through the single fractured core plugs.

- The amount of temperature decrease in fracture is increased while temperature profile increase along fracture is reduced with increasing outer temperature from 70 to 90 °C. This can be attributable to the increase in volumetric heat capacity of matrix that reducing thermal conduction at high temperatures.

- The convective heat transfer coefficients calculated by energy balance and analytical model cannot justify the values of temperature in fracture outlet whereas the convective heat transfer coefficients calculated directly using experimental values of heat flux and the values of temperature difference at matrix-fracture interface in numerical model can represent matrix-fracture heat transfer.

- The current study represents that thermal properties of matrix influence on the amount of convective heat transfer coefficient and temperature difference at matrix-fracture interface in diffusive dominant heat transfer mechanism (low flow rate) whereas flow characteristics have important effect on those at advective dominant heat transfer mechanism (high flow rate).

- The local and transient values of convective heat transfer coefficient were introduced to analysis matrix-fracture heat transfer because of variable values of heat flux and temperature difference at matrix-fracture interface with respect to space and time.

- According to experimental and numerical studies, the local convective heat transfer coefficient depends mainly on temperature difference along matrix-fracture interface. However, transient values of heat flux determine principally the transient convective heat transfer coefficient.

8.2. Matrix-Fracture Solute Transport

- The solution of Rhodamine B was used as a non-reactive tracer solution for investigation of matrix-fracture solute transport. As it is a fluorescent dye, the fluorescence spectrometry was used to measure concentration of tracer solution based on induced fluorescence.

- The numerical model of tracer solution injection through single fractured core plug was built using CMG STARS simulator to analyze matrix-fracture mass transfer in non-isothermal conditions. The numerical model calibrated with experimental values of outlet concentration of tracer was used to determine the anisotropic values of dispersion coefficient. Also, it makes investigation of the effect of flow rate in fracture and thermal properties of matrix on matrix-fracture solute transport in different core plugs.

- The analysis of breakthrough curves shows that the outlet concentrations increase for all single fractured core plugs over tracer injection period. This can be referred to advective dominant mechanism of solute transport. The tracer effluents hover around a relatively steady value at the end of tracer solution injection because of solute equilibrium between matrix and fracture. Also, tracer breakthrough curves indicate that the high value of permeability in porous matrix results in low outlet concentration over tracer injection experiments through single fractured core plugs. Core plugs # 1 and 8 with large values of permeability and dispersion coefficient due to more dispersion within matrix have lower outlet concentrations while

core plugs # 3 and 10 with low values of physical properties of matrix have high outlet concentrations of tracer over tracer injection through matrix-fracture systems.

- The level of solute penetration from fracture into matrix can be considered as an index of matrix-fracture mass transfer. In addition, it can be evaluated by the tracer breakthrough concentration, steady concentration profile in fracture, and the amount of mass remained in matrix.

- The numerical simulation model illustrates that the outlet concentration of tracer and concentration profile along fracture are high at large injection rates due to short contact time of solute at matrix-fracture interface that declines the solute penetration into matrix.

- The numerical model indicates that thermal properties of matrix control solute transport in matrix-fracture systems in addition to physical properties of matrix. The thermal properties of matrix through establishment of temperature gradient that causes Soret effect have a pivotal role on solute transport in matrix-fracture systems. Core plugs # 1 and 8 with high increase in the values of matrix thermal properties over outer temperature rise from 70 to 90 °C have large temperature gradient along matrix-fracture interface that more solute migrates from fracture to matrix, decreasing outlet concentrations of tracer and tracer concentration profile along fracture. But in the case of core plugs # 3 and 10 low increase in thermal properties of matrix over temperature increase from 70 to 90 °C causes low temperature gradient that results

in low migration of solute from fracture to matrix, in turn, high outlet concentrations of tracer and tracer concentration profile along fracture.

- Among the range of injection flow rates, the tracer concentration difference at matrix-fracture increases with rising flow rate due to more penetration into matrix, reaching maximum amount at flow rate 1.5 (cc/min). With increasing flow rate, the short contact time of the solute at matrix-fracture interface contributes to decrease concentration difference due to less solute penetration into matrix.

- The thermal properties of matrix can affect on tracer concentration difference through the establishment of temperature gradient at matrix-fracture interface and Soret effect. In the case of core plug # 3 the less Soret effect causes decrease in solute migration and concentration difference at 90 °C. On the other hand, the concentration difference is relatively high for core plug # 1 due to large Soret effect in non-isothermal tracer injection processes.

- The amount of mass remained in matrix decreases exponentially with increasing injection flow rate due to short contact time of tracer at matrix-fracture interface.

- Thermal properties of matrix by Soret effect can be effective in the amount of mass remained in matrix. In the case of core plugs # 1 and 8 with high Soret effect the amount of mass remained in matrix increases over outer temperature increase from 70 to 90 °C while the amount of mass remained in matrix decreases for core plugs # 3 and 10 due to low Soret effect.

- The Soret effect is predominant phenomenon in low injection rate over non-isothermal mass transfer.

8.3. Matrix-Fracture Particles Transport

- The breakthrough of micro particles suspension is faster than that of solute. It can be due to lack of micro particles penetration into matrix.

- Lower attachment of micro particles to matrix grains due to low permeability of matrix, smaller pore throat size of matrix, and similar charge of particles results in the plug flow form in breakthrough curve.

REFERENCES

Abbasi, M., Khazali, N., Sharifi, M., 2017. Analytical model for convection-conduction heat transfer during water injection in fractured geothermal reservoirs with variable rock matrix block size. Geothermics 69, 1-14.

Abdallah, G., Thoraval, A., Sfeir, A., Piguet, J.P., 1995. Thermal convection of fluid in fractured media. International Journal of Rock Mechanics and Mining Sciences & Geomechanics Abstracts 32(5), 481-490.

Abdelfatah, E., Pournik, M., Shiau, B.J.B., Harwell, J., 2017. Mathematical modeling and simulation of formation damage associated with nanoparticles transport in porous media, SPE SPE-184894-MS, Latin America and Caribbean Mature Fields Symposium. Society of Petroleum Engineers, Salvador, Bahia, Brazil.

Akin, S., 2001. Analysis of tracer tests with simple spreadsheet models. Computers & Geosciences 27(2), 171-178.

Akin, S., Okandan, E., 1995. Reservoir characterization by tracer testing, World Geothermal Congress. International Geothermal Association Florence, Italy, pp. 1145-1150.

Alaskar, M., Li, K., Horne, R., 2014. Transport of temperature nanosensors through fractured tight rock: an experimental study, SPE-172208-MS, Saudi Arabia Section Technical Symposium and Exhibition. Society of Petroleum Engineers, Al-Khobar, Saudi Arabia.

Alaskar, M.N., Ames, M.F., Connor, S.T., Liu, C., Cui, Y., Li, K., Horne, R.N., 2012. Nanoparticle and Microparticle Flow in Porous and Fractured Media-An Experimental Study. SPE Journal 17(04), 1,160-161,171.

Amini, S., Mohaghegh, S., 2019. Application of machine learning and artificial Intelligence in proxy modeling for fluid flow in porous media. Fluids 4(3), 126-143.

Axelsson, G., 2013. Tracer tests in geothermal resource management, EPJ Web of Conferences. EDP Sciences, p. 02001.

Bagalkot, N., Kumar, G.S., 2015. Thermal front propagation in variable aperture fracture–matrix system: A numerical study. Sadhana 40(2), 605-622.

Bagalkot, N., Kumar, G.S., 2018. Colloid transport in a single fracture–matrix system: Gravity effects, influence of colloid size and density. Water 10(11), 1531-1548.

Bagalkot, N., Zare, A., Kumar, G., 2018. Influence of fracture heterogeneity using linear congruential generator (LCG) on the thermal front propagation in a single geothermal fracture-rock matrix system. Energies 11(4), 916-929.

Baston, D.P., Falta, R.W., Kueper, B.H., 2010. Numerical modeling of thermal conductive heating in fractured bedrock. Ground Water 48(6), 836-843.

Bergman, T.L., Lavine, A.S., Incropera, F.P., DeWitt, D.P., 2011. Fundamentals of Heat and Mass Transfer 7th ed. John Wiley & Sons, New York, US.

Berre, I., Doster, F., Keilegavlen, E., 2019. Flow in fractured porous media: A review of conceptual models and discretization approaches. Transport in Porous Media 130(1), 215-236.

Bijeljic, B., Rubin, S., Scher, H., Berkowitz, B., 2011. Non-Fickian transport in porous media with bimodal structural heterogeneity. Journal of contaminant hydrology 120, 213-221.

Bird, R.B., Steward, W.E., Lightfood, E.N., 2002. Transport phenomena, 2nd ed. John Wiley & Sons   New York.

Biswas, S., Mishra, U., 2015. Continuous fixed-bed column study and adsorption modeling: removal of lead ion from aqueous solution by charcoal originated from chemical carbonization of rubber wood sawdust. Journal of Chemistry 2015, 9.

Bodin, J., Delay, F., De Marsily, G., 2003. Solute transport in a single fracture with negligible matrix permeability: 1. fundamental mechanisms. Hydrogeology journal 11(4), 418-433.

Boon, M., Bijeljic, B., Krevor, S., 2017. Observations of the impact of rock heterogeneity on solute spreading and mixing. Water Resources Research 53(6), 4624-4642.

Boving, T.B., Grathwohl, P., 2001. Tracer diffusion coefficients in sedimentary rocks: correlation to porosity and hydraulic conductivity. Journal of contaminant hydrology 53(1-2), 85-100.

Bozbiyik, B., Van Assche, T., Lannoeye, J., De Vos, D.E., Baron, G.V., Denayer, J.F., 2017. Stepped water isotherm and breakthrough curves on aluminium fumarate metal–organic framework: experimental and modelling study. Adsorption 23(1), 185-192.

Brouyère, S., Carabin, G., Dassargues, A., 2005. Influence of injection conditions on field tracer experiments. Ground Water 43(3), 389-400.

Cavalcante, C.C., Maschio, C., Santos, A.A., Schiozer, D., Rocha, A., 2017. History matching through dynamic decision-making. PloS one 12(6), e0178507.

Charette, V.J., Evangelista, E., Chertcoff, R., Auradou, H., Hulin, J.-P., Ippolito, I., 2007. Influence of the disorder on tracer dispersion in a flow channel. European Physical Journal Applied Physics.

Cheng, A., GhassemiÜ, A., Detournay, E., 2001. Modeling heat extraction from a fracture in hot dry rock using an integral equation method. Cerca con Google.

Chowdhury, Z.Z., Hamid, S.B.A., Zain, S.M., 2015. Evaluating design parameters for breakthrough curve analysis and kinetics of fixed bed columns for Cu (II) cations using lignocellulosic wastes. BioResources 10(1), 732-749.

CMG STARS Manual, Advanced Process and Thermal Reservoir Simulator, (2013) CMG STARS, version 2013. Computer Modelling Group Ltd., Calgary, AB, Calgary, Canada.

Coronado, M., Ramírez-Sabag, J., Valdiviezo-Mijangos, O., Somaruga, C., 2009. A test of the effect of boundary conditions on the use of tracers in reservoir characterization. Geofísica internacional 48(2), 185-193.

Crhribi, A., Chlendi, M., 2011. Modeling of fixed bed adsorption: application to the adsorption of an organic dye. Asian Journal of Textile 1, 161-171.

Dietrich, P., Helmig, R., Sauter, M., Hötzl, H., Köngeter, J., Teutsch, G., 2005. Flow and transport in fractured porous media. Springer Science & Business Media, Berlin, Heidelberg.

Geiger, S., Cortis, A., Birkholzer, J., 2010. Upscaling solute transport in naturally fractured porous media with the continuous time random walk method. Water Resources Research 46(12), W12530.

Grisak, G.E., Pickens, J.F., 1980. Solute transport through fractured media: 1. The effect of matrix diffusion. Water Resources Research 16(4), 719-730.

Grisak, G.E., Pickens, J.F., 1981. An analytical solution for solute transport through fractured media with matrix diffusion. Journal of hydrology 52(1-2), 47-57.

Heidari, L., Gervais, V., Le Ravalec, M., Wackernagel, H., 2011. History matching of reservoir models by ensemble Kalman filtering: the state of the art and a sensitivity study, in: Ma, Y.Z., La Pointe, P.R. (Eds.), Uncertainty analysis and reservoir modeling: AAPG Memoir 96. pp. 249-264.

Heinze, T., Hamidi, S., Galvan, B., 2017. A dynamic heat transfer coefficient between fractured rock and flowing fluid. Geothermics 65, 10-16.

Incropera, F.P., DeWitt, D.P., 2002. Fundamentals of heat and mass transfer, 5th ed. John Wiley & Sons, New York.

Jiang, P.-X., Ren, Z.-P., 2001. Numerical investigation of forced convection heat transfer in porous media using a thermal non-equilibrium model. International Journal of Heat and Fluid Flow 22(1), 102-110.

Kaviany, M., 1995. Principles of heat transfer in porous media, 2nd ed. Springer, Berlin-Heidelberg.

Khuzhayorov, B., Mustofokulov, Z., 2019. The Adsorbed Solute Transport with Diffusion Effects. Journal of Applied and Computational Mathematics 8(1), 1-4.

Khuzhayorov, B., Mustofoqulov, Z., 2018. Transport of active solute in a fractured porous medium with nonequilibrium adsorption. International Journal of Advanced Research in Science, Engineering and Technology 5(12), 7589-7597.

Klump, J., Galkin, A., Giraldo, C., Schicks, J.M., 2011. Using hydrocarbon reservoir modeling software for numerical modeling of laboratory experiments on gas hydrates Proceedings of the 7th International Conference on Gas Hydrates (ICGH 2011). Edinburgh, Scotland, UK.

Kuiken, G.D., 1994. Thermodynamics of irreversible processes: applications to diffusion and rheology. Wiley New York.

Kumar, S.S., 2012. A review on fluid dynamics of fractured reservoir geology. International Journal of Geology 6(2), 45-52.

Lenormand, R., Le Romancer, J., Le Gallo, Y., Bourbiaux, B., 1998. Modeling the diffusion flux between matrix and fissure in a fissured reservoir, SPE 49007, Annual Technical Conference and Exhibition. New Orleans, Louisiana.

Li, Y.V., Cathles, L.M., Archer, L.A., 2014. Nanoparticle tracers in calcium carbonate porous media. Journal of nanoparticle research 16(8), 2541.

Lienhard, J.H., 2013. A heat transfer textbook. Courier Corporation, 5th ed. John Wiley & Sons, New York.

Luo, J., Qi, Y., Zhao, Q., Tan, L., Xiang, W., Rohn, J., 2018. Investigation of flow and heat transfer characteristics in fractured granite. Energies 11(5), 1228-1243.

Luo, J., Zhu, Y., Guo, Q., Tan, L., Zhuang, Y., Liu, M., Zhang, C., Xiang, W., Rohn, J., 2017. Experimental investigation of the hydraulic and heat-transfer properties of artificially fractured granite. Scientific Reports 7, 39882.

Malgaresi, G., Zhang, H., Chrysikopoulos, C., Bedrikovetsky, P., 2019. Cotransport of suspended colloids and nanoparticles in porous Media. Transport in Porous Media 128(1), 153-177.

Martinez, A.R., Roubinet, D., Tartakovsky, D., 2014. Analytical models of heat conduction in fractured rocks. Journal of Geophysical Research: Solid Earth 119(1), 83-98.

Mohammadi, H., Manshad, A.K., Montazeri, G., 2012. A reservoir simulation approach for modeling of naturally fractured reservoirs. Egyptian Journal of Petroleum 21(2), 125-133.

Moorthy, M., Senthilvadivu, K., 2012. Soret and Dufour effects on natural convection flow past a vertical surface in a porous medium with variable viscosity. Journal of Applied Mathematics 2012, 15.

Narasimhan, A., 2013. Essentials of heat and fluid flow in porous media. Boca Raton, FL : CRC, Taylor & Francis/Ane Books Pvt. Ltd. .

Nield, D.A., Bejan, A., 2006. Convection in porous media, 3rd ed. Springer, New York, US.

Olasolo, P., Juárez, M., Morales, M., Liarte, I., 2016. Enhanced geothermal systems (EGS): A review. Renewable and Sustainable Energy Reviews 56, 133-144.

Pal, D., Chatterjee, S., 2013. Soret and Dufour effects on MHD convective heat and mass transfer of a power-law fluid over an inclined plate with variable thermal

conductivity in a porous medium. Applied Mathematics and Computation 219(14), 7556-7574.

Patel, H., 2019. Fixed-bed column adsorption study: a comprehensive review. Applied Water Science 9(3), 45.

Polak, A., Grader, A.S., Wallach, R., Nativ, R., 2003. Tracer diffusion from a horizontal fracture into the surrounding matrix: measurement by computed tomography. Journal of contaminant hydrology 67(1-4), 95-112.

Pruess, K., van Heel, T., Shan, C., 2005. Tracer testing for estimating heat transfer area in fractured reservoirs, Proceedings World Geothermal Congress. Antalya, Turkey.

Rai, S.K., Bera, A., Mandal, A., 2015. Modeling of surfactant and surfactant–polymer flooding for enhanced oil recovery using STARS (CMG) software. Journal of Petroleum Exploration and Production Technology 5(1), 1-11.

Ramírez-Sabag, J., Valdiviezo-Mijangos, O., Coronado, M., 2005. Inter-well tracer tests in oil reservoirs using different optimization methods: A field case. Geofísica internacional 44(1), 113-120.

Reddy, D.S., Govardhan, K., 2015. Effect of viscous dissipation, soret and dufour effect on free convection heat and mass transfer from vertical surface in a porous medium. Procedia Materials Science 10, 563-571.

Reddy, P.S., Rao, K.S., Rao, D.P., Mamatha, E., 2010. Thermo-Diffusion and Diffusion–Thermo Effects on Convective Heat and Mass Transfer through a Porous Medium in a Circular Cylindrical Annulus with Quadratic Density Temperature Variation–A Finite Element Study. International Journal of Dynamics of Fluids 6(1), 97-106.

Reddy, P.S., Rao, V., 2012. Thermo-Diffusion and Diffusion-Thermo Effects on Convective Heat and Mass Transfer through a Porous Medium in a Circular

Cylindrical Annulus with Quadratic Density Temperature Variation- Finite Element Study. Journal of Applied Fluid Mechanics 5(4), 139-144.

Sahimi, M., 2011. Flow and transport in porous media and fractured rock: from classical methods to modern approaches, 2nd ed. John Wiley & Sons.

Sanaee, R., Oluyemi, G.F., Hossain, M., Oyeneyin, B.M., 2012. Fracture-matrix flow partitioning and cross flow: numerical modeling of laboratory fractured core flood, Proceedings of the 2012 COMSOL conference. Milan.

Schmelling, S.G., Ross, R.R., 1989. Contaminant Transport in Fractured Media: Models for Decision Makers. US Environmental Protection Agency. EPA/540/4-89/004.

Shahkarami, A., Mohaghegh, S.D., Hajizadeh, Y., 2015. Assisted history matching using pattern recognition technology, SPE Digital Energy Conference and Exhibition. Society of Petroleum Engineers, Texas, USA.

Shaik, A.R., Rahman, S.S., Tran, N.H., Tran, T., 2011. Numerical simulation of fluid-rock coupling heat transfer in naturally fractured geothermal system. Applied thermal engineering 31(10), 1600-1606.

Tachi, Y., Ito, T., Akagi, Y., Satoh, H., Martin, A.J., 2018. Effects of Fine-Scale Surface Alterations on Tracer Retention in a Fractured Crystalline Rock From the Grimsel Test Site. Water Resources Research 54(11), 9287-9305.

Tang, D., Frind, E., Sudicky, E.A., 1981. Contaminant transport in fractured porous media: Analytical solution for a single fracture. Water Resources Research 17(3), 555-564.

Tunnish, A., Shirif, E., Henni, A., 2019. History matching of experimental and CMG-STARS results. Journal of Petroleum Exploration and Production Technology 9(1), 341-351.

Werth, C.J., Cirpka, O.A., Grathwohl, P., 2006. Enhanced mixing and reaction through flow focusing in heterogeneous porous media. Water Resources Research 42(12),W12414.

Wiegand, S., 2004. Thermal diffusion in liquid mixtures and polymer solutions. Journal of Physics: Condensed Matter 16(10), R357.

Wu, Y.-S., Ye, M., Sudicky, E., 2010. Fracture-flow-enhanced matrix diffusion in solute transport through fractured porous media. Transport in Porous Media 81(1), 21-33.

Yamaguchi, S., Akibayashi, S., 1992. Heat transfer process in a hot dry rock geothermal reservoir, 14th New Zealand Workshop. New Zealand, pp. 133-138.

Yu, J., An, C., Mo, D., Liu, N., Lee, R.L., 2012. Study of adsorption and transportation behavior of nanoparticles in three different porous media, SPE-153337-MS, improved oil recovery symposium. Society of Petroleum Engineers, Tulsa, Oklahoma, USA.

Zhang, G., Zhu, J., Li, J., Wang, Q., 2015. The analytical solution of the water-rock heat transfer coefficient and sensitivity analyses of parameters, Proceedings World Geothermal Congress. Melbourne, Australia.

Zhao, J., 1992. Analytical and experimental studies of heat convection by water flow in rock fractures, in: RockMechanics, T.W. (Ed.) The 33th US Symposium on Rock Mechanics (USRMS). American Rock Mechanics Association.

Zhao, J., Tso, C., 1993. Heat transfer by water flow in rock fractures and the application to hot dry rock geothermal systems. International Journal of Rock Mechanics and Mining Sciences and Geomechanics Abstracts 30(6), 633-641.

Zhao, Z., 2014. On the heat transfer coefficient between rock fracture walls and flowing fluid. Computers and Geotechnics 59, 105-111.

Zhu, Y., Zhan, H., 2018. Quantification of solute penetration in an asymmetric fracture-matrix system. Journal of hydrology 563, 586-598.

Zhu, Y., Zhan, H., Jin, M., 2016. Analytical solutions of solute transport in a fracture–matrix system with different reaction rates for fracture and matrix. Journal of hydrology 539, 447-456.

Zou, L., Jing, L., Cvetkovic, V., 2016. Assumptions of the analytical solution for solute transport in a fracture-matrix system. International Journal of Rock Mechanics and Mining Sciences 83, 211-217.
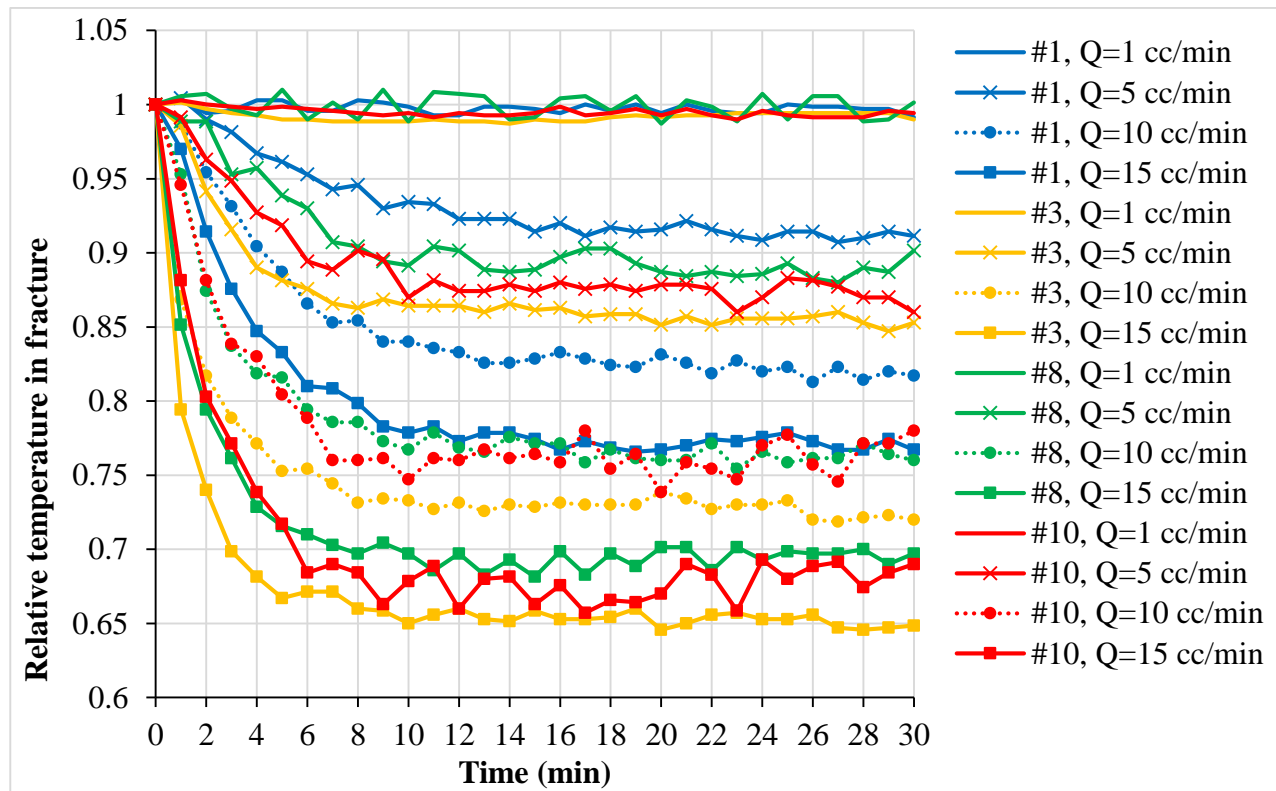
APPENDICES

Matrix-Fracture Heat Transfer

Figure A.1. Experimental relative temperature decrease in fracture at outer temperature 70 °C
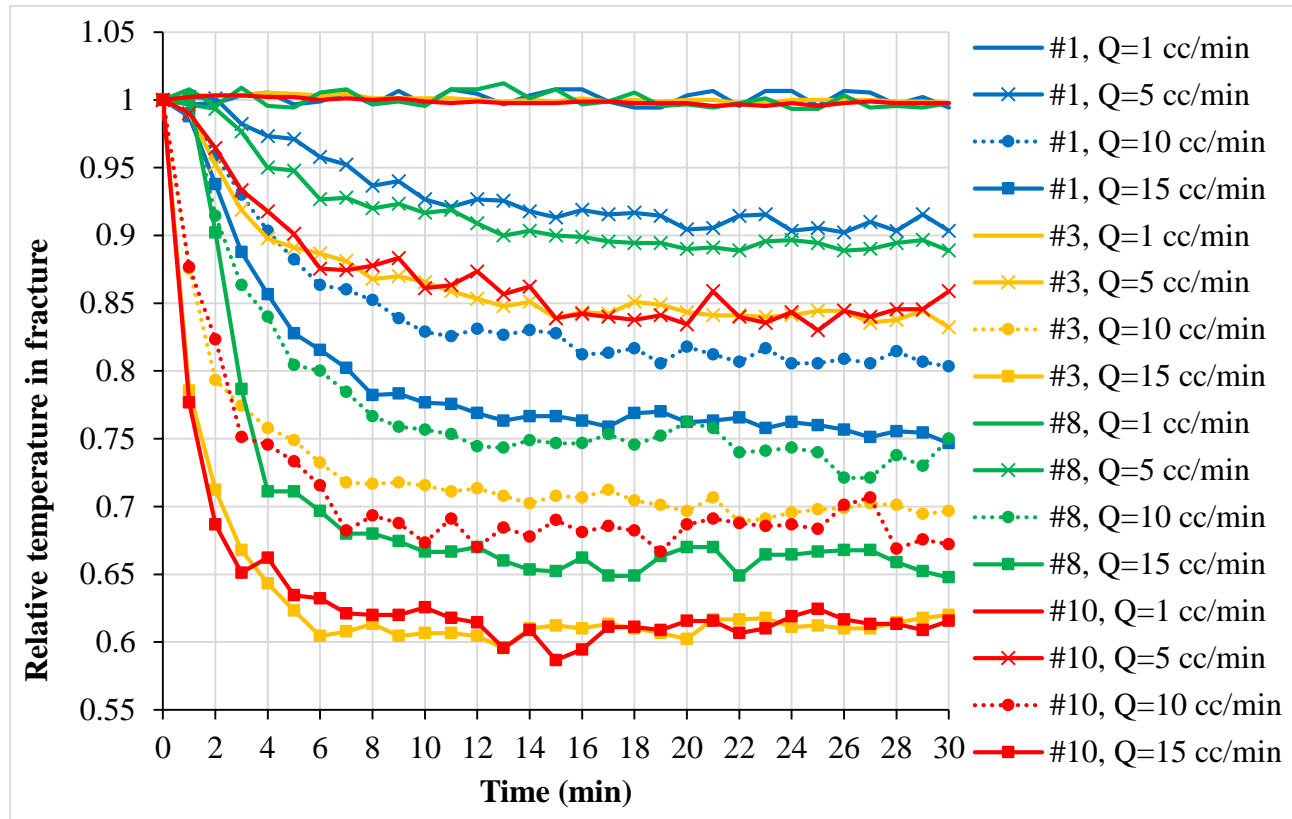
Figure A.2. Experimental relative temperature decrease in fracture at outer temperature 90 °C
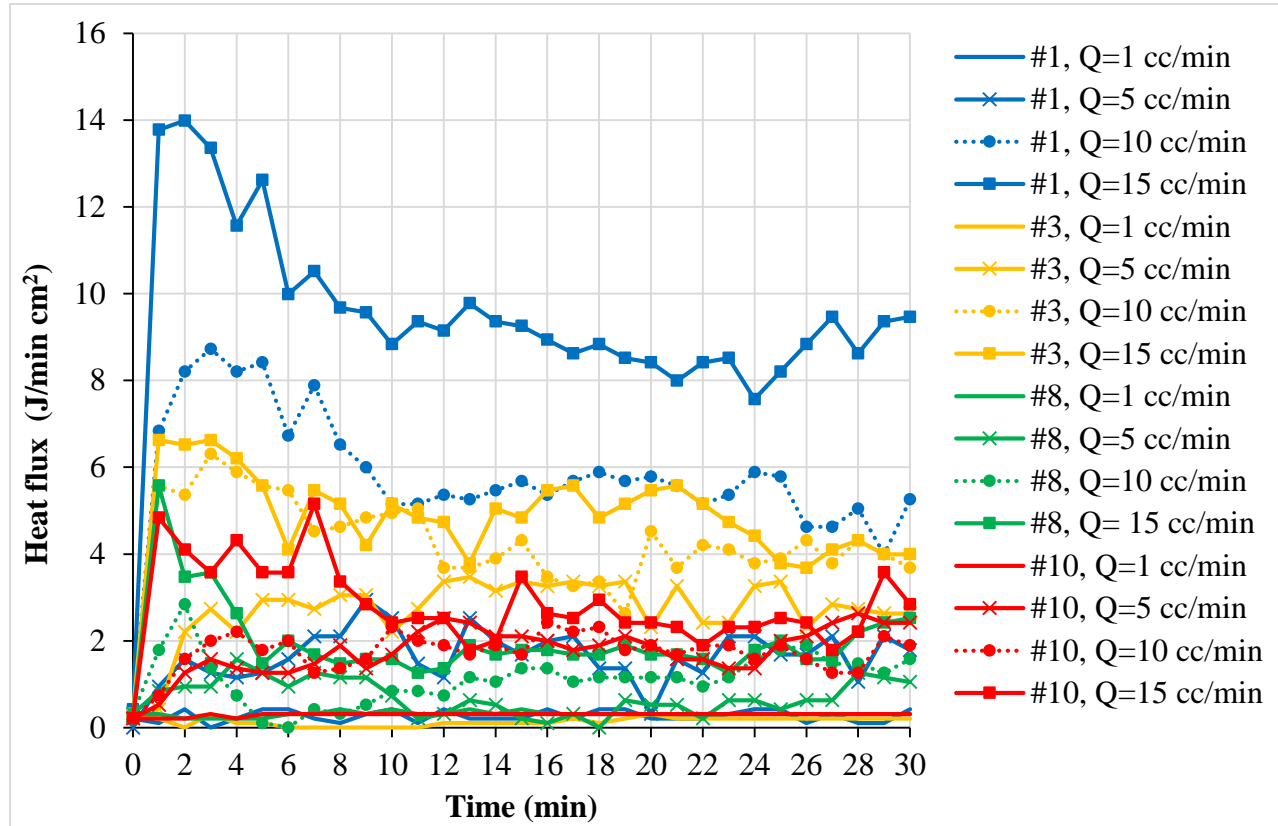
Figure A.3. Experimental heat flux at matrix-fracture interface at outer temperature 70 °C
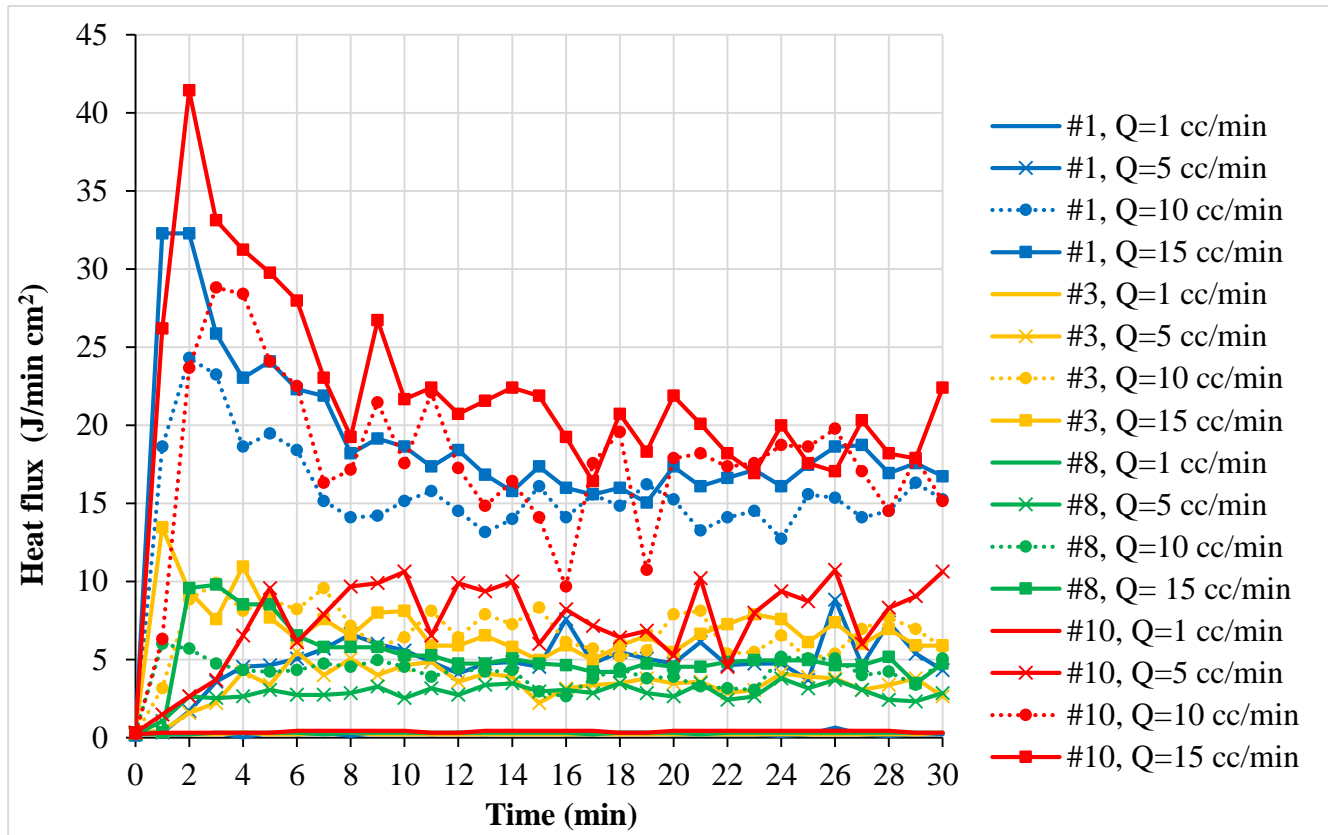
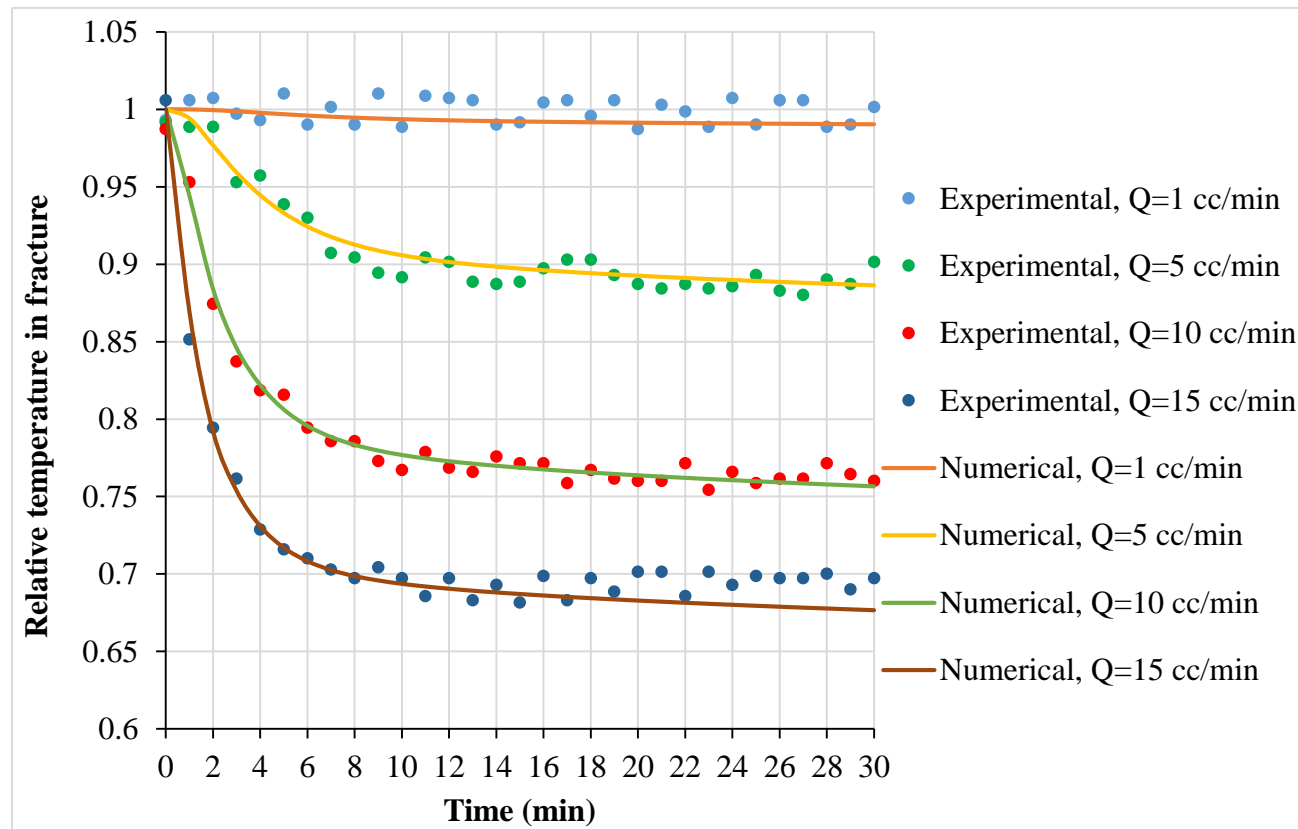*Figure A.4.* Experimental heat flux at matrix-fracture interface at outer temperature 90 °C

Figure A.5. History matching of temperature in fracture for core plug #8 at outer temperature 70°C
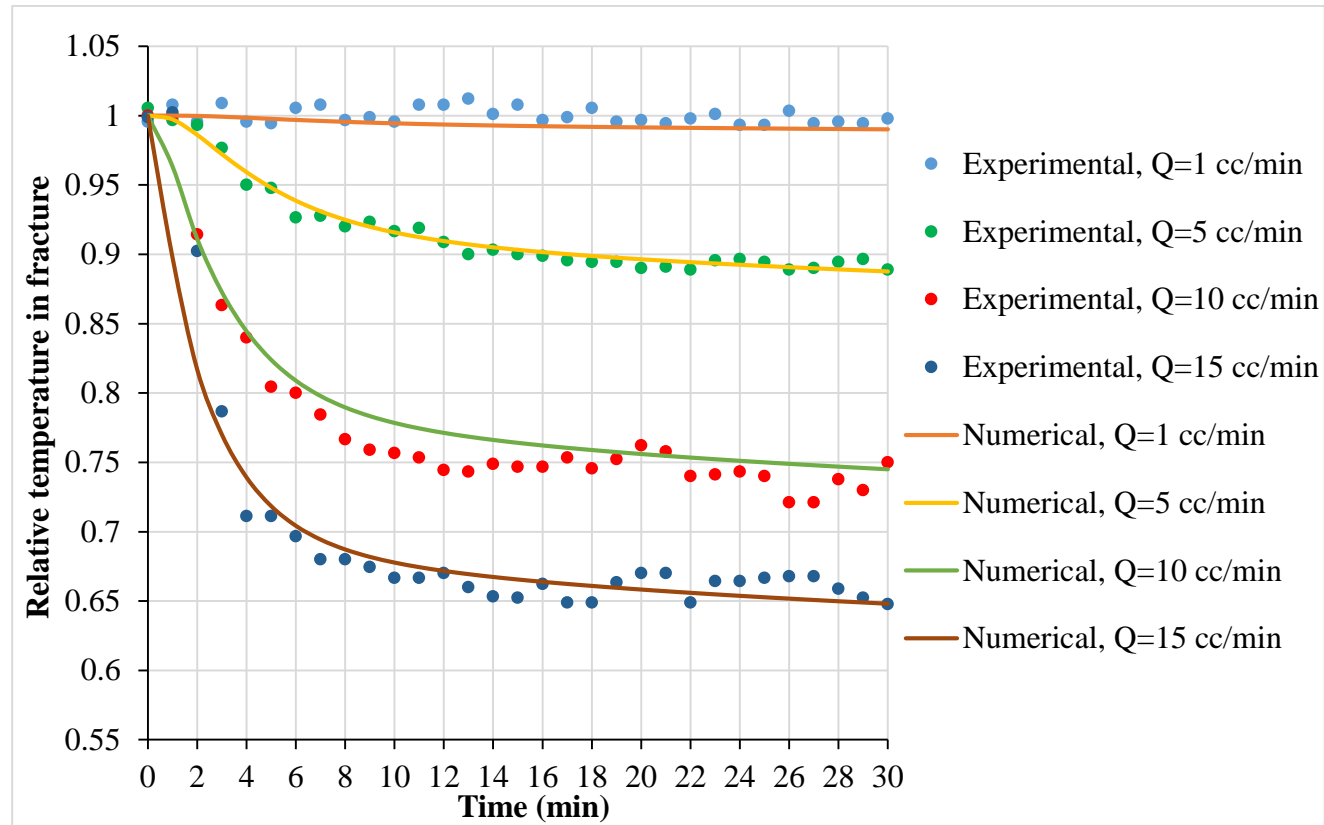
Figure A.6. History matching of temperature in fracture for core plug #8 at outer temperature 90°C
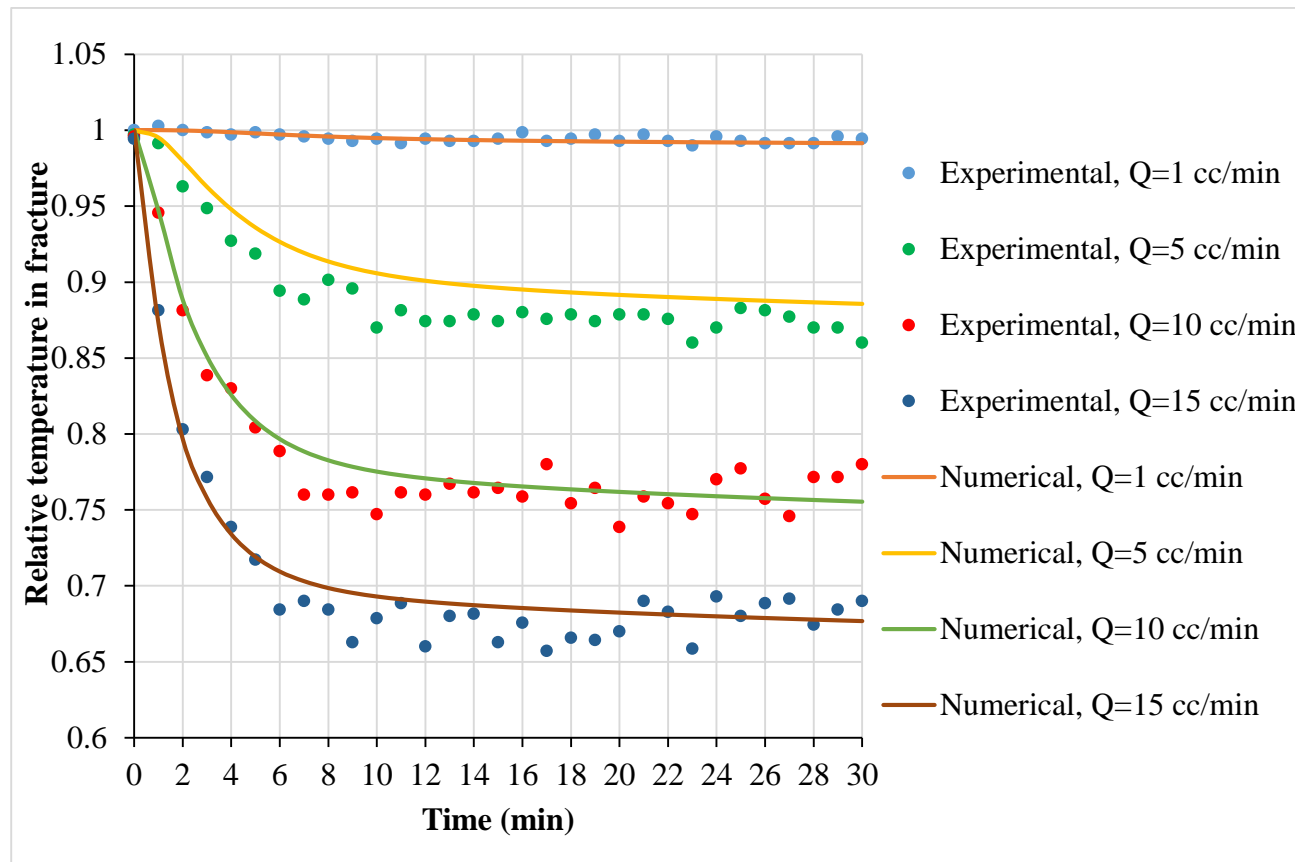
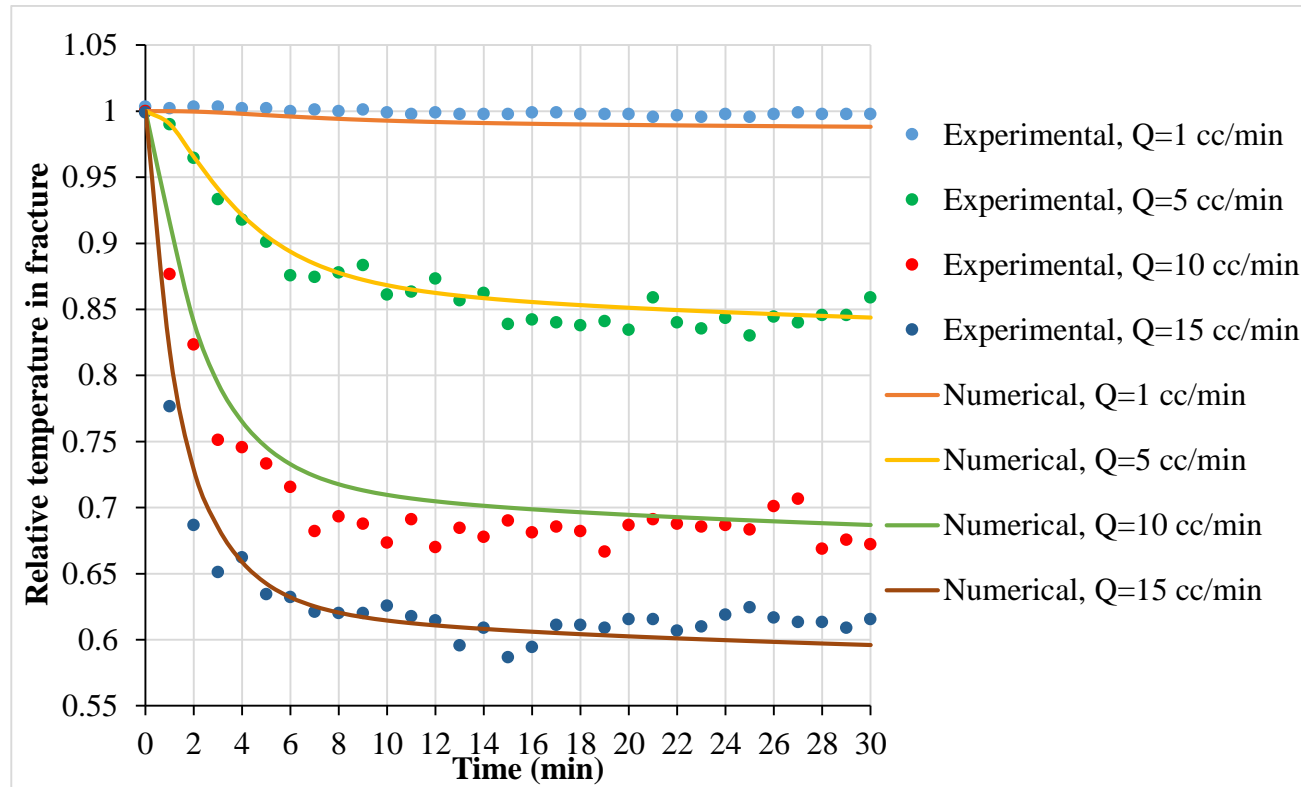*Figure A.7.* History matching of temperature in fracture for core plug #10 at outer temperature 70°C

Figure A.8. History matching of temperature in fracture for core plug #10 at outer temperature 90°C

CURRICULUM VITAE

PERSONAL INFORMATION

Surname, Name	:	Tavakkoli Osgouei **,** Yashar
Nationality	:	Iranian
Date of Birth	:	16 August 1979
E-mail	:	yashar.osgouei@metu.edu.tr

EDUCATION

Degree	Institution	Year of Graduation
Ph.D.	METU-Ankara, Petroleum and Natural Gas Engineering	2020
M.Sc. (II)	METU-Ankara, Petroleum and Natural Gas Engineering	2013
M.Sc. (I)	Azad University, Iran, Applied Chemistry	2005
B.Sc.	Azad University, Iran, Applied Chemistry	2003

EXPERIENCE

Year	Place	Enrollment
2016	ITALY	Summer School on Energy 2016
2015	METU-NCC	Teaching and Research Assistant
2014	ITALY	Math Mods Summer School 2014

LANGUAGES

English, Turkish, Azeri, Persian

PUBLICATIONS (<u>Journal Papers</u>)

1. Y. Tavakkoli Osgouei, S. Akin, "Experimental and Numerical Study of Flow and Thermal Transport in Fractured Porous Media", Springer Journals, Heat and Mass Transfer, 2020. (In Press)

2. Y. Tavakkoli Osgouei, M. Parlaktuna," Effects of Minerals on Steam Distillation during Thermal Heavy-Oil Recovery: An Experimental Investigation", Journal of Energy Sources, Part A: Recovery, Utilization, and Environmental Effects, VOL. 40, NO. 6, 662–672, 2018.

3. A. Salem, Y. Tavakkoli Osgouei, "The Effect of Particle Size Distribution on Barite Reduction", Journal of Materials Research Bulletin, No.44, pp 1489-1493, 2009.

4. A. Salem, Y. Tavakkoli Osgouei, S. Jamshidi, "Kinetic Study of Barite Carbothermic Reduction in Presence of Sodium Carbonate as Catalyst", Iranian Journal of Chemical Engineering, Vol.7, No.2 (Spring), pp 58-67, 2010.